

January 2012

# Development and Application of an F/M Based Anaerobic Digestion Model and the RT-RiboSyn Molecular Biology Method

Matthew Raymond Cutter

*University of South Florida*, [cutter\\_matthew@hotmail.com](mailto:cutter_matthew@hotmail.com)

Follow this and additional works at: <http://scholarcommons.usf.edu/etd>

 Part of the [American Studies Commons](#), [Environmental Engineering Commons](#), and the [Molecular Biology Commons](#)

---

## Scholar Commons Citation

Cutter, Matthew Raymond, "Development and Application of an F/M Based Anaerobic Digestion Model and the RT-RiboSyn Molecular Biology Method" (2012). *Graduate Theses and Dissertations*.  
<http://scholarcommons.usf.edu/etd/4023>

This Dissertation is brought to you for free and open access by the Graduate School at Scholar Commons. It has been accepted for inclusion in Graduate Theses and Dissertations by an authorized administrator of Scholar Commons. For more information, please contact [scholarcommons@usf.edu](mailto:scholarcommons@usf.edu).

Development and Application of an F/M Based Anaerobic Digestion Model and the  
RT-RiboSyn Molecular Biology Method

by

Matthew R. Cutter

A dissertation submitted in partial fulfillment  
of the requirements for the degree of  
Doctor of Philosophy  
Department of Civil and Environmental Engineering  
College of Engineering  
University of South Florida

Major Professor: Sarina Ergas, Ph.D.  
Daniel Yeh, Ph.D.  
Ryan Toomey, Ph.D.  
Stuart Wilkinson, Ph.D.  
James Garey, Ph.D.

Date of Approval:  
March 23, 2012

Keywords: precursor rRNA, reverse transcription, wastewater, dynamic modeling,  
chloramphenicol

Copyright ©2012, Matthew R. Cutter

## **ACKNOWLEDGEMENTS**

I'd like to thank my friend and first advisor, Dr. Peter Stroot, for the opportunity to come to Florida and be his first Ph.D. student. I wish you luck in your future endeavors.

I'd especially like to thank my advisor, Dr. Sarina Ergas, for being there for me in the bottom of the 9<sup>th</sup> inning. You've been a tremendous help to me these last several months, and I will always be grateful to you for your efforts. I would also like to thank my committee for their help and support over the years.

A big thank you to my fellow Team Stroot friends and cohorts: Sam, Andrea, Kathryn, Ray, Steve, and Lina. We've all been through a lot of lab and research difficulties, as well as a good deal of beer and lunches together. I appreciate all those times that we've helped each other out with research, and wish nothing but the best for all of you. I also want to thank the great friends that I've lived with over the years: Ken, Kimi, Claire, Marisa, Ashton, and Brandel - I really enjoyed living with all of you and wish you all the best. I am also very grateful for all of the guidance and friendship from Mary Beth Colter, Ph.D. at the H. Lee Moffitt Cancer Center & Research Institute. It was great being an honorary Core member! Finally, I'd like to thank my parents and family for their love and support these last several years.

## TABLE OF CONTENTS

LIST OF TABLES	iii
LIST OF FIGURES	v
ABSTRACT	viii
CHAPTER 1: INTRODUCTION	1
CHAPTER 2: DEVELOPMENT OF A SIMPLE F/M-BASED ANAEROBIC DIGESTION MODEL FOR CONTINUOUSLY-STIRRED TANK REACTORS	4
2.1 Introduction to Wastewater Treatment	4
2.2 Anaerobic Digestion	5
2.3 Review of Anaerobic Digestion Models	10
2.4 Model Review Conclusions	24
2.5 Model Development	25
2.5.1 Model Concept	25
2.5.2 Model Nomenclature	28
2.5.3 The F/M-Based CSTR Model	28
2.6 Methods and Materials	40
2.6.1 Specific Biogas Generation Test	40
2.6.2 Sludge Characterization	41
2.6.3 Laboratory-Scale Anaerobic Digesters	42
2.6.4 Analytical Methods	44
2.6.5 BioWin 3 Anaerobic Digestion Modeling Software	44
2.7 Results and Discussion	46
2.7.1 Specific Biogas Generation Test	46
2.7.2 Laboratory-Scale Anaerobic Digesters as Compared to the F/M Model	50
2.7.3 Laboratory-Scale Anaerobic Digesters as Compared to BioWin 3 Simulations	57

CHAPTER 3: DEVELOPMENT OF THE RT-RIBOSYN METHOD	61
3.1 Introduction	61
3.2 Background and Description of the RT-RiboSyn Method	63
3.3 Methods and Materials	67
3.3.1 Information on Wastewater and Sludge Sources	67
3.3.2 RT-RiboSyn with Pure Bacteria Culture	68
3.3.3 RT-RiboSyn Method with Activated Sludge from a High-Purity Oxygen System	70
3.3.4 RT-RiboSyn Method with Pure Methanogen Culture and Anaerobic Digester Sludge	72
3.3.5 Analytical Methods	74
3.4 Results and Discussion	75
3.4.1 RT-RiboSyn with Pure Bacteria Culture	75
3.4.2 RT-RiboSyn Method with Activated Sludge from High-Purity Oxygen System	82
3.4.3 RT-RiboSyn Method with Pure Methanogen Culture and Anaerobic Digester Sludge	88
3.4.4 Results from <i>M. barkeri</i> RNA	88
3.4.5 RT-RiboSyn Results with Anaerobic Digester Sludge and Arch915 Primer	92
3.4.6 RT-RiboSyn Results with Anaerobic Digester Sludge and Eub338 Primer	97
CHAPTER 4: CONCLUSIONS	100
4.1 F/M-Based Anaerobic Digestion Model	100
4.2 RT-RiboSyn Method	101
REFERENCES	103
APPENDICES	112
Appendix A F/M Anaerobic Digestion Model Supplemental Material	113
Appendix B Expanded Methods and Materials	118
Appendix C Reprint of Published RT-RiboSyn Article	138
Appendix D Beckman-Coulter CEQ-8000 Detection Limits	143
ABOUT THE AUTHOR	END PAGE

## LIST OF TABLES

Table 1	Measured and calculated model parameters for the F/M CSTR model.	42
Table 2	Total and volatile solids concentrations from primary, waste-activated, and blended sludges used for all experimental work.	43
Table 3	Comparison of experimental reactor and model biogas production rates (mL biogas per liter sludge per day) for laboratory-scale reactors operated at 10, 15, and 20 day HRTs.	53
Table 4	Average predicted (steady-state) and minimum/maximum (entire model simulation) F/M values for each reactor by feed type.	56
Table 5	Comparison of Total Volatile Solids (TVS) results from the 10-day and 20-day HRT reactors as compared to F/M and BioWin 3 model predictions	59
Table 6	General and statistical data for calculated ratios of precursor 16S rRNA to mature 16S rRNA, including primer used, culture temperature (°C), time of exposure to chloramphenicol (minutes), mean pre16S:16S, standard deviation ( $\sigma$ ), number of samples (n), and the coefficient of variance (COV).	80
Table 7	Specific rate of ribosome synthesis, $r$ , and specific growth rate, $\mu$ , as calculated by RT-RiboSyn and spectrophotometry, as well as the % difference between the measurements.	81
Table 8	Predicted lengths of 16S rRNA and pre16S rRNA fragments from RT&PE using the Arch915 primer for several methanogens.	92
Table B1	Annealing temperatures for selected WellRed-labelled primers	131
Table B2	Washing buffer formulation depending on formamide concentration in the hybridization buffer	137

Table D1 Expected mass of rRNA available in a standard sample of anaerobic digester sludge (2 mL) and per RT reaction (10 µg total) for several examples of syntrophic bacteria and methanogens found in anaerobic digester sludge

145

## LIST OF FIGURES

Figure 1	Simplified process schematic of a typical large wastewater treatment plant: 1.) wastewater generation, 2.) grinder and bar screen to remove large debris, 3.) primary settling tank to separate bulk of solid wastes from liquid wastes, 4.) aeration basin with activated sludge for oxidation/nitrification, 5.) secondary clarifier, 6.) chlorine contact chamber, 7.) gravity settling for WAS, 8.) anaerobic digestion, 9.) belt filter press and stabilized solids drying, 10.) landfill disposal or land application.	6
Figure 2	Sequential stages in the anaerobic digestion process: a.) Hydrolysis and fermentation, b.) VFA oxidation, and c.) biogas formation	9
Figure 3	Process flowchart of PS and WAS digestion and wasting processes	31
Figure 4	Process flowchart of microbial growth, wasting, and decay processes	35
Figure 5	Process flowchart of biogas production	37
Figure 6	Mass balance and material flow of the model reactor	39
Figure 7	Specific biogas production rates that characterize PS (◆) and WAS (■) digestion using seed sludge from a full-scale anaerobic digester.	49
Figure 8	Daily biogas production rates from reactors (◆), and predictions from the F/M model (■) for 10, 15, and 20-day HRT reactors.	52
Figure 9	Simplified description of cell doubling (a), ribosome synthesis (b), and inhibition of ribosome synthesis by chloramphenicol (c).	64
Figure 10	Example of pre16S:16S versus time, in this case a T = 30°C sample using the Eub338 primer with <i>A. calcoaceticus</i> .	77
Figure 11	Typical electropherograms of RT-RiboSyn products derived from <i>A. calcoaceticus</i> incubated in nutrient broth at 25 °C after exposure to chloramphenicol for (a) zero minutes and (b) 20 minutes.	78

Figure 12	Typical electropherogram of RT-RiboSyn products derived from <i>A. calcoaceticus</i> incubated in nutrient broth at 25 °C after exposure to chloramphenicol for a.) zero minutes and b.) twenty minutes.	79
Figure 13	Images from FISH analysis of activated sludge from HPO system at Howard F. Curren Advanced Wastewater Treatment Plant.	83
Figure 14	Filtered sample COD measurements versus time (minutes) from the master reactor.	84
Figure 15	Electropherograms of RT-RiboSyn products taken from reactor with HPO system activated sludge at (a) zero minutes and (b) 28 minutes using the Eub338 primer.	86
Figure 16	RT&PE fragment analysis for RNA from pure culture of <i>M. barkeri</i> generated with the Arch915 primer.	89
Figure 17	Example of how to estimate 16S and pre16S rRNA fragment lengths.	91
Figure 18	RT&PE fragment analysis for anaerobic digester sludge at t=4 hours using the Arch915 primer.	94
Figure 19	RT&PE fragment analysis for anaerobic digester sludge at t=24 hours using the Arch915 primer.	95
Figure 20	RT&PE fragment analysis for sludge at t=24 hours using the Eub338 primer.	99
Figure B1	Dotting sample(s) on slide well(s)	134
Figure B2	Placing sample slide and folded Kimwipe in hybridization chamber	135
Figure C1	Electropherogram of RT-RiboSyn products derived from <i>A. calcoaceticus</i> incubated in nutrient broth at 25 °C after exposure to chloramphenicol for zero minutes.	140
Figure C2	Electropherogram of RT-RiboSyn products derived from <i>A. calcoaceticus</i> incubated in nutrient broth at 25 °C after exposure to chloramphenicol for twenty minutes.	141
Figure D1	16S peak height vs. dilution factor from CEQ fragment analysis	146

Figure D2	Pre16S peak height vs. dilution factor from CEQ fragment analysis	146
Figure D3	16S peak height vs. total fragment mass	147
Figure D4	Pre16S peak height vs. total fragment mass	147

## ABSTRACT

A simple anaerobic digestion model has been developed for a continuously-stirred tank reactor (CSTR), which links the specific biogas production rate to the food/microorganism ratio (F/M). The model treats the various microbial populations involved in the sequential biological processes involved in anaerobic digestion as a composite and links the entire biomass specific growth rate directly to the specific biogas production rate. The model was calibrated by determining the specific gas production rate for a range of F/M values using a municipal wastewater seed sludge. The model predictions for steady-state biogas production rates were compared to observed biogas production and volatile solids destruction results from three laboratory-scale anaerobic digesters that were operated at hydraulic retention times of 10, 15, and 20 days. The F/M model results were shown to agree with reactor biogas output for 10, 15, and 20 day hydraulic retention times to within 5.0%, 14.3%, and 9.5%, respectively. A commercial wastewater treatment plant model, BioWin 3, was also used to model anaerobic digestion as a comparison. Agreement for the BioWin 3 model results, as compared to the 10, 15, and 20-day hydraulic retention time reactors, was within 66.2%, 114.1%, and 105.1%, respectively. In all cases the BioWin 3 model over-predicted biogas output as compared to the reactors.

A molecular biology method called RT-RiboSyn was developed to measure the specific growth rate of microbial populations. RT-RiboSyn, is an *ex situ* method that

utilizes a reverse transcription and primer extension (RT&PE) method to analyze the rRNA extracted from a time series of samples treated with chloramphenicol. The method measures the rate of ribosome synthesis over time through the increase in precursor 16S rRNA (pre16S rRNA) relative to the mature 16S rRNA (16S rRNA). A single fluorescently labeled primer that targets an interior region of both pre16S and 16S rRNA for a distinct population is used to generate two pools of reverse transcription product. The ratio of pre16S and 16S rRNA is then determined by separating these pools by length using capillary electrophoresis, and measuring the fluorescent intensity of each pool of fragments.

Results from three different log growth cultures of *Acinetobacter calcoaceticus* indicate that RT-RiboSyn, as compared to spectrophotometer readings, was able to predict specific growth rates within -3.1% to 10% and -3.3% to 21.0% when using a primer targeting Eubacteria and *Acinetobacter*, respectively. The RT-RiboSyn results from a stationary phase culture predicted no growth and possible 16S rRNA degradation.

Further work was completed to determine whether the RiboSyn method would successfully measure growth rates of specific microbial populations in environmental samples. The first of these was activated sludge from a high-purity oxygen system in a wastewater treatment facility located in Tampa, Florida. The organism targeted was the *Acinetobacter* genus, which was shown to be prevalent via fluorescence *in situ* hybridization results. RT-RiboSyn results indicated that growth was not measureable for the *Acinetobacter* present in the system; however, since the sludge was taken at the end of the process, *Acinetobacter* may have been in stationary phase when the samples were collected.

Attempts were made to apply the method to methanogens in both pure culture and anaerobic digester sludge samples. An analysis of samples of RNA from *Methanosarcina barkeri* indicated that the presence of 16S rRNA could be measured; however, capillary electrophoresis instrument limitations prevented the detection of pre16S rRNA fragments. Additional testing of anaerobic digester sludge for both bacterial and Archaeal population was successful for detecting 16S rRNA and possibly precursor 16S rRNA fragments of a variety of lengths. However, specific growth rates could not be determined for the Archaea present in these samples, either due to capillary electrophoresis limitations or very slow growth rates. The results show that the RT-RiboSyn method is applicable to pure cultures; however, a modification of the method is needed to overcome the limitations apparent in populations with low specific growth rates.

## **CHAPTER 1: INTRODUCTION**

Anaerobic digestion is a commonly used process for the treatment of wastes to minimize their effect on the environment. Other than stabilized solids, one useful byproduct is methane gas which can be used for energy production. In industrialized countries, anaerobic digestion is commonly used for the treatment of municipal sludges and industrial wastewater. This extends from large wastewater treatment facilities treating millions of gallons of wastewater per day, to swine lagoons for treating animal wastes, to septic tanks in rural areas not serviced by municipal sewage lines. Anaerobic digestion processes are an important step in preventing environmental problems inherent to the release of unstabilized sludges or raw wastewater.

Engineers seek to understand and improve upon engineered processes, and anaerobic digestion is no exception. There have been many anaerobic digestion models created in past decades to aid in this effort, some of which will be described later. These models range in their applicability from specific to broad in their treatment of anaerobic digestion processes. While these models are designed well and have found use in research and commercial modeling software, a model for a variety of anaerobic digestion processes that is simple and easy to use would be beneficial.

In addition to a simpler model, the use of molecular biology methods could prove helpful to the understanding of anaerobic digestion processes. The ability to determine the specific growth rate of microbial populations in their environment without needing to

isolate them under laboratory conditions would aid in this goal. Such a method would allow for the measurement of specific growth rates under a variety of conditions. These growth rates would be useful in making anaerobic digestion models more accurate.

The following hypotheses were formulated during this investigation:

- A simple anaerobic digestion model based upon the food to microorganism ratio can be created to encompass the important kinetic parameters of the anaerobic digestion process without specifically knowing the values of each parameter.
- The model may be calibrated quickly around the specific feed source(s) and sludge type of interest, and can give accurate predictions of biogas production.
- The measurement of the specific rate of ribosome synthesis can be used to determine the specific growth rate of a microbial population.
- Since the current method to determine the specific growth rate of a microbial population entails measuring the optical density of a pure culture in log growth phase with a spectrophotometer, comparing the rate of specific ribosome synthesis to this method may allow for a molecular biology method as an alternative to the spectrophotometric method.
- As determining the rate of ribosome synthesis requires the use of molecular biology methods and oligonucleotide primers specific to the organisms of interest, it may be possible to determine the specific growth rate of a distinct population in a mixed environmental sample.

The approach to answering these questions entailed several experiments. A series of laboratory-scale anaerobic digesters was operated for a lengthy period of time with daily volumetric measurements of biogas production. These digesters were seeded with municipal anaerobic digester sludge and fed with a blend of wastewaters from the same municipal treatment plant. A series of anaerobic digestion batch reactors were operated at a series of increasing food to microorganism ratios based upon the volatile solids content of two feed streams and digester seed sludge. The biogas output from each reactor was linked to the biomass present in each reactor, and the resulting data was used to calibrate a simple F/M-based anaerobic digestion model. A commercially-available anaerobic digestion model was also used to predict biogas output from the F/M model.

A molecular biology method was created to measure the specific rate of ribosome synthesis as an analog to the specific growth rate of microbial populations. The method was verified against spectrophotometric growth rate measurements with a pure culture of bacteria. The method was then used to attempt to measure the specific growth rate of distinct populations within wastewater samples.

## **CHAPTER 2: DEVELOPMENT OF A SIMPLE F/M-BASED ANAEROBIC DIGESTION MODEL FOR CONTINUOUSLY-STIRRED TANK REACTORS**

### **2.1 Introduction to Wastewater Treatment**

The modern wastewater treatment plant (WWTP) has become a standard urban fixture, and has greatly reduced the impact of human waste on the environment. This is accomplished by removing most of the oxygen demand caused by chemical and organic wastes in the wastewater prior to its return to the environment. While there is a great deal of variety in processes and equipment used at WWTPs, the basic processes are common to most large plants. A typical process flow at a WWTP is shown in Figure 1, starting with 1.) wastewater generated by homes and industry that is pumped via the wastewater system to the WWTP. Once it has arrived at the plant, the waste water goes through a 2.) grinder and bar screen to catch any large debris, followed by a grit chamber to allow for any pebbles/grit to settle out of the wastewater. Following this settling, 3.) the primary settling tank, or clarifier, allows for the separation of solid and liquid wastes. The liquid wastes, which are rich in dissolved organic carbon and ammonia, are 4.) sent into the aeration basin where the wastewater is aerated to allow for the bacterial oxidation of organic matter and nitrification of the ammonia. In facilities with Biological Nitrogen Removal (BNR), denitrification converts the nitrate to nitrogen gas which is accomplished in either a separate reactor or by reconfiguring and altering redox conditions in the aeration basin. Once completed, the 5.) wastewater is allowed to settle

in a secondary clarifier where biomass generated from the breakdown of the wastes in the aeration basin is allowed to settle out of the liquid. A portion of this activated sludge is recycled back to the aeration basin, and is called return activated sludge (RAS). The rest of the settled sludge is wasted to the anaerobic digesters and is called waste-activated sludge (WAS). The clarified water from the secondary clarifier is sent to a 6.) chlorine contact chamber and/or an ultraviolet light disinfection process. This water can then be released to the environment, often to other waterways, or used as reclamation water. The settled sludge from the secondary clarifier is thickened 7.) by using a gravity settling to thicken the solids prior to their pumping to the anaerobic digesters along with the 3.) settled waste solids from the primary clarifier. The anaerobic digestion process 8.) is used to stabilize the solid wastes to render them safe for disposal or use as a soil amendment. A byproduct of this process is biogas, which is a mixture of methane and carbon dioxide that can be flared off to the environment, or used as a fuel source to offset electrical costs for the treatment process. Once the digestion is complete, the solids are dewatered 9.) and allowed to dry so that it can be sent to a landfill, or possibly used for 10.) land application as a soil amendment.

## **2.2 Anaerobic Digestion**

Anaerobic digestion is used as a means of stabilizing wastes for release to the environment, as well as generating a source of energy from methane gas. It is common practice to use methane emissions from wastewater treatment plants and landfills to produce energy to offset energy costs for these facilities. Besides the common use of stabilizing sewage wastes, anaerobic digestion is also used for treatment of industrial

wastes such as from wineries and distilleries (Moletta, 2005), paper production, and slaughterhouses (Rajeshwari *et al.*, 2000).

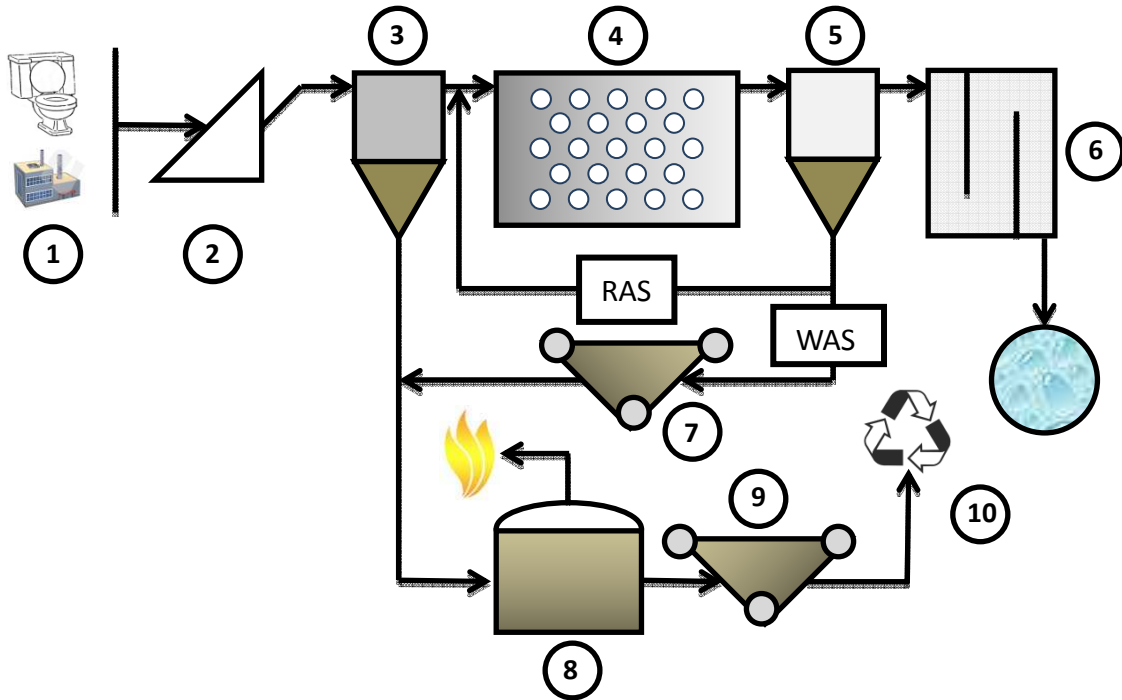


**Figure 1.** Simplified process schematic of a typical large wastewater treatment plant: 1.) wastewater generation, 2.) grinder and bar screen to remove large debris, 3.) primary settling tank to separate bulk of solid wastes from liquid wastes, 4.) aeration basin with activated sludge for oxidation/nitrification, 5.) secondary clarifier, 6.) chlorine contact chamber, 7.) gravity settling for WAS, 8.) anaerobic digestion, 9.) belt filter press and stabilized solids drying, 10.) landfill disposal or land application.

Anaerobic digestion is also being used on farms for dairy (Ince, 1998) and other livestock (Angelidaki and Ahring, 1993) wastes. Anaerobic digestion is even being used for wastewater streams from multiple sources, such as with municipal wastewater

(Sosnowski *et al.*, 2003). This research is focused on wastewater sewage sludge.

However, the findings could be applied to these various wastewater types.

Anaerobic digestion is a multi-step process by which organic solids are degraded and converted to methane and carbon dioxide, commonly referred to collectively as biogas. The organic solids consist of proteins, carbohydrates, and lipids, which are converted to biogas through three sequential, metabolic stages as shown in Figure 2: a.) hydrolysis and fermentation, b.) volatile fatty acid (VFA) oxidation and c.) biogas formation (Metcalf & Eddy, 2003). The hydrolysis and fermentation stages involve the breakdown of the organic components into short chain VFAs, such as propionate and butyrate. VFA oxidizers break down these VFAs into acetate, hydrogen, and carbon dioxide. Acetogens form acetate from hydrogen and carbon dioxide. During the biogas formation stage, methanogens (acetoclastic and CO<sub>2</sub> reducing) utilize the acetate, hydrogen, and carbon dioxide to form methane. Acetoclastic methanogens split acetate into methane and carbon dioxide.

Methanogens are a group of single-celled life that belong to the domain Archaea, and are noted for their unusual coenzymes (Woese, 1987) that allow for the production of methane. Methanogens are strict anaerobes (Balch *et al.*, 1979), and are commonly found in anaerobic environments such as peat bogs (Hales *et al.*, 1996), marine sediments (Hallam *et al.*, 2003), soil (Leuders *et al.*, 2001), hydrothermal vents (Dhillon, 2005), and mammalian digestive tracts (Garcia *et al.*, 2000). The methane emissions of ruminants (such as cattle, sheep, and deer) represent approximately 15% of the total methane emissions in the atmosphere (Moss, 1993).

Although in widespread use, anaerobic digestion is at times problematic due to fundamental lack of understanding of the growth of the Bacteria and Archaea present in digesters. Specifically, how operating conditions affect the growth of methanogens and syntrophic bacteria in anaerobic digesters is not well understood. Methanogens perform as a hydrogen sink for the hydrogen produced during acidogenesis, and under normal conditions keep the partial pressure of hydrogen very low (Metcalf & Eddy, 2003). This low partial pressure drives the fermentation reaction to produce more oxidized products such as formate and acetate. However, there is a difference in growth rates between acidogens and the slower growing methanogens. If there is a disruption to the hydrogen utilization rates of the methanogens, then VFA buildup can reduce the pH in the digester (Metcalf & Eddy, 2003). This "sour digester" situation will kill or slow the substrate utilization rates of the microbial populations responsible for waste stabilization, and the digestion reactions will slow or stop. Incorporating specific growth rates of organisms responsible for these digestion processes in an anaerobic digestion model would be of benefit in reducing the risk of a sour digester condition, as well as other changes within the reactor.

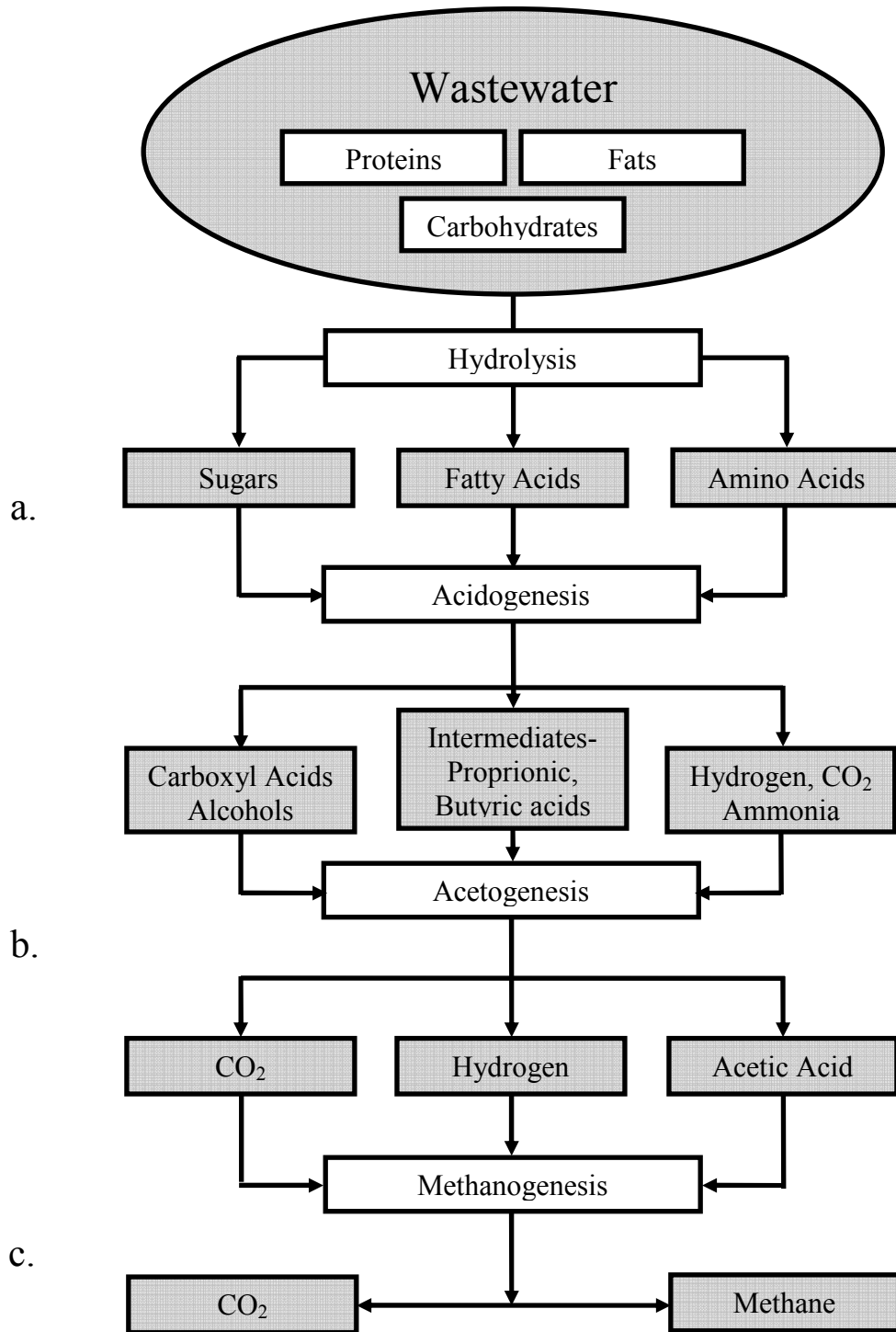


**Figure 2.** Sequential stages in the anaerobic digestion process: a.) Hydrolysis and fermentation, b.) VFA oxidation, and c.) biogas formation

### 2.3 Review of Anaerobic Digestion Models

There are several models available for the simulation of the anaerobic digestion of wastewater solids and sludges. Some of these models focus on a specific component of anaerobic digestion, such as microbial kinetics, while others attempt to encompass the overall digestion process.

Kleerebezem and Stams (1999) discuss the microbial conversions that occur at close to thermodynamic equilibrium, and the consequences of this condition on the kinetics of reactions in anaerobic methanogenesis. The fermentation of butyrate was used as an example. The major thrust of the paper is that, due to the metabolic network stoichiometry, there is a coupling between the  $\Delta G$  based balances in the cell and the transfer of substrates and products in the catabolic and anabolic reactions (Kleerebezem and Stams, 1999). The authors assume in their model that the ATP-consumption and electron translocation are dependent on the cellular concentration ratio of ATP and ADP. This model shows that using Monod-based kinetics to describe these conversions is not feasible, since “substrate conversion and biomass growth are proposed to be uncoupled” (Kleerebezem and Stams, 1999). They propose that this method has advantages over Monod-based equations for describing substrate consumption. There are limitations, however. One such limitation is the assumption that the electrochemical gradient across the cell membranes is constant. Another is the omission of a term accounting for energy used in cell maintenance. Due to the large number of assumptions and uncertainties pertaining to biochemical processes, the model is not very suitable for engineering purposes. Making it so would require simplified descriptions of microbial growth near thermodynamic equilibrium. The authors conclude with the comment that anaerobic

fermentations occur at high rates and for extended periods of time with almost no energy lost in the enzymatic conversions. They propose further research to investigate the high efficiency of these organisms.

Hoh and Cord-Ruwisch (1996) investigated the inhibitory effects of end products in biological systems, and the failure of the Michaelis-Menten model to account for these inhibitory effects. As a result, reaction rates are often overestimated. Correcting this model to account for end product accumulation usually involves incorporating a variety of inhibition factors. However, the authors show that these factors are insufficient for reactions close to thermodynamic equilibrium. In fact, several models investigated violate thermodynamic laws under this condition due to endproduct concentrations. In order to prevent this, the authors use a modified reversible kinetic model. Normally, the large number of empirical parameters needed for a reversible model renders it impractical for use. In this case, the authors simplify the model by using steady-state kinetics and thermodynamic equations to make it practical for bioprocess modeling when close to equilibrium. The model was comparable to the Michaelis-Menten model for highly exergonic reactions, and was correct in its rate predictions when close to equilibrium. The new model also accounted for all substrates and products, and so was able to predict the inhibition effect resulting from multiple end products. The biggest drawback to this model is that the authors assumed that microbial transformation will reach thermodynamic equilibrium. The nature of biological systems dictates that often reactions stop before equilibrium is reached. However, the authors believe that their model could be used as an alternative to the Michaelis-Menten equation to improve existing complex models.

Sanders *et al.* (2000) focused primarily on particle size and how it pertains to gas production rate in anaerobic digestion. The authors described a Surface Based Kinetics (SBK) model for the surface related hydrolysis kinetics of particulate substrates, using a mathematical description of the kinetics with spherical particles. Experiments were performed with starch substrates, obtained by blending fresh potatoes with distilled water, and then sieving the mixture through two sieves (125 and 45  $\mu\text{m}$ ) to divide the feed into two fractions of different particle sizes. A third particle size was obtained from a vendor (Merck). Each group of particles was digested in anaerobic digesters (30° C) with batch experiments. Hydrolysis was monitored via VFA and glucose analyses. At the end of the experiment, it was found that the gas production rate is inversely proportional to the particle diameter. The authors conclude that the hydrolysis rate is directly related to the substrate surface area available. However, they also state that particle breaking should increase the available surface area and thus increase the hydrolysis rate. Their experiment showed that the hydrolysis rate decreased with prolonged digestion time, and therefore the surface area available for hydrolysis must not equal the total surface area available. They conclude the fine particles that are formed may not be totally available for hydrolysis. Although the SBK model is limited to spherical particles, it accounts for surface area whereas the empirical first order model does not. The authors state that  $k_h$  values (first order hydrolysis constants) taken from literature are not applicable for anaerobic digester designs for complex substrates unless the substrate composition and particle size distribution are both taken into account.

Valentini *et al.* (1997) sought to develop a reliable model for the anaerobic hydrolysis of wastewater with high suspended solids content. Four kinetic equations were combined

(Michaelis-Menten, Biomass first order, Substrate first order, and Biomass half order) to develop a new general equation that allows for more accurate modeling of hydrolysis. A series of batch reactor tests were completed for model verification (stirred, 35° C) with a substrate of cellulose particles of known diameter distribution (3-90  $\mu\text{m}$ ). It was assumed that particles would degrade into smaller ones. The data from the experiments were fitted by adjusting the degradation kinetics coefficients to yield equations that contain an “A” parameter (between 0 and 1) and the particle diameter. The “A” parameter optimal average value for their experiments was 0.42. The model essentially describes the degradation kinetics of a given substrate under given conditions. The physical meaning relates the increase in biomass concentration to the limited availability of substrate surface, and is less than linearly proportional. The authors concluded that the “A” parameter is likely related to the biodegradability of the substrate in question. For kinetic studies, it is suggested that an appropriate “A” value is determined first.

Wastewater treatment modeling is not always targeting municipal treatment methods, but can address wastewater generated by the food production industry. Batstone *et al.* (1997) presented a kinetic model based on the anaerobic digestion of pig slaughterhouse wastewater, where high rate degradation is difficult due to the presence of particulates and fats. The authors expand upon an earlier carbohydrate degradation model (Costello *et al.*, 1991 expanded by Ramsay *et al.*, 1994 to include protein degradation) to include the degradation of particulates and fats. Particulates can be difficult to digest due to the need for enzymatic degradation before fermentation, and fats can coat substrate granules and decrease solute transport. In addition, particulate substrate can entrap biomass and cause washout. These problems are addressed with a dynamic model that can help with the

design and operation of anaerobic digesters for complex wastewater. The model was validated via a sampling program with a two-stage anaerobic treatment plant (1200 m<sup>3</sup>/day). The first stage was an equalization/acidification plant, and the second a fixed volume hybrid reactor. Variations in influent flow and concentration were used to monitor plant performance. Three primary substrates consisted of soluble and insoluble fats, proteins, and carbohydrates. Using the simulation package NIMBUS™ (Newell and Cameron, 1991), the authors created a model that allowed for a flexible structure. A series of measurements were rated for ability to quantify the ability of the model to simulate the experimental data. These were (in order of importance): reactor biogas, reactor feed acids (acetic, propionic, butyric, and valeric), and equalization pH. After tuning the model, it was found that an average fit of 77% of the data could be achieved. The model also showed that the VFA concentrations were the most important component for the equalization tank since they are better indicators of influent overload. The model also under-simulated gas flows when substrate loading was low. The authors recommend verifying the model on similar digester plants; however, they maintain that the model is well suited for design and optimization of plants for protein and fat based wastewater.

Vavilin and Lokshina (1996) created a model to analyze VFA degradation kinetics in order to help create a new version of the generalized <METHANE> model, which was described earlier in another paper (Vasiliev *et al.*, 1993). The authors maintain that a series of papers has shown that the sub-processes of anaerobic digestion (except for hydrolysis) are adequately modeled by Monod kinetics. However, a variety of measured values for Monod kinetic coefficients for VFA degradation in mixed cultures has led the authors to use Haldane kinetics in a subprogram for the general model. Both the Monod

and Haldane kinetics models were tested against experimental data from previous work (Noike *et al.*, 1985), where continuous-flow reactors were operated under a variety of acetate-loading conditions. It was found that the model failed under high influent concentrations of acetate due to the inhibition effects on both types of kinetics model. In addition, the model failed to simulate the effluent acetate concentration, and a correction was needed. The correction involved the addition of changeable half-saturation coefficients to the Monod and Haldane functions.

Batstone *et al.* (2000a ; 2000b) created a model that is capable of simulating the degradation of complex wastewater containing significant levels of proteins, fats, or particulates. High-rate anaerobic digestion of these waste streams is desirable due to the economic and environmental reasons; however, the lack of understanding of the degradation mechanisms prevents widespread utilization of the process for these ends. A set of equations for liquid phase, gas phase, physico-chemical reactions, and biological activity are used. There are ten generic biological and three enzymatic groups using different kinetic parameters to calculate degradation rates of various substrates. The rates are dependent on substrate and biomass concentrations as well as pH and hydrogen inhibition. Enzyme production rates are dependent on growth rates of the various bacteria groups. The pH is determined by the physico-chemical reactions, which also determine the gas-liquid transfer of carbon dioxide and the associated carbonate species. The biological equations use Monod equations modified with hydrogen and pH inhibition.

Protein degradation is assumed to be controlled by coupled Strickland reactions, while fatty acid fermentation occurs through  $\beta$ -oxidation. Bacterial inhibition due to long chain fatty acids (LCFA) is not included in the model. Yield is assumed to be 10g per mole of

ATP generated, and the bacterial decay rate is dictated by first order kinetics. Other assumptions for the model include: reactor is a homogeneously mixed continuously-stirred tank reactor (CSTR), gas phases are ideal, residence times for all types of substrate are equal, biological rather than diffusion reaction rates are limiting, temperature effect on association constants are ignored, and some strong acids and bases are not included. Also of note is the set of parameters that describe a group of species instead of a single species in each bacterial group. The model was developed to be very flexible and applicable to a variety of reactors and waste streams with minimal changes to the biological kinetic parameters. However, the model is limited to a liquid environment.

The second part of this paper details the use of slaughterhouse effluent to estimate parameters and validate the model. The reactor in this case is a two-stage hybrid upflow anaerobic reactor that was close to a CSTR hydraulic condition. Data from the operation of the reactor without recycle were used for parameter estimation.

The model allows for the influent to be split into the components of particulate/soluble fats, proteins, and carbohydrates. Analyses of the influent were performed to determine these concentrations, as well as VFA content and pH. A tracer study was also performed to determine the hydraulic retention time of the reactor vessel. A variety of measurements were required for parameter estimation including, soluble nitrogen and chemical oxygen demand (COD) for protein and fat hydrolysis, effluent ammonia for amino acid degradation, and reactor pH.

After parameter estimation was completed, model simulations revealed that particulate matter accumulated in the reactor. This caused problems with overloading in the long term. In addition, due to discrepancies in organic acid concentrations and soluble COD in

the final experimental data set, the model simulations indicated that gas output was diminished. The authors concluded that some of the organic acids were adsorbing onto the surface of the biomass. This led to poor model performance because of an over-prediction of the VFA concentrations in the acidification reactor when recycle was included.

The limitations of this model are minor. It currently does not include any mechanism for inhibition caused by LCFA or sulfide. However, the flexibility of the model will allow their inclusion. The strength of this model is that it could be used for practical or theoretical applications. It appears to be especially useful for predicting the formation of intermediates during protein degradation.

In 1997, a modeling task group was formed at the 8<sup>th</sup> World Congress on Anaerobic Digestion with the goal of developing a general model of anaerobic digestion (IWA Anaerobic Digestion Modeling Task Group, 2002). Although there were many specific models available to the industry, very few were used for practical applications. The group aimed to develop a model that included several desired outcomes:

- Increased model usage for plant design, optimization, and operation
- Further development and validation studies to allow for model implementation in full-scale plants
- A common basis for further model development
- Assist transfer of technology from research to industry

In the end, the group desired to create a model that was a “standard” from which operators and researchers could speak a common language to improve anaerobic digestion.

This model, which the IWA called Anaerobic Digestion Model No. 1 (ADM1), combined the work of several of the authors earlier efforts in anaerobic digestion modeling. It combines biochemical and physico-chemical processes, as well as the degradation of particulates to carbohydrates, lipids, and proteins. As these components are hydrolyzed to sugars, amino acids, and LCFAs, and then follow steps for acidogenesis and acetogenesis. The model then follows the reaction steps as described in the introduction of this paper. All told, the model uses twenty-six dynamic state concentration variables, and eight implicit algebraic variables per reactor vessel or element.

There are three overall biological steps used in ADM1: acidogenesis, acetogenesis, and methanogenesis, as well as extracellular disintegration and hydrolysis steps. Hydrolysis in ADM1 is modeled using first order kinetics. For all intracellular biochemical processes, substrate uptake is modeled with Monod-type kinetics. Biomass death is modeled with first order kinetics, and dead biomass is maintained in the system as particulate material of composite composition. The ADM1 model also takes the following inhibition functions into account: pH, hydrogen, and free ammonia. The model also uses physico-chemical reactions to account for any reactions not driven biologically. These include liquid-liquid and gas-liquid reactions, as well as liquid-solid transformations. The model does not include precipitation reactions. The three primary gas components are carbon dioxide, methane, and hydrogen. Reaction kinetics for the

model differs by process. The hydrolysis reactions are based on first order kinetics. Acidogenesis is governed by Strickland reactions. Fatty acid degradation is determined by  $\beta$ -oxidation.

The ADM1 model has a few limitations that could hinder its use in practical applications. Modeling the liquid phase physico-chemical processes requires a differential equation solver for the mass balance equation. There are a lot of kinetic rate equations that require extensive investigation into the biological process in question. For use in practice, the user would need to understand the kinetic parameters for the various bacterial groups present in the reactor. This is not always practical at the plant level. ADM1 probably lends itself better to research and development for this reason. However, it is still a powerful tool that promises to spawn many improvements in anaerobic digestion process development. The ADM1 model has been incorporated into water modeling software packages such as WEST (Worldwide Engine for Simulation, Training, and Automation, HEMMIS software, Belgium) and GPS-X (General Purpose Simulator, Hydromantis, Canada), which will broaden the use of ADM1 among wastewater industry professionals.

Vavilin *et al.* (2003) developed a model for the anaerobic degradation of municipal solid waste in a 1-D bioreactor. The model includes pH adjustment and leachate recirculation, and was developed to analyze the balance between polymer hydrolysis/acidogenesis and methanogenesis. The model was validated with previously published experimental data (Vasiliev *et al.*, 1993).

The model is structured such that the rate-limiting steps are hydrolysis and methanogenesis processes. To simplify the model, all of the transformation processes

converting VFAs to methane are made into a single step in the model. Five parabolic partial differential equations were used to model various concentrations of substrate in the reactor (solid waste, total VFA, methanogenic biomass, and sodium) as well as the methane production rate.

The model shows that methane production increases with specific liquid (leachate) flow rate, and did not occur at all at zero recirculation rate. The higher flow rate homogenizes the liquid phase and helps to prevent inhibition in the biological reactions. Further modeling and comparison to published data showed that an initial period of non-mixing followed by an increase in mixing intensity is beneficial to methanogenesis. Overall, the authors conclude that degradation time can be reduced if a balance between hydrolysis and methanogenesis rates is reached. Conditions favorable to methanogenesis are important in the early stage, followed by favorable conditions for hydrolysis in the later stages. The reason for this is because of the reduced accumulation of VFAs allows for hydrolysis/acidogenesis to proceed. The authors conclude that waste degradation and methane production are improved when inhibitory factors are prevented early on in the process by increasing the flow rate of leachate throughout the reactor.

Vavilin *et al.* (2004) demonstrated that a high concentration of food waste in bioreactors can lead to inhibition of biodegradation due to a buildup of VFAs in the absence of methanogenic populations. They suggest the addition of lean solid waste (non-food) waste to provide sites for methanogens to be protected from rapid acidogenesis. Combined with leachate recirculation, good rates of biodegradation can be achieved.

The authors combine the previous surface-related kinetics model (Vavilin *et al.*, 1996), along with the distributed model of solid waste anaerobic digestion (Vavilin *et al.*,

2003) for an overall improved model. The surface-related model paper showed that the Contois model (uses a single parameter to demonstrate the saturation of both biomass and substrate) is just as good at fitting the data as the surface-related model. The basic distributed model uses five parabolic partial differential equations as described previously (Vavilin *et al.*, 2003). Both grey and food waste degradation were modeled.

The data from grey waste degradation were fitted better by the Contois than first-order kinetics. For the degradation of a mixture of rich (food) and lean wastes, a distributed model with different hydrolysis rates was developed. It was shown that an initial separation between food waste and inoculum in the reactor enhanced methane production if the VFAs diffusing into the methanogenic areas were consumed efficiently. For those areas in the reactor where biomass concentration was initially low and VFA diffusion took place, methanogenesis was inhibited. By refraining from mixing early in the degradation process, the inhibition can be avoided by allowing these low biomass concentration areas to begin methanogenesis properly. This model should provide adequate performance simulations of high-solids landfill bioreactors with leachate recycling.

Parker (2005) examined the application of the ADM1 model to investigate several advanced anaerobic digestion configurations. To do so, the model is applied to a variety of existing data sets to test the predictive accuracy of ADM1 for this variety of anaerobic digestion configurations. All of the data sets selected had used actual sludges from municipal wastewater treatment plants. The large number of coefficients and constants used by the ADM1 model prevented exact calibration of the model with the selected data sets, so whenever needed the recommended model parameters were used. The data sets

represented several digestion configurations, including: single-stage mesophilic digestion, acid phase digestion, temperature-phased anaerobic digestion, and two-phase digestion.

For the single-stage digestion, the ADM1 model over predicted the acetate concentration at low SRTs, while under predicting the concentrations of the VFAs propionate, valerate, and butyrate. ADM1 also predicted a 40% decrease in aceticlastic methanogenesis at the lower SRTs due to increased concentrations of ammonia. Along with incorrect assumptions of feed composition, this assumption about the methanogens may have caused this predictive disparity.

The acid phase data set, when modeled with ADM1, showed under predictions of organic acid concentrations at lower SRTs, and over predictions of the same at higher SRTs. The originators of the data set observed methane production from the sludge at higher SRTs, while ADM1 predicted no appreciable methane production. This could be due to methanogens actually being less sensitive to pH than the pH inhibition functions in the model predict.

The temperature-phased anaerobic digestion (TPAD) data set showed mostly steady methane production and VFA concentrations at all SRTs tested. The ADM1 model increasingly over predicted both methane production and VFA concentrations as SRT decreased. The authors suggested that the reason for the inconsistencies may be found in the biokinetic coefficients for temperature employed by ADM1. As suggested in the ADM1 paper, a constant correction factor should be used for all microbial species present, which would predict increased VFA accumulation at higher temperatures.

For the two-stage anaerobic digestion data set, two SRTs were examined (3 and 7 days) for a two stage mesophilic reactor. The model under predicted VFA concentration, pH, and ammonia concentration for the 3 day SRT, and over predicted these parameters for the 7 day SRT. However, with the exception of the VFA concentration, the predictions were close to the experimental results for the 7 day SRT reactor. It should be noted that the reported ranges for experimental results were wide, so a rigorous evaluation of the model in this instance is challenging.

The paper provides an evaluation of the ADM1 model with a variety of data sets from experimental reactor operations, and has shown some predictive inconsistencies between the model and experimental results. However, the use of suggested values for many of the coefficients and constants used by the model may be a source for many of these errors. As seen with the TPAD data, treating all microbial species the same with regards to biokinetic constants may lend more inaccuracies to the ADM1 model.

A different approach uses an Adaptive Neuro-fuzzy interference system (ANFIS) model, which is based on linguistic uncertain expressions rather than numerical statistical or probabilistic methods (Cakmakci, 2007). The model was applied to primary settled sludge from the Kayseri municipal WWTP in Turkey, which services a population of approximately 700,000. The ANFIS model is used to predict volatile solid (VS) concentration in the effluent and methane production. The independent input parameters taken from the Kayseri data were pH, VS concentration, pre-thickened sludge flow rate, and temperature. This predicted VS concentration is then used to predict methane production. The results of the model indicated good agreement between predicted and actual VS effluent concentration and methane production. It was found that all four

independent input parameters were required to get good agreement between predicted and actual effluent VS concentration. Accurate predictions of effluent VS concentration then allowed for accurate predictions of methane production. What is remarkable about this model is that accurate predictions of the effluent VS concentration and methane production can be made without defining all of the complex reactions inherent to anaerobic digestion. The author noted that the highly nonlinear structure of the ANFIS model is what allows for the easy modeling of a complex system such as anaerobic digestion. The approach is a novel one as compared to traditional models.

## **2.4 Model Review Conclusions**

A lot of time and effort have gone into developing and testing models to better understand the behavior of anaerobic digestion processes. Many of the early models addressed very specific portions of the process, such as hydrolysis or fermentation. Later models addressed the digestion of specific and often difficult to digest substrates, such as particulate matter or fats. Variables such as surface area available for digestion were included in these models. Other models were created for waste streams other than sewage sludge. ADM1 was created to tie together a large number of models and their contributions so that “one big model” could be available for research and operation efforts. Later models, such as ANFIS, take a different modeling approach altogether to avoid the complexity of the reactions inherent to anaerobic digestion.

Clearly, as computing advances make complex calculations more efficient, the depth and power of these models is increasing. Using them to test new reactor designs and

processes prior to actual construction should make for better designs and shorter startup times. However, it is important to develop models for people other than researchers. A lot of the models published in scientific and engineering journals are simply too complex and unwieldy for average plant manager and operator. A simple anaerobic digestion model that requires a short list of process inputs might be a welcome tool for wastewater treatment plant personnel and others.

## **2.5 Model Development**

### **2.5.1 Model Concept**

While there are many anaerobic digestion models available, one concern is that many of these models are quite complex and may be difficult to calibrate. Some of the models are very specific in their application, and some attempt to be as encompassing of anaerobic digestion as possible. Both approaches are worthy goals, and find their applicability in a variety of anaerobic digestion processes. However, these models might have difficulty with rapidly changing conditions in a reactor. Should the feed stream(s) change quickly, or sludge condition be altered, a model could quickly become unreliable as a method of process analysis. The more complex the model, the more demand exists for accurate measurement of parameters. If conditions change quickly, so might the parameters upon which a model is based.

Must a model be complex in order to accurately capture reactor performance? Complex analysis is often a more suitable activity for researchers than for process operators and engineers. In the business of wastewater treatment, decisions sometimes

need to be made quickly. Suppose a situation demands changing the ratio of PS to WAS being fed into an anaerobic digester and a decision must be made quickly. Or perhaps a new feed type needs to be introduced, such as a high-fat or high-fiber feed type. Perhaps a load of toxic material has been released upstream and it is necessary to determine possible effects on the digester operation. Is it possible to create a model that is simple to operate and set-up according to changing conditions, and yet require fewer explicit parameters?

Designing a simple model that uses fewer inputs requires determining those inputs that are most important during the operation of an anaerobic digester. In the interest of simplicity, the model was designed to use feed inputs, microbial growth, and biogas output, which were considered to be the variables that have the most impact on an anaerobic digestion process.

During early bench-scale reactor work, a hypothesis was tested that led to the development of this model. When combining wastewater with anaerobic digester sludge at increasing ratios of food (wastewater) to microorganisms (digester sludge) in small reactors, the biogas output was found to increase on a per-gram of biomass basis. In other words, it appeared that when the biomass was exposed to greater concentrations of usable substrate per unit of biomass, the organisms were creating more biogas per gram of microorganisms. It became apparent that the food to microorganism ratio (F/M) could be an important consideration in anaerobic digestion modeling.

As discussed previously, the purpose of anaerobic digestion is to remove the oxygen demand from wastes prior to their release to the environment. This is accomplished via

the microbial consumption of the constituent substrates of the wastewater. Earlier work by Monod describes the expressions for this behavior (Monod, 1942, 1949):

$$r_{su} = - \frac{kXS}{K_S + S} \quad (1)$$

where  $r_{su}$  is the rate of change in substrate concentration from utilization ( $\text{g/m}^3 \cdot \text{day}$ ),  $k$  is the maximum substrate utilization rate ( $\text{g substrate /g of organisms} \cdot \text{day}$ ),  $X$  is the biomass concentration ( $\text{g/m}^3$ ),  $S$  is the growth-limiting substrate concentration ( $\text{g/m}^3$ ), and  $K_S$  is the half-velocity constant, substrate concentration at half the maximum specific substrate utilization rate ( $\text{g/m}^3$ ). A variation of this equation can utilize the specific biogas generation rate as the specific substrate utilization rate, and the  $F/M$  as the substrate concentration. This relation can be linearized to generate equations for the wastewater substrate utilization rates of interest:

$$\frac{1}{q} = \frac{K_S}{q_{max}} \left( \frac{1}{S} \right) + \frac{1}{q_{max}} \quad (2)$$

where  $q$  is the specific biogas generation rate ( $\text{ml biogas/g biomass} \cdot \text{day}$ ),  $q_{max}$  is the maximum specific biogas generation rate ( $\text{ml biogas/g biomass} \cdot \text{day}$ ),  $K_S$  is substrate concentration at half of  $q_{max}$  ( $\text{g/mL}$ ), and  $S$  is the substrate concentration ( $\text{g/mL}$ ).

A model built on this principle may be used for any food and any sludge source rather than limiting it to domestic wastewater-fed digesters. However, since anaerobic digesters are most commonly used for domestic and municipal wastewater treatment, the initial work done to create a model was focused there. Since continuously-stirred tank reactors

(CSTR) are prevalent in the wastewater treatment industry, an F/M-based model was created for use with CSTRs.

### 2.5.2 Model Nomenclature

The following symbols are used with the model description, and are selected using guidelines previously published (Corominas *et al.*, 2010).

$d$	hydraulic retention time (time, days)
$F_{PS}, F_{WAS}$	degradable fraction of the incoming feed, for PS ( $F_{PS}$ ) and WAS ( $F_{WAS}$ )
$FM_P, FM_W$	food to microorganism ratio, for PS ( $FM_P$ ) and WAS ( $FM_W$ )
$G_{FD}$	volume of biogas per mass of feed destroyed, for PS, WAS, and biomass (mL biogas $g^{-1}$ feed destroyed)
$G_{PS}, G_{WAS}, G_D$	biogas production rate, for PS ( $G_{PS}$ ), WAS ( $G_{WAS}$ ), and biomass decay ( $G_D$ ) (volumetric flow rate, mL $d^{-1}$ )
$G_{TOT}$	total biogas production rate (volumetric flow rate, mL $d^{-1}$ )
$q_P, q_W$	specific biogas generation rate from PS ( $q_P$ ) and WAS ( $q_W$ ), (mL biogas per day per gram of microbial biomass)
$S_{PS}, S_{WAS}$	incoming degradable feed, for PS ( $S_{PS}$ ) and WAS ( $S_{WAS}$ ) (mass, g)
$S_{UP}, S_{UW}$	non-degradable feed, for PS ( $S_{UP}$ ) and WAS ( $S_{UW}$ ) (mass, g)
$S_{TVSP}, S_{TVSW}$	total volatile solid content of incoming feed, primary sludge ( $S_{TVSP}$ ) and WAS ( $S_{TVSW}$ ) (mass, g)
$X_a$	total active microbial biomass (mass, g)
$X_D$	fraction of daily microbial mass lost to decay
$X_G$	newly grown microbial biomass (mass, g)
$X_W$	wasted microbial biomass (mass, g)
$X_{WPS}, X_{WWAS}$	wasted degradable feed, for PS ( $X_{WPS}$ ) and WAS ( $X_{WWAS}$ ) (mass, g)
$X_{WUP}, W_{WUW}$	wasted non-degradable feed, for PS ( $X_{WUP}$ ) and WAS ( $W_{WUW}$ ) (mass, g)
$X_{DP}, X_{DW}$	digested feed, for PS ( $X_{DP}$ ) and WAS ( $X_{DW}$ ) (mass, g)
$Y_P, Y_W$	yield, growth of microbial biomass per gram of primary sludge ( $Y_P$ ) and WAS ( $Y_W$ )

### 2.5.3 The F/M-Based CSTR Model

The Continuously-Stirred Tank Reactor (CSTR) model consists of five distinct components: degradable feed ( $S$ ), non-degradable feed ( $S_U$ ), microbial growth ( $X_G$ ), food

to microorganism ratio (FM), and biogas production (G). Each of these components, with the exception of microbial growth, is divided into primary solids (PS) and waste activated sludge (WAS) streams. Figures 3, 4, and 5 illustrate these processes and how they relate to one another within the model. The symbols used on these three figures were selected as a simple process flowchart of the feed processes based on symbols used in the STELLA modeling program (v. 6.0.1, HPS, Inc., Lebanon, NH), which was used to create the mathematical model. When using the model, the following inputs are used: initial mass of each type of volatile solids (PS and WAS), initial biomass, degradable fraction of each type of solids (PS and WAS), yield, hydraulic retention time (HRT), and the specific biogas production rates for each feed stream (PS and WAS).

Figure 3 shows the process used for digestion and wasting of both primary and waste-activated solids. As feed enters the reactor, it is modeled as degradable and non-degradable solids. The degradable feed is the volatile fraction of the total mass of each feed type entering the reactor as determined by solids testing. The remaining solids are non-degradable.

The equations governing the feed digestion and wasting processes for the degradable and non-degradable feed streams are described below. Equations 3 through 8 are used for the degradable PS and WAS streams, whereas Equations 8 through 11 are for the non-degradable PS and WAS feed streams.

Equation 3 shows that the degradable PS feed stream ( $S_{PS}$ , grams) is the product of the total volatile solids content of the incoming PS feed ( $S_{TVSP}$ , grams) and the degradable fraction of the PS feed ( $F_{PS}$ ):

$$S_{PS} = S_{TVSP} * (F_{PS}) \quad (3)$$

Similarly, the degradable WAS stream ( $S_{WAS}$ , grams) is a product of the total solids content of the incoming WAS feed ( $S_{TVSW}$ , grams) and the degradable fraction of the WAS feed ( $F_{WAS}$ ) as shown in Equation 4:

$$S_{WAS} = S_{TVSW} * (F_{WAS}) \quad (4)$$

The wasted streams are also divided by PS and WAS fractions.

The wasted PS stream ( $X_{WPS}$ , grams per day) is the difference between the incoming PS feed and the digested PS feed ( $X_{DPS}$ , grams), divided by the hydraulic retention time (HRT, days), as shown in Equation 5:

$$X_{WPS} = (S_{PS} - X_{DP})/HRT \quad (5)$$

The wasted stream for the WAS ( $X_{WWAS}$ , grams per day) is calculated in the same way; where the difference between the incoming WAS feed and the digested WAS feed ( $X_{DW}$ , grams) is divided by HRT, as shown in Equation 6:

$$X_{WWAS} = (S_{WAS} - X_{DW})/HRT \quad (6)$$

The remaining degradable feed that is not wasted is used to calculate F/M.

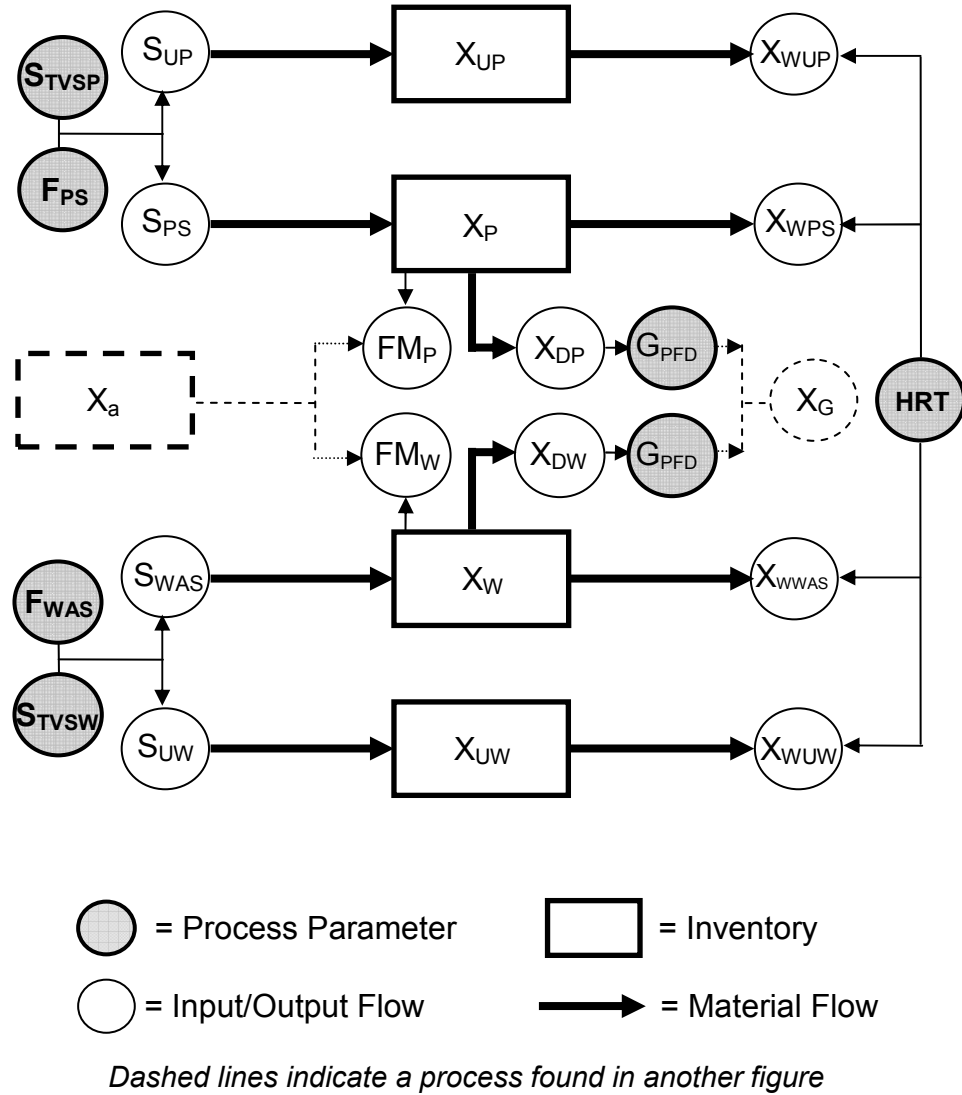


**Figure 3.** Process flowchart of PS and WAS digestion and wasting processes.

The digested feed per each feed type is determined by Equations 7 and 8. Equation 6 shows that digested primary solids ( $X_{DP}$ ) are the quotient of the gas production from the digestion of primary solids ( $G_{PS}$ , mL) and the volume of biogas per mass of feed destroyed ( $G_{FD}$ , mL biogas per gram of feed destroyed) as determined by stoichiometric

calculations (see Appendix A-1) for anaerobic digestion processes (Rittmann and McCarty, 2001):

$$X_{DP} = G_{PS}/G_{FD} \quad (7)$$

Equation 8 shows the same determination of the digested waste-activated solids ( $F_{DW}$ , grams) as the quotient of the gas production from digestion of WAS ( $G_{WAS}$ ) and the  $G_{FD}$ :

$$X_{DW} = G_{WAS}/G_{FD} \quad (8)$$

Non-degradable feed consists of those components, such as inorganic solids and inert solids, which do not factor into the F/M ratio. The non-degradable solids are included in the model so that their buildup can be monitored and used to determine total solids in the reactor, and are governed by Equations 9 through 12. These too are split into PS and WAS streams.

Equation 9 shows the determination of the non-degradable mass of the incoming PS feed stream ( $S_{UP}$ , grams) to be the product of the  $S_{TVSP}$  and the remaining non-degradable fraction of the PS feed stream ( $1 - F_{PS}$ ):

$$S_{UP} = S_{TVSP} * (1 - F_{PS}) \quad (9)$$

Equation 10 is the calculation for the non-degradable mass of the incoming WAS stream ( $F_{UW}$ , grams) is also the product of the  $S_{TVSP}$  and the remaining non-degradable fraction of the WAS feed stream ( $1 - F_{WAS}$ ):

$$S_{UW} = S_{TVSW} * (1 - F_{WAS}) \quad (10)$$

Much the same way as determined for the wasted degradable feed streams, the wasted non-degradable feed streams are split between PS and WAS feed streams. The wasted non-degradable PS stream ( $X_{WUP}$ , grams per day) is the quotient of the incoming non-degradable PS stream ( $S_{UP}$ , grams) and the HRT as shown in Equation 11:

$$X_{WUP} = S_{UP}/HRT \quad (11)$$

Equation 12 shows the calculation for the wasted non-degradable WAS stream ( $W_{NDFW}$ , grams per day) as the quotient of the incoming non-degradable WAS stream ( $F_{INDW}$ , grams) and the HRT:

$$X_{WUW} = S_{UW}/HRT \quad (12)$$

The second major component of the CSTR F/M model deals with the microbial population of the digester sludge. Microbial mass and growth are largely affected by two variables: initial mass of the digester sludge, and the yield (Y). The initial mass is determined by volume and the volatile mass concentration of the digester sludge. Yield

determines the new microbial mass per time step of the HRT. The wasted mass of microbes is also determined by the HRT.

Figure 4 shows a flowchart of the microbial growth, wasting, and decay processes. The microbial biomass density is governed by Equations 12 through 14. New microbial biomass is considered to be the microbial mass grown (grams) as a result of the digestion of the PS and WAS feed streams (grams), and is represented by the yield fractions  $Y_P$  and  $Y_W$ , respectively.

Equation 13 controls the addition of new microbial biomass, and is split into two products representing the digested PS and WAS feed streams:

$$X_G = (Y_P * X_{DP}) + (Y_W * X_{DW}) \quad (13)$$

Equation 14 shows how the wasted biomass ( $X_W$ , grams per day) is determined, and is the quotient of the total active biomass ( $X_a$ , grams) and the HRT:

$$X_W = X_a / \text{HRT} \quad (14)$$

The decay of biomass ( $X_D$ , grams per day) is determined by Equation 15, and is the product of  $X_a$  and the decay rate coefficient ( $K_D$ ,  $\text{day}^{-1}$ ):

$$X_D = X_a * K_D \quad (15)$$

The remaining degradable feed and dynamic mass of microbes in the sludge is used to determine the F/M ratio.

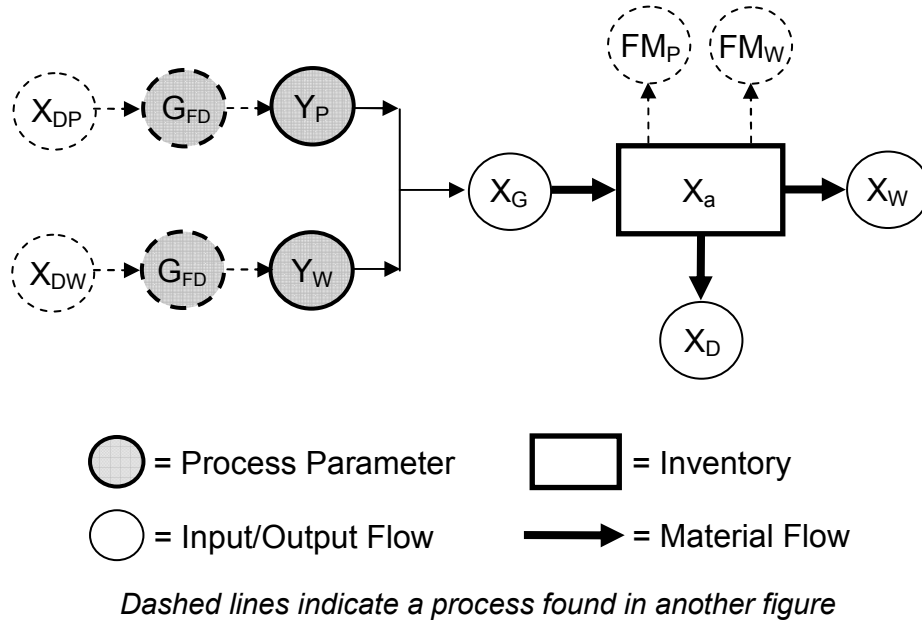


**Figure 4.** Process flowchart of microbial growth, wasting, and decay processes.

Equations 16 and 17 determine the F/M ratios that directly affect the model biogas production via the Specific Biogas Generation tests. Equation 16 calculates the F/M with regards to the PS ( $FM_P$ ), and is the quotient of degradable PS feed stream and the total microbial mass:

$$FM_P = S_{PS}/X_a \quad (16)$$

Equation 17 is used to determine the F/M with regards to the WAS ( $FM_W$ ), and is the quotient of degradable WAS feed stream and total microbial mass:

$$FM_W = S_{WAS}/X_a \quad (17)$$

The remaining process in the model is biogas production process, and a flowchart of this process is shown in Figure 5. The biogas production rate is determined by the F/M ratio in conjunction with the specific biogas generation rates. As the F/M ratio changes during model operation, the biogas production rate changes accordingly.

Biogas production is determined by Equations 18 through 23. As the specific biogas generation for each feed stream is integral to the determination of the volume of biogas produced, these relations for the PS and WAS are represented by Equations 18 and 19, respectively.

Equation 18 is based on Equation 2 and shows the specific biogas generation rate for the PS stream ( $1/q_P$ ), where  $(K_S/q_{max})_P$  is slope of the curve, and  $(1/q_{max})$  is the y-intercept:

$$1/q_P = (K_S/q_{max})_P (1/S) + (1/q_{max}) \quad (18)$$

Equation 19 shows the specific biogas generation rate for the WAS stream ( $1/q_W$ ), where  $(K_S/q_{max})_W$  is slope of the curve, and  $(1/q_{max})$  is the y-intercept:

$$1/q_W = (K_S/q_{max})_W (1/S) + (1/q_{max}) \quad (19)$$

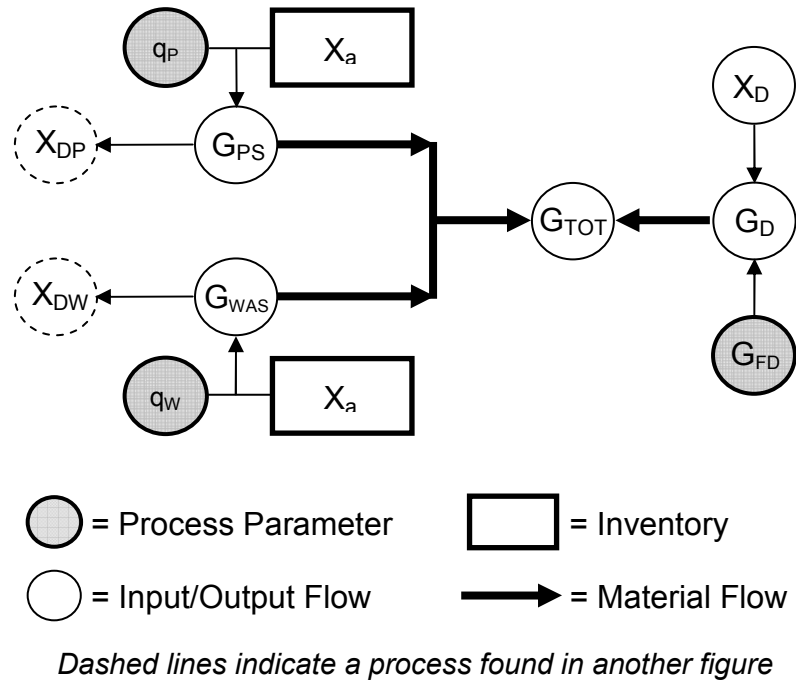


**Figure 5.** Process flowchart of biogas production.

Equation 20 is used to determine the gas production rate from digestion of PS ( $G_{PS}$ , mL biogas per day) using the factors from Equation 18, and is the product of the  $q_P$  (mL biogas per day per gram of microbial biomass) and  $X_a$ :

$$G_{PS} = q_{\max} * (FM_P / K_S + FM_P) * X_a \quad (20)$$

Equation 21 shows how the biogas determination for the digestion of WAS ( $G_{WAS}$ , mL biogas per day) is calculated, and is the product of the  $q_w$  (mL biogas per day per gram of microbial biomass) and  $X_a$ :

$$G_{WAS} = q_{max} * (FM_W/K_S + FM_W) * X_a \quad (21)$$

As decaying microbial biomass lyses to return the interior contents of the cells to the sludge, this new substrate becomes available for biogas production. This is shown in Equation 22, wherein the biogas production due to microbial decay ( $G_D$ , mL biogas per day) is the product of  $G_{FD}$  (mL biogas per gram of feed destroyed) and microbial decay ( $X_D$ , grams):

$$G_D = G_{FD} * X_D \quad (22)$$

Finally, the total daily biogas production rate ( $G_{TOT}$ , mL biogas per day) is shown in Equation 23, and is the sum of  $G_{PS}$ ,  $G_{WAS}$ , and  $G_D$ , or simply the sum of equations 20 through 22:

$$G_{TOT} = G_{PS} + G_{WAS} + G_D \quad (23)$$

This summation is simply used for reporting purposes in the model. The full code for the model from the Stella software package is presented in Appendix A-2.

Figure 6 shows the material flow and mass balance of the model using the name of the parameters given by equations 3 through 23.

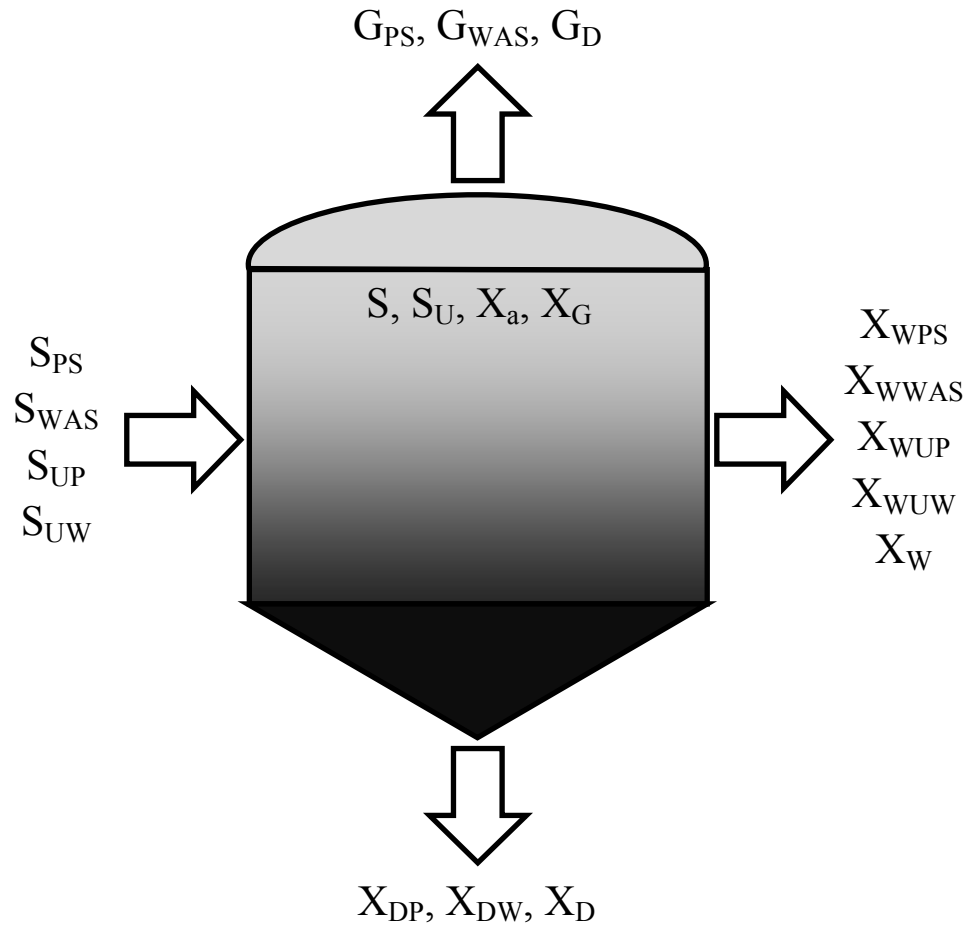


**Figure 6.** Mass balance and material flow of the model reactor.

## **2.6 Methods and Materials**

### **2.6.1 Specific Biogas Generation Test**

The model is flexible in that it incorporates the biogas generation per gram of biomass of the actual sludge of the reactor being modeled. This is accomplished via the determination of the specific biogas generation (SBG) for PS and WAS. This is done by using a series of bench-scale anaerobic digesters that contain mixtures of wastewater and digester sludge at increasing levels of F/M. The F/M ratios in the reactors follow a progression of 1:1, 2:1, 4:1, 8:1, and 16:1 so that a wide range of mixture possibilities is covered. Biomass is determined by measuring volatile solids content of the digester sludge.

Due to the differences in their constituents, specific biogas generation data were determined for both primary sludge (PS) and waste-activated sludge (WAS) independently. Digester sludge and feed wastewater (PS or WAS) were mixed for a range of F/M (1:1, 2:1, 4:1, 8:1, and 16:1) based on volatile solids in sealable 50 mL serum bottles with a working volume of 40 mL. The serum bottles were placed in a shaker-incubator (35°C) for four hours, constantly shaken at 120 rpm. Each bottle was fitted with a butyl rubber stopper and an aluminum cap to allow for syringe needle puncture for biogas volume measurement. The volume of the biogas generated in each serum bottle was measured by water displacement, and was used to determine the specific biogas production rate (Equation 2).

### 2.6.2 Sludge Characterization

Anaerobic digester sludge, primary sludge and waste-activated sludge were collected from the Glendale Street Wastewater Reclamation Plant in Lakeland, FL. The Lakeland facility is a 13.7 MGD wastewater treatment plant with activated sludge and anaerobic digestion processes. In 1987, a 1400 acre artificial wetlands treatment system became the primary discharge point for treated effluent, with a annual average flow to the wetlands of 8 MGD. The anaerobic digestion process is a two-stage process with two 750 thousand gallon tanks, each having a 15-day hydraulic retention time (B. Kruppa, personal communication, October 13<sup>th</sup>, 2011).

At the time of sampling, the Lakeland plant was feeding only primary sludge to the 2-stage mesophilic digester. For the laboratory-scale anaerobic digesters used to verify the model, PS and WAS were blended in a dry solids ratio of 1.79:1 (PS/WAS) to simulate a typical blended feed for anaerobic digestion (Griffin *et al*, 1998). Table 1 shows a summary of the calculated and assumed parameters for the F/M model as applied to the bench scale reactor system used in this study.

**Table 1.** Measured and calculated model parameters for the F/M CSTR model.

	<b>Model Parameter</b>	<b>Type</b>	<b>Value</b>
<b>Measured Parameters</b>	Daily feed blend	Total solids	0.186 g
		Volatile solids	0.157 g
	10-day HRT	PS loading rate	1.22 g VS L-reactor <sup>-1</sup> d <sup>-1</sup>
		WAS loading rate	0.91 g VS L-reactor <sup>-1</sup> d <sup>-1</sup>
	15-day HRT	PS loading rate	0.81 g VS L-reactor <sup>-1</sup> d <sup>-1</sup>
		WAS loading rate	0.61 g VS L-reactor <sup>-1</sup> d <sup>-1</sup>
	20-day HRT	PS loading rate	0.61 g VS L-reactor <sup>-1</sup> d <sup>-1</sup>
WAS loading rate		0.46 g VS L-reactor <sup>-1</sup> d <sup>-1</sup>	
<b>Calculated/Set Parameters</b>	Biomass fraction of inoculum		0.1 (1)
	Biomass decay rate coefficient	R <sub>D</sub>	0.1 d <sup>-1</sup> (2)
	Biogas per gram of feed destroyed	G <sub>FD</sub>	803 mL biogas g <sup>-1</sup> feed destroyed (3)
	Yield (Y)	PS	0.1 d <sup>-1</sup> (4)
	Yield (Y)	WAS	0.1 d <sup>-1</sup> (4)
	Degradable fraction of volatile solids	F <sub>PS</sub> , F <sub>WAS</sub>	0.7, 0.5 (5), (6)
	Model time step		5 minutes
<b>References:</b> (1) Arnaiz <i>et al.</i> (2006) (4) Metcalf and Eddy (2003) (2) Siegrist <i>et al.</i> (2002) (5) Pasztor <i>et al.</i> (2009) (3) Rittmann McCarty (2001) (6) Kabouris <i>et al.</i> (2008)			

### 2.6.3 Laboratory-Scale Anaerobic Digesters

Three laboratory-scale anaerobic digesters were operated with HRTs of 10, 15, and 20 days using anaerobic digester sludge collected from the Glendale Wastewater Reclamation Plant in Lakeland, FL as the inoculum. The operation was semi-continuous, with daily maintenance that included: biogas volume measurement, removal of waste sludge, and the addition of new blended feed. The reactors were operated for a total of 60 days in order to show results for at least three HRT per reactor.

The feed for the reactors consisted of a blend of PS and WAS from the Lakeland plant. After blending, the total solids content was determined to be 2.33% with a volatile solids content of 84.1%. Table 2 shows the results of the total and volatile solids content for the PS and WAS separately, as well as after blending. The feed blend was partitioned into small quantities and frozen at -20°C. Small quantities of this blended sludge were kept thawed for use as a daily feed sludge for the laboratory-scale anaerobic digesters.

The laboratory-scale anaerobic digesters were a series of 50 mL serum bottles with rubber stoppers and aluminum crimp caps. The liquid volume in each bottle was 40 mL, and the remaining headspace was about 10 mL. For ease of daily feeding and wasting, 8 mL of feed blend was fed to each reactor series, which determined the total volume for each reactor series. As a result, the total volumes for the 10, 15, and 20-day HRT reactor series were 80 mL, 120 mL, and 160 mL of digester sludge, respectively. Biogas output is on a per-liter of sludge basis.

**Table 2.** Total and volatile solids concentrations from primary, waste-activated, and blended sludges used for all experimental work.

<b>Sludge Type</b>	<b>TS (%)</b>	<b>VS (% of TS)</b>
PS	3.47	84.5
WAS	1.41	78.7
Blended Feed	2.33	84.1

All reactors were incubated at 35°C and shaken constantly at 120 rpm. Biogas volume was measured directly from each reactor by water displacement.

In order to maintain the HRT, sludge was wasted daily from each reactor and the remaining sludge was mixed with fresh feed. After feeding, the headspace for each reactor was flushed with an anaerobic mixture of gases (20% CO<sub>2</sub>: 80% N<sub>2</sub>). Laboratory-scale reactors were operated for sixty days, to allow for at least three HRTs for each reactor. After sixty days of operation, the solids content of the anaerobic digester sludge was determined (American Public Health Association, 1999).

#### **2.6.4 Analytical Methods**

Total and volatile solids analysis was performed using Method #2540 (American Public Health Association, 1999). The equipment used was a Fisher Scientific 3511 FS drying oven (Fisher Scientific, Hampton, NH), a Thermo Scientific Model 48000 furnace (Thermo Scientific, Waltham, Mass.), and a Denver Instrument APX-60 precision balance (Denver Instrument, Bohemia, NY). Sludge pH was measured using an Oakton pH/°C/Ion/mV meter (Oakton Instruments, Vernon Hills, IL). Biogas volume was measured via a buffered water displacement system.

#### **2.6.5 BioWin 3 Anaerobic Digestion Modeling Software**

The results from the F/M model were compared with a published commercial model. The software chosen was the BioWin 3 model (v. 3.1, EnviroSim Associates, Ltd., Hamilton, Ontario), which is a dynamic full treatment plant model and simulation package with a variety of process modules to allow for a great deal of versatility. In this case, the module used was the anaerobic digestion process module. A simple model was

created using the anaerobic digestion module with split feed streams consisting of PS and WAS.

The digester volume was set to 100 liters due to modeling constraints, and the biogas output reported on a per-liter of digester sludge basis. Feed input was set to the same values as used with the experimental reactors, which in turn determined the model HRT. Temperature was also set to 35° C as was the case for the experimental reactors. The time step for the model was set to 5 minutes. Yield and decay coefficients are broken out by organism type whereas the F/M model treats the microbial biomass as a composite. These values were not changed in the BioWin 3 model, since the rates in the BioWin 3 model included not only methanogens but fermentative bacteria yield rates.

The BioWin 3 anaerobic digestion model uses dozens of parameters to simulate the process, any of which can be modified by the user. As the F/M model was set up for simple operation without having to measure or calculate most of these parameters, the BioWin 3 model was operated with the seed values that are pre-set in the model. These parameters were input from a variety of published sources by EnviroSim Associates. EnviroSim has noted that the ADM1 model (IWA Anaerobic Digestion Modeling Task Group, 2002), while a comprehensive anaerobic digestion model, was too limited to be included into a plant-wide simulation software package.

## 2.7 Results and Discussion

The discussion of results will first address the Specific Biogas Generation tests, followed by the experimental reactor results as compared to the F/M model and BioWin 3 model predictions.

### 2.7.1 Specific Biogas Generation Test

The results of the SBG tests of the PS and WAS are shown in Figure 7. The linearized plots of  $1/q$  versus  $1/(FM)$  show curves for PS and WAS as described previously (Equation 2). A linear regression was used with each set of data to determine the equations for each line. The  $R^2$  values for the PS and WAS lines are 0.994 and 0.867 respectively, indicating a good fit to both sets of data. Equation 24 is the linear regression equation for the PS test:

$$1/q_p = 0.0101*(1/FM_p) + 0.00007 \quad (24)$$

where the values for  $q_{max} = 14285.7$  and  $K_S = 144.3$ . Similarly, Equation 25 is the regression equation for the WAS test:

$$1/q_w = 0.0163*(1/FM_w) + 0.0006 \quad (25)$$

where the values for  $q_{max} = 1666.7$  and  $K_S = 27.2$ . There is a significant difference between the  $q_{max}$  values for PS and WAS, which is supported by previously published

data (Pavlostathis and Gossett, 1986). The biomass content of the inoculum was assumed to be 10% of the volatile solids (Arnaiz *et al.*, 2006). Since the Lakeland digesters were only fed with PS, the remainder of the volatile solids in the digester sludge was assumed to be from PS only and was added to the total PS volatile solids for correction of F/M. The WAS specific biogas generation determination was treated differently in this respect, with the PS present in the inoculum disregarded in the F/M determination. However, the portion of the biogas output due to the PS as determined by a mass fraction of the total feed solids was subtracted from the total biogas output for the WAS test.

The  $1/q$  from Equation 2 was determined with the assumed biomass and biogas output from the serum bottles in each of the tests. Both  $1/q$  (PS and WAS) were further modified by subtracting the biogas output due to the assumed microbial biomass decay rate ( $0.1 \text{ d}^{-1}$ ) (Siegrist *et al.*, 2002) during the duration of the test.

These calculations were made for each of the five reactors in the PS and WAS tests, and plotted vs. the respective corrected  $1/(F/M)$  value. A regression analysis was performed and trend lines fitted to the data to determine the values of  $q_{\max}$  and  $K_S$  for the specific biogas generation for the digestion PS and WAS.

This method was simplified due to the lack of WAS in the digester sludge; however, if the model is set up for digesters running both feed types, the initial conditions will require an iterative process to determine the initial feed solids load. Software packages that can do such iterative calculations would be beneficial in such applications.

As Equations 24 and 25 indicate, the actual biogas generation due to WAS is low as compared to the biogas output due to the degradation of PS. The digestion of WAS is difficult due to the hydrolysis of the waste being a rate-limiting step, which requires

longer retention times to degrade the waste (Eastman and Ferguson., 1981). Another possible contributor to the decreased biogas production is that the Lakeland digesters not being used to digest WAS at the time, and therefore the microbial populations may be less acclimated to digest WAS. This insensitivity to WAS will lead to a buildup of WAS in the reactor due to decreased digestion rates. Adding to the difficulty in digesting the WAS, the Lakeland plant does not use any sort of pretreatment steps for WAS streams prior to digestion. Pretreatment of WAS is commonly used to improve WAS utilization in anaerobic digesters. In the cases of thermal pretreatment (Haug *et al.*, 1978) or ultrasonic pretreatment (Tiehm *et al.*, 2001), biogas production and solids digestion can be significantly improved. The SBG test could be a simple and useful approach to quickly evaluate the effectiveness of WAS pretreatment strategies.

The versatility of the SBG test lends itself to use with other feed types, such as animal and dairy wastes, as well as other organic wastes not typically treated at a wastewater treatment plant. As long as the volatile solids content is known for the feed and seed sludge, the test can be operated as has been done in this work. Due to the short operation time of the test, however, some waste streams may not be degradable enough to generate correct specific biogas generation rates as compared to a long term digestion of said wastes. The SBG test captures the degradability of readily-degradable substrates. For some applications, periodic repetitions of the SBG may be needed to recalibrate the

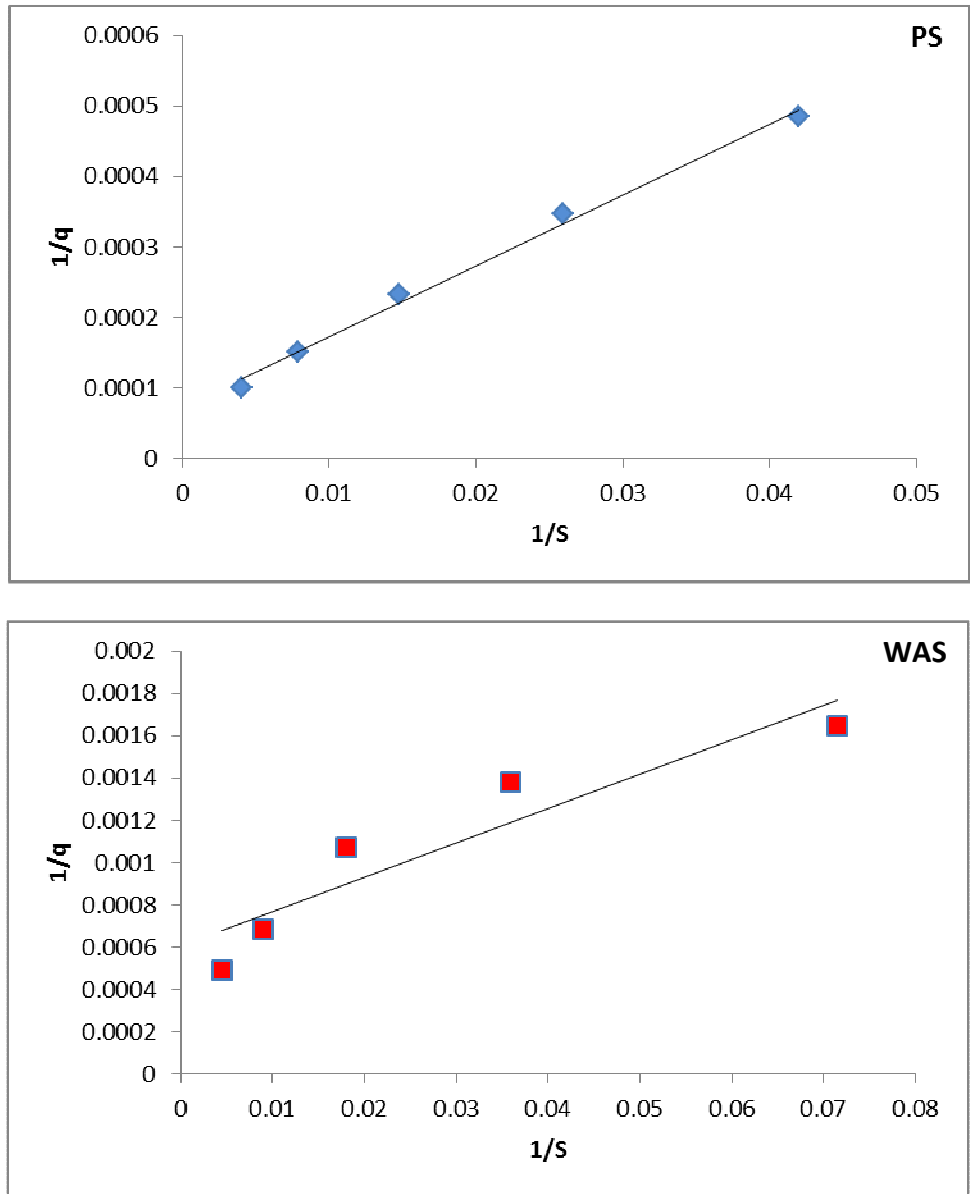


**Figure 7.** Specific biogas production rates that characterize PS (◆) and WAS (■) digestion using seed sludge from a full-scale anaerobic digester. The equations for the linear regressions shown are Equations 24 and 25 for the PS and WAS data, respectively.

model as conditions in the digester changes. The test would also be helpful in assessing the effects of an digester upset event, and be useful in determining a course of action to recover the normal operation of the digester.

Further examination of the Equations 24 and 25 also indicates that as F/M increases, the biogas generation rate increases as well. Since the biogas generation rate is dependent on microbial biomass, the increase in biogas production rate suggests that the microbial specific growth rate ( $\mu$ ,  $\text{day}^{-1}$ ) is increasing as F/M increases. Taking this into account, this model may be useful for processes with higher F/M values; such as in plug flow reactors (PFR) with recycle.

### **2.7.2 Laboratory-Scale Anaerobic Digesters as Compared to the F/M Model**

Daily biogas production rates (BPR) for the three reactors are shown in Figure 8. The BPR of the 10-day HRT reactor began to decrease after the second retention period until the end of the experiment, indicating some changes in the reactor. The 15-day and 20-day reactors exhibited small increases in the average daily BPR until the end of the experiment. The 10-day HRT reactor demonstrates a longer term reduction in the BPR, which may be explained by microbial population changes, a buildup of recalcitrant wastes, or the reduction in pH due to accumulation of volatile fatty acids.

However, the final pH of each of the three reactors was near neutral at 6.70, 6.77, and 7.04 for the reactors operated at 10, 15, and 20-day HRT, respectively, which suggests that VFA did not accumulate and impact pH significantly.

The biogas production rates of the laboratory-scale reactors and the model results, as well as the percent difference between both values, are provided in Table 3. Data are

reported for each HRT period. Operating the reactors for a total of 60 days allowed for at least three HRT periods for each reactor.

In the first HRT period for the 15-day and 20-day HRT reactors, the F/M model over-predicts the biogas production rates as compared to the experimental production rates by 30% in both reactors. This is likely due to the assumed residual PS in the inoculum being different from the actual residual PS in the inoculum. F/M model predictions for the three reactors show the 15-day and 20-day HRT reactors reaching steady state in the second retention period, while the 10-day HRT reactor reaches it in the first retention period. The initial F/M for the 10-day HRT reactor are closer to the steady state F/M value as compared to the other reactors, allowing for a faster attainment of steady state biogas production.

For F/M model calculations, the feed solids are modeled as not completely degradable; just as in actual anaerobic digesters. However, the SBG equations (Equations 24 and 25) are generated over a short period of time (4 hours), so it unlikely digestion of anything other than readily-digestible substrates and intermediates is occurring. The digestible fraction of the feed streams is adjusted in the model to a level that creates the best agreement between the model and the reactors. For these experiments, it was found that a digestible fractions of 0.7 and 0.5 for the PS and WAS, respectively, provided good agreement.

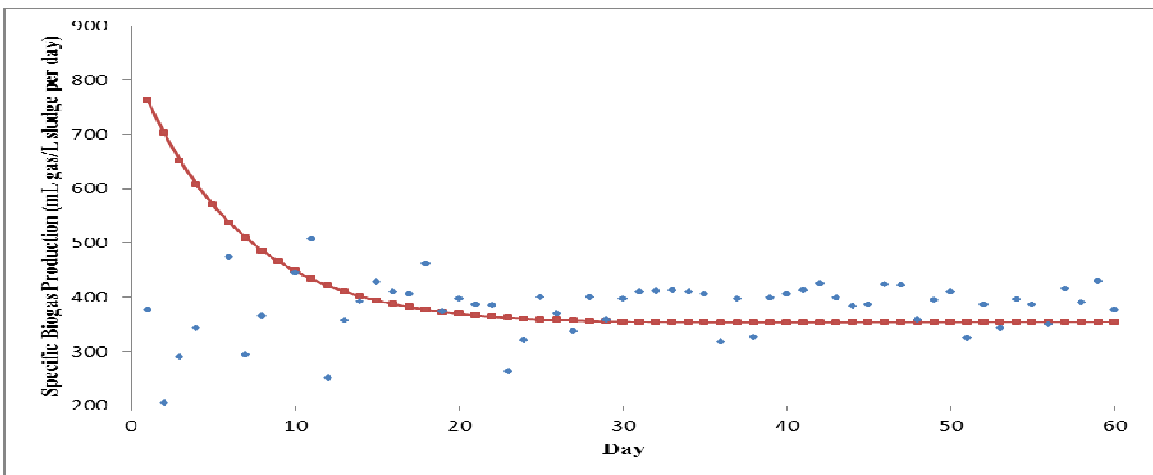
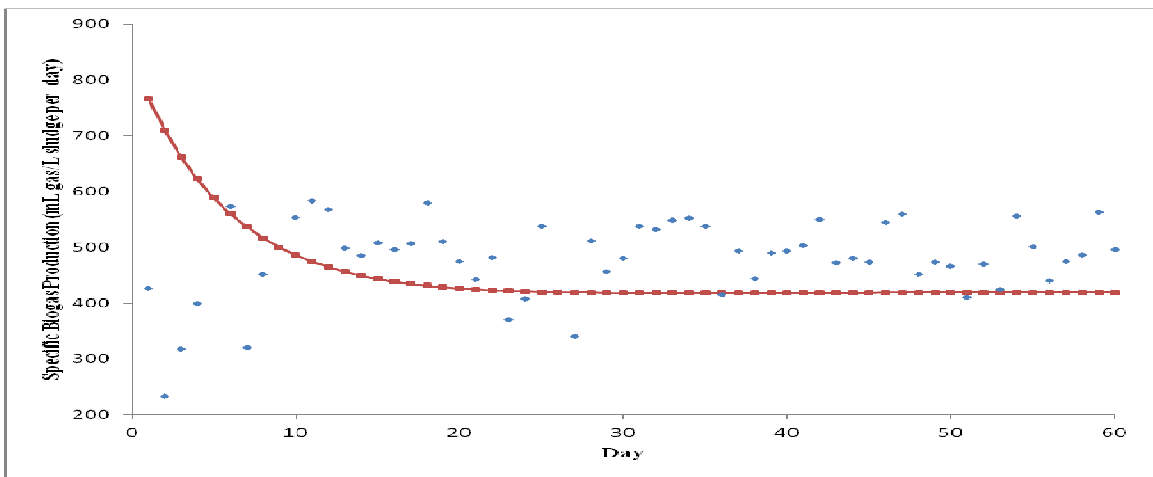
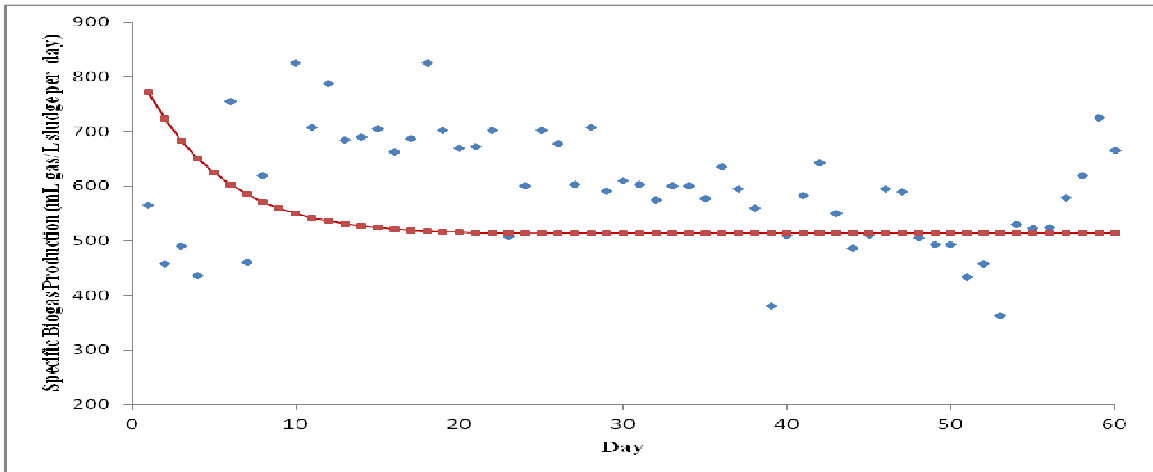


**Figure 8.** Daily biogas production rates from reactors ( $\blacklozenge$ ), and predictions from the F/M model ( $\blacksquare$ ) for 10, 15, and 20-day HRT reactors.

**Table 3.** Comparison of experimental reactor and model biogas production rates (mL biogas per liter sludge per day) for laboratory-scale reactors operated at 10, 15, and 20 day HRTs. Each model result is given with the percentage difference as compared to the experimental reactor results.

HRT (days)	Type	HRT Period					
		1	2	3	4	5	6
10	Experimental	<b>576</b>	<b>652</b>	<b>647</b>	<b>625</b>	<b>608</b>	<b>542</b>
	F/M Model	<b>632</b> -8.9%	<b>528</b> 19.0%	<b>514</b> 20.6%	<b>514</b> 17.8%	<b>515</b> 15.3%	<b>515</b> 5.0%
	BioWin 3	<b>957</b> -66.2%	<b>957</b> -46.8%	<b>957</b> -47.9%	<b>957</b> -53.1%	<b>957</b> -57.4%	<b>957</b> -43.4%
15	Experimental	<b>456</b>	<b>454</b>	<b>471</b>	<b>489</b>		
	F/M Model	<b>549</b> -20.4%	<b>426</b> 6.2%	<b>418</b> 11.3%	<b>419</b> 14.3%		
	BioWin 3	<b>957</b> -109.9%	<b>957</b> -114.1%	<b>957</b> -114.1%	<b>957</b> -95.7%		
20	Experimental	<b>376</b>	<b>376</b>	<b>391</b>			
	F/M Model	<b>485</b> -29.0%	<b>357</b> 5.1%	<b>354</b> 9.5%			
	BioWin 3	<b>771</b> -105.1%	<b>740</b> -96.8%	<b>739</b> -89.0%			

These values are in agreement with empirical data found previously (Pasztor *et al.*, 2009; Kabouris *et al.*, 2008) for the digestible portion of municipal wastewater. There are methods that determine the anaerobic degradability of water-soluble (Baumann and Müller, 1997) and solid (Kolář *et al.*, 2005) substrates as well as possible others that can be used prior to model setup to determine the degradable fractions. Another possibility is

to use the SBG test conducted over longer time periods to determine degradability of recalcitrant wastes.

Once the reactors are at steady state in the third retention period, the differences between the experimental and F/M model biogas production rates for the 10-day, 15-day, and 20-day HRT reactors are 5.0%, 14.3%, and 9.5%, respectively. The later retention periods for the 10-day HRT reactor show lesser disparity between the F/M model and experimental biogas production rates, decreasing to a 5.0% difference at sixty days of operation. For the 15-day HRT reactor, the F/M model initially over-predicts the biogas output, but model performance changes in subsequent retention periods ending at a 14.3% with slightly increasing differences through the second through fourth retention periods. Similar performance was observed in model predictions for the 20-day HRT, which also features good agreement between the F/M model and experimental biogas production rates.

F/M model predictions are less accurate at greater than 10-day HRT values, indicating that the model is neither fully capturing the complexity (i.e., unidentified variables or parameters) in the bioconversion of sludge nor accounting for changes in the microbial ecology. The initial loading conditions of the reactors may have created an overload condition that was corrected over time, but which more accurately reflects the conditions in the SBG test reactors. Neither VFA concentration nor biogas composition was determined for these experiments, so it is possible that the biogas generation for the each reactor in the early retention periods is more carbon dioxide and hydrogen.

The daily organic loading rate (OLR) for the 10-day, 15-day, and 20-day HRT reactors are 2.13, 1.42, and 1.07 g VS L<sup>-1</sup> reactor d<sup>-1</sup>, respectively, which are close to the

typical daily OLR for high-rate anaerobic digesters ( $1.6 - 4.8 \text{ g VS L}^{-1} \text{ reactor d}^{-1}$ ) (Metcalf & Eddy, 2003). Based on the assumed residual PS content in the inoculum, the initial OLR for the combined feed for the 10-day, 15-day, and 20-day HRT reactors is 10.29, 9.57, and 9.22  $\text{g VS L}^{-1} \text{ reactor d}^{-1}$ , respectively. These high OLR values indicate that the initial conditions for the reactors were likely in an overload condition. While the biomass is considered a composite by the F/M model, it is possible that the various microbial populations grow at different rates during the organic overload condition (Michaud *et al.*, 2001). Fermenting and VFA-oxidizing bacteria may be growing at greater rates in the presence of the higher feed concentration than the methanogens, creating a situation where the biogas quality is decreased but the biogas quantity still increases. As seen in Table 3, the 10-day HRT experimental reactor exhibited a lower BPR during the later retention periods. The overload condition may correct itself over time as VFA concentration reduces to a steady state value due to dilution and turnover by syntrophic bacteria and methanogens.

Table 4 shows the F/M model steady-state average daily F/M values for the PS in the 10-day, 15-day, and 20-day HRT reactors are 12.1, 9.5, and 8.3, respectively. Similarly, the steady-state F/M values for the WAS in the reactors are 12.7, 10.7, and 9.7, respectively. These represent the average F/M values as the 10, 15, and 20-day HRT reactor model results reached steady state in the 3<sup>rd</sup>, 2<sup>nd</sup>, and 2<sup>nd</sup> HRT periods, respectively.

Table 4 also lists the predicted minimum and maximum F/M values for each reactor by feed type for the full length of the experiment. The predicted maximum PS F/M for the 10-day HRT reactor is 20% greater than in the 15-day HRT reactor, which may

explain its somewhat erratic BPR. The elevated PS F/M could indicate the buildup of VFAs in the reactor, despite the OLR remaining within the typical range (Metcalf & Eddy, 2003) for high-rate anaerobic digesters.

**Table 4.** Average predicted (steady-state) and minimum/maximum (entire model simulation) F/M values for each reactor by feed type.

Reactor (HRT)	PS			WAS		
	Average <sub>SS</sub>	Minimum <sub>T</sub>	Maximum <sub>T</sub>	Average <sub>SS</sub>	Minimum <sub>T</sub>	Maximum <sub>T</sub>
10-day	12.0	8.7	12.0	8.9	1.0	8.9
15-day	9.6	7.5	9.6	7.5	0.7	7.7
20-day	8.3	6.6	8.5	6.7	0.5	7.0
Notation: SS: Steady-state value    T: Total length of simulation						

Despite the predicted F/M in the 10-day HRT reactor being greater than in the 20-day HRT reactor, the final total and volatile solids contents for the 10-day and 20-day HRT experimental reactors were nearly identical. The total solids (TS) and volatile solids (VS) content for the inoculum sludge was 2.29% and 74.3%, respectively. Total volatile solids (TVS) is the percentage of the sludge represented by the volatile portion of the total solids content. For the 10-day and 20-day HRT reactors after 60 days of operation, the %TS/%VS/%TVS were 1.28%/74.3%/0.95% and 1.27%/70.8%/0.90%, respectively, while the F/M model TVS content for the 10-day and 20-day HRT reactors is 1.55% and 1.27%, respectively.

The 10-day HRT reactor exhibits a greater VS destruction rate, leading to increased BPR during the conversion of VS to intermediates. This increased BPR may explain the BPR disparity between the 10-day and 20-day HRT reactors.

Microbial communities are not static or immune to environmental conditions, so it stands to reason that reactor operation parameters will affect the microbial community structure and performance. Operating reactors at low or high F/M will select for microbial populations that thrive in those conditions. Higher F/M will select for microbial populations that accommodate greater OLR. This is an important consideration when modifying the model for use with other reactor configurations, such as plug flow reactors (PFR) with recycle. The higher F/M values present in PFRs is a difficult problem to overcome when considering the possibility of dynamic changes in microbial community structure. ADM1, for instance, provides for numerous biochemical reactions that are assumed to be characteristic of a functional group of microorganisms, but it does not account for changes in the kinetic rate constants due to dynamic changes in the actual microbial community structure. The F/M model does not address this issue either, but the model could be corrected over time by periodic SBG tests. One intriguing possibility would be the integration of the F/M model with ADM1, which may be able to model the turnover of soluble intermediates due to high F/M operation.

### **2.7.3 Laboratory-Scale Anaerobic Digesters as Compared to BioWin 3 Simulations**

The data from the BioWin 3 simulations are shown in Table 3. These are daily biogas production as compared to the daily biogas production from the experimental reactors.

In all cases, the BioWin 3 model package significantly over-predicts the daily biogas production rates for each of the three reactors. For the 10-day HRT reactor, the BioWin 3 model results are the closest in value to the experimental results with a biogas production over-prediction of 43.4% in the 6<sup>th</sup> HRT period to 66.2% in the 1<sup>st</sup> HRT period. The model predictions for the 15-day HRT reactor range from an over-prediction in biogas generation of 95.7% in the 4<sup>th</sup> HRT period to 114.1% in the 2<sup>nd</sup> HRT period. The model predictions for the 20-day HRT reactor also over-predict the biogas production rates, with an 89.0% over-prediction in the 3<sup>rd</sup> HRT period and a 105.1% over-prediction in the 1<sup>st</sup> HRT period.

The exact reasons for these inaccuracies are not known, as there are many possible sources of error in a model with so many parameters. The greatest source of error is likely the degradable fraction of the volatile solids being set to 1 as compared to the fractions in the F/M model being set to 0.7 and 0.5 for PS and WAS, respectively. This would increase the biogas production rate by a significant amount as compared to the F/M model.

As can be seen in Table 3, the only BioWin 3 model predictions to not reach steady state conditions immediately are the model results for the 20-day HRT reactor. The F/M model predictions exhibit similar behavior; however, the overall daily biogas production rates compare more favorably to the experimental reactor rates. It appears that the SBG tests do capture more accurately the kinetic parameters of the anaerobic digesters than those included in the BioWin 3 model, at least for the 60-day time period in which these experiments were run. The BioWin 3 model is created for long-term operation of a wastewater treatment plant, whereas the SBG test will capture short term biogas

generation results. While modeling a wastewater treatment process, the parameters in the BioWin 3 model are calibrated to the empirical data. This was not done for this case, as little data was available from the experimental reactors for this sort of calibration. It should also be noted that the F/M model is quite limited in the number of parameters that can be changed as compared to the BioWin 3 model.

After 60 days of operation, the TVS predictions for the 10-day and 20-day HRT reactors are 1.24% and 0.99%, respectively. Table 5 shows these results from the reactors and the two models.

**Table 5.** Comparison of Total Volatile Solids (TVS) results from the 10-day and 20-day HRT reactors as compared to F/M and BioWin 3 model predictions

	<b>Reactor Sludge</b>	<b>F/M Model</b>	<b>BioWin 3 Model</b>
<b>10-day HRT</b>	0.95%	1.55%	1.24%
<b>20-day HRT</b>	0.90%	1.27%	0.99%

The BioWin 3 model results are more comparable to those from the reactor sludge for both reactors; however the biogas rate is over-predicted in all cases. Perhaps the model is producing too much biogas per gram of volatile solids destroyed via the kinetic parameters used in the model. Estimates of the microbial biomass community composition may also be incorrect, which would also directly affect the use of the kinetic parameters. Both of the models over-estimate the remaining TVS in the effluent, which indicates that perhaps the batch feeding of the reactors may have caused the sludge to

acclimate to periods of higher F/M. As a result of batch feeding, the microbial biomass may have become more efficient at the breakdown of volatile solids in the sludge.

## CHAPTER 3: DEVELOPMENT OF THE RT-RIBOSYN METHOD

### 3.1 Introduction

The analysis of microbial communities in natural and engineered environments is a crucial practice for environmental engineers and scientists. Some of the most useful tools for understanding environmental systems are the growth rates of microbial communities.

Typically, growth rate information is obtained by letting cells grow suspended in a nutritive media and taking a time series of spectrophotometer measurements of the suspension's turbidity. But this method only measures the bulk growth rate, and does not provide independent simultaneous measures of growth rate for each constituent species in the population. Using current molecular biology methods, we can identify and enumerate distinct microbial populations, as well as determine function (Amann *et al*, 1998), but we would further benefit from knowing how fast microbes are growing under a variety of environmental conditions. To date, developing a valid technique has been attempted with radioactively-labeled DNA and DNA hybridization (Pollard, 1998). In addition to the restrictions and difficulties of using radioactive material, this approach suffers because not all bacteria incorporate the thymidine used in the assay. Other techniques, such as *in situ* identification of uncultured bacteria and microbial community composition that target ribosomal RNA (rRNA), have been useful (Amann, 2000) for studying microbial communities in wastewater systems. A relatively new method, fluorescence *is situ* hybridization (FISH) with microautoradiography (FISH-MAR), identifies which

individual cells are consuming a particular compound (Lee *et al*, 1999), as well as the substrate uptake rate (Nielsen *et al*, 2003). However, the substrate uptake rate has not been correlated with specific growth rate. While a powerful method appropriate for certain applications, FISH-MAR suffers from a few cumbersome limitations. It is a notably difficult method to master, involving several days of work, and is limited to laboratories authorized to work with radioisotopes. Traditional methods of measuring microbial growth are suited for pure cultures, or may only reveal composite growth rates for an environmental sample. A faster, simpler method would be beneficial for the investigation of natural and engineered systems.

A means to determine the specific growth rate of microorganisms may come from taking advantage of the action of ribosomes within cells as they are growing rapidly. As cells prepare to split into two new daughter cells, the number of ribosomes in the cell must double so that the daughter cells have the same number of ribosomes as the original cell. Ribosome genesis is best understood in the bacteria *Escherichia coli*, as it has been heavily studied. Greater detail pertaining to ribosome synthesis in *E. coli* can be found in earlier published works (Srivastava and Schlessinger, 1990; Jemiolo, 1996). However, an important aspect of ribosome synthesis is that two types of 16S ribosomal RNA (rRNA) are created during the process. These two types, referred to as precursor (pre16S rRNA) and mature (16S rRNA), differ in length. Pre16S rRNA is processed during ribosome synthesis into 16S rRNA, at which time the ribosomes have been completely synthesized.

Further, it has been found that antibiotics, such as chloramphenicol, can disrupt this process (Britschgi and Cangleosi, 1998), allowing for the continued buildup of pre16S rRNA in relation to 16S rRNA. As the synthesis of ribosomes is analogous to the rate at

which new cells are created, a measurement of the ribosome synthesis rate may be used to determine the specific growth rate of microbial populations.

### **3.2 Background and Description of the RT-RiboSyn Method**

A molecular biology based method was developed to determine the specific growth rate,  $\mu$ , of a distinct microbial population in an environmental sample by measurement of the specific rate of ribosome synthesis,  $r$  (shown schematically in Figure 9). This new method has been named RT-RiboSyn, based upon ribosome synthesis and the use of reverse transcription and primer extension (RT&PE) to measure the specific rate of ribosome synthesis as shown in Equation 26:

$$r = \frac{\ln 2}{t_D} \quad (26)$$

where  $t_D$  is the ribosome doubling time.

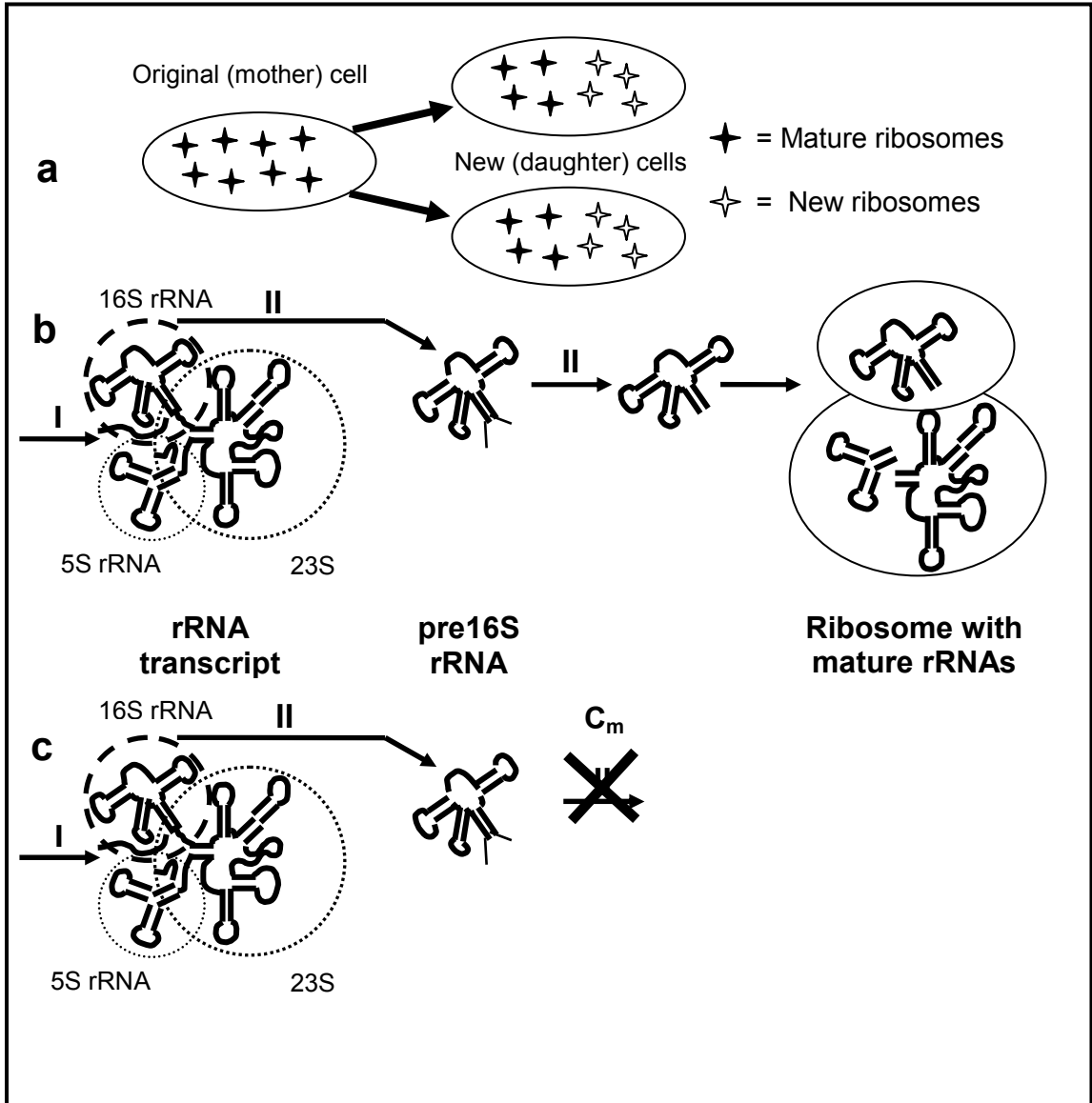


**Figure 9.** Simplified description of cell doubling (a), ribosome synthesis (b), and inhibition of ribosome synthesis by chloramphenicol (c). The steps in each process are: I) Expression, II) 1° processing, and III) 2° processing.  $C_m$  is chloramphenicol exposure.

As Figure 9 indicates, cell synthesis is dependent on the creation of new ribosomes. During log growth, each cell is actively synthesizing new ribosomes to be divided into

the two new daughter cells (Figure 9a). For a constant specific growth rate, the average number of ribosomes per cell remains constant. Thus, the specific rate of ribosome synthesis ( $r$ ) is the same as the specific growth rate of the cell ( $\mu$ ). Ribosome synthesis starts with expression, which generates a polycistronic rRNA transcript that contains the three rRNAs. RNase III cleaves this transcript of the *rrn* operon enzymatically into 5S, 16S, and 23S segments, and each of these “precursor” segments has extraneous RNA from the 5’ and 3’ ends removed to form “mature” rRNA for assembly into ribosomes.

Ribosomes contain the mature rRNA and ribosomal proteins. The precursor rRNA represents new ribosomes, while the mature rRNA represents the extant, functional ribosomes (Figure 9b). The RT-RiboSyn method targets 16S rRNA to determine the ratio of pre16S rRNA to 16S rRNA as it changes over time in cells experiencing disruption of normal ribosome synthesis. This is accomplished by adding the antibiotic chloramphenicol to the sample (Figure 9c) and taking samples over time. At the beginning of the time series, the processing of pre16S rRNA is stopped at the second step by adding the antibiotic chloramphenicol, which disrupts the processing of pre16S rRNA to 16S rRNA (Pace, 1973). Once exposed to chloramphenicol, the bacterial cells continue to create pre16S rRNA while the 16S rRNA remains constant outside of normal degradation processes (Stroot and Oerther, 2003).

Monitoring pre16S rRNA synthesis has been used in previous work (Cangleosi and Brabant, 1997; Oerther *et al*, 2002; Stahl *et al.*, 1988; Stroot and Oerther, 2003) as an indicator of growth response, and has been shown (Oerther *et al.*, 2002) to dramatically increase as compared to total 16S rRNA. RT-RiboSyn takes this concept a step further,

and uses it to determine a specific rate of ribosome synthesis by using a primer that specifically targets a population of interest.

The abundance of the new pre16S rRNA relative to the abundance of 16S rRNA can be measured over time. This is accomplished by extracting the RNA in bulk, removing extraneous DNA from the extracted RNA, annealing a DNA primer with an attached fluorochrome to the pre16S rRNA and 16S rRNA, extending the primer toward the 5' end using reverse transcriptase, then enzymatically removing the RNA and performing capillary electrophoresis on the fluorescently labeled ssDNA. Since pre16S rRNA has additional ribonucleotides at the 5' end compared to the 16S rRNA, ssDNA derived from pre16S rRNA will be longer than those derived from 16S rRNA.

Thereafter, it is possible to separate and quantify the two pools based upon their length using a capillary electrophoresis system. Thus separated, measuring relative abundance of the two ssDNAs is a matter of measuring the relative fluorescent intensity of each ssDNA. Each distinct microbial population in the sample of interest can be targeted with a specific primer complementary to a sequence within the pre16S and 16S rRNA that is unique among the microbial populations present in the mixture. Over a time series, this increase in pre16S rRNA as compared to the 16S rRNA allows for the determination of the ribosome doubling time (Figure 10). This ribosome doubling time is then used to determine the specific growth rate by using Equation 26.

The RT-RiboSyn method was verified in several steps. First, it was used to determine the specific growth rate of a pure culture of *A. calcoaceticus*. The results were compared to spectrophotometer optical density measurements which is the traditional method to determine specific growth rates of pure cultures. Next, the method was used with an

environmental sample, in this case activated sludge from a high purity oxygen (HPO) system at a wastewater treatment plant. Finally, the method was applied to the RNA of a pure culture of *Methanosarcina barkeri*, followed by anaerobic digester sludge to measure specific growth rates of archaea.

### **3.3 Methods and Materials**

This methods and materials section details the application of the RT-RiboSyn method to a pure bacterial culture, bacteria present in a wastewater treatment process, and to archaea in a pure culture and wastewater sample. Appendix B contains expanded methods and materials that pertain to this section.

#### **3.3.1 Information on Wastewater and Sludge Sources**

Activated sludge samples and primary effluent were obtained from the Howard F. Current Advanced Wastewater Treatment plant located in Tampa, Florida. The plant is the wastewater treatment facility for the city of Tampa, with a daily average (2009) flow rate of 54.2 million gallons per day (MGD) and a designed capacity of 96 MGD. The High Purity Oxygen (HPO) system is a secondary treatment process for the removal of carbonaceous biological oxygen demand (BOD), and is the source for the activated sludge and primary effluent used in these experiments. The solids retention time (SRT) for the process is 12 hours, and the hydraulic retention time (HRT) is 4 hours (T. Ware, personal communication, October 28, 2011).

Anaerobic digester sludge samples were obtained from the Glendale Wastewater Reclamation Plant located in Lakeland, Florida. The average daily flow through the

facility is 13.7 MGD, with a discharge point to an artificial wetlands constructed around the plant in 1987. The anaerobic digester in use at the time of these experiments was a two-stage system (primary and secondary tanks) with a total capacity of 1.5 million gallons, and an HRT of 15-20 days depending on loading (B. Kruppa, personal conversation, November 3, 2011). The system was run at an average temperature of about 35° C, making it a mesophilic digestion process. Samples were obtained via a sampling port from the primary digester.

### **3.3.2 RT-RiboSyn with Pure Bacteria Culture**

*A. calcoaceticus* (ATCC# 23055) was cultured in sterile nutrient broth (Difco Nutrient Broth #234000) and shaken at 250 rpm to generate four distinct growth conditions including mid-log growth phase cultures incubated 25, 30, and 35 °C, and a stationary phase culture incubated at 30 °C. Chloramphenicol (20 mg/L) was added to a 50 mL subsample from each master culture to inhibit the secondary processing of pre16S rRNA (Pace, 1973). Sub-samples (4 mL) were collected from each 50 mL sample at 0, 10, 20, and 30 minutes of exposure to chloramphenicol, centrifuged (10,000 g for 5 minutes), decanted, and stored promptly in a -80 °C freezer. Appendix B-1 provides a more detailed description of the sampling protocol.

The optical density (OD) of the four master cultures was measured periodically at 684 nm using a spectrophotometer and the specific growth rate was determined for the time of sample collection.

RNA was extracted from the subsamples using the phenol:chloroform method (Schmid *et al.*, 2001). See Appendix B-2 for a detailed account of the steps involved in

the phenol:chloroform extraction. Following the RNA extraction, the samples were purified further using the RNAqueous<sup>®</sup> kit (Ambion, Inc., Carlsbad, CA). See Appendix B-3 for detailed steps taken while using the RNAqueous<sup>®</sup> kit. Residual DNA was removed using a DNaseI treatment (DNAfree<sup>™</sup> kit by Ambion, Inc., Carlsbad, CA). Appendix B-4 lists the detailed steps for using the DNAfree<sup>™</sup> kit. Finally, RT&PE using the ImProm-II<sup>™</sup> Reverse Transcription System (Promega Corporation, Fitchburg, WI) was performed according to manufacturer's instructions with a MgCl<sub>2</sub> concentration of 2.5 mM. Appendix B-5 details the steps required in usage of the ImProm-II<sup>™</sup> kit.

The WellRed-labeled primers (Sigma-Genosys, The Woodlands, TX) used in the RT&PE reaction were Eub338 (5' GCTGCCTCCCGTAGGAGT 3') and Acin0659 (5' CTGGAATTCTACCATCCTCTCCCA 3'), which target conserved sites of the pre16S and 16S rRNA for all Eubacteria and *Acinetobacter*, respectively (Loy, *et al*, 2003; Oerther *et al*, 2000). The primer extension step was 1 hour at 42° C and 47° C for the Eub338 and Acin0659 primers, respectively. The RT&PE samples were analyzed by capillary electrophoresis with the CEQ 8000 Genetic Analysis System (Beckman-Coulter, Brea, CA), with resulting electropherograms used for analysis. The WellRed labeled size standards were the GenomeLab DNA Size Standard Kit (600 nt) for the Eub338 RT&PE samples, and the MapMarker<sup>®</sup> 1000 (Bioventures, Inc., Murfreesboro, TN) size standard for the Acin0659 RT&PE samples. Appendix D presents an analysis of the lower threshold detection limits for the CEQ-8000 system.

Capillary electrophoresis separates the two RT&PE products by length, and using the same primer for both products allows for the comparison of the two peaks by area of the peaks. The fragment lengths correspond to the predicted lengths of the pre16S and 16S

RT&PE products (Stroot, 2004). The ratio of the pre16S and 16S RT&PE products (pre16S/16S) was determined for each sub-sample and plotted versus time of chloramphenicol exposure. A trend line was fitted to these data and the equation determined. Using the slope (m) of the equation, the ribosome doubling time was determined. Specific rates of ribosome synthesis were then determined using Equation 26.

### **3.3.3 RT-RiboSyn Method with Activated Sludge from High-Purity Oxygen System**

Prior to deciding to attempt to determine the specific growth rate of *Acinetobacter* genus in a wastewater treatment facility, samples were taken for fluorescence *in situ* hybridization (FISH) from the HPO system at the Howard F. Curren Advanced Wastewater Treatment Plant located in Tampa, Florida. FISH allows for the identification and enumeration of organisms of interest. Samples of sludge were taken from a sampling port at the effluent end of the HPO system and centrifuged at 10,000 g for 4 minutes in 2 mL micro-centrifuge tubes. The sludge samples were then decanted and resuspended in 4% paraformaldehyde (PFA) solution to disrupt the cell walls of the bacteria present to prepare the sample for FISH. After 3 hours in 4% PFA, the samples were centrifuged again at 10,000 g and decanted. The samples were then resuspended in a 1:1 ethanol:phosphate buffered saline (PBS) solution to preserve the samples. Samples were then stored at -20° C. Later FISH analysis using the Acin0659 probe with a Cy-3 fluorescent marker indicated the presence of *Acinetobacter* genus in the sludge, so further sampling was then performed. For a full description of the FISH method, see Appendix B-6.

Activated sludge and primary effluent samples were taken from the HPO system at the Howard F. Curren plant. Both sample types were taken from sampling ports as sampling from other locations in the process was not possible due to its design. The primary effluent sample (fresh wastewater ready for treatment processes) was collected in two large Pyrex bottles and sealed with a screw-on lid. The activated sludge was collected in a bottle that permitted ample headspace to provide oxygen for microorganisms during transit to the laboratory. The samples were collected in the early morning.

Upon return to the laboratory, several air stones connected to aquarium air pumps were placed into the activated sludge to provide aeration while sample collection preparation was completed. The master reactor was a 4 L beaker that contained 2 L of primary effluent and 1 L of activated sludge and was placed on a magnetic stir plate. Three air stones provided aeration while a large stir bar mixed the contents of the reactor at a high rate. During sampling, periodic measurements of dissolved oxygen (DO) and chemical oxygen demand (COD) were made. According to DO measurements, aeration and stirring were high enough that reactions were not oxygen-limited ( $DO \geq 7.6$  mg/L).

For the RT-RiboSyn sampling, 200 mL subsamples were taken from the master reactor and placed in 500 mL beakers with an air stone and a magnetic stir bar to keep the sludge mixture aerated. At time zero, a 2000 mg/L chloramphenicol solution was added to the subsample to bring the final chloramphenicol concentration to 200 mg/L. Samples were taken at 0, 7, 14, 21, and 28 minutes of exposure to chloramphenicol and were collected in two 15 mL conical tubes at each time step. Samples were centrifuged at 10,000 g, decanted, and promptly stored at -80 ° C. RNA extractions, purification, and reverse transcription procedures were as described in 3.3.2, with the exception that a

higher concentration of chloramphenicol (200 mg/L vs. 20 mg/L) was used in order to overcome any absorption effects from extraneous material in the sludge. Environmental samples often contain extraneous materials that could absorb these antibiotics and prevent their inhibitory effects on populations of interest. RNA from a pure culture of *A. calcoaceticus* was used as a positive control for the RT&PE process and was analyzed along with the RNA from the sludge samples on the CEQ-8000 Genetic Analysis System.

### **3.3.4 RT-RiboSyn Method with Pure Methanogen Culture and Anaerobic Digester Sludge**

Pure methanogen culture work was performed by obtaining a slab culture of *M. barkeri* from the Oregon Collection of Methanogens at the Portland State University. The sample was provided with a small supply of MS Medium (Boone *et al*, 1989) which was used to grow a pure culture of *M. barkeri*. RNA was extracted and purified as described in 3.3.2.

One major difference between applying the RT-RiboSyn method to bacteria versus archaea is that the mechanism by which chloramphenicol inhibits growth in bacteria does not work with archaea. Rodriguez-Fonseca *et al* (1995) demonstrated that the antibiotic anisomycin is an analog to chloramphenicol that will inhibit pre16S rRNA processing in archaea, so this antibiotic was substituted for chloramphenicol in these studies. The sampling and extraction procedures outlined for pure cultures in 3.3.2 was the same as the wastewater samples, with the exception that a higher concentration of chloramphenicol (200 mg/L) or anisomycin (250 mg/L) was needed to overcome absorption effects. As detailed in work with *Methanococcus voltae* (Possot *et al.*, 1988), a

minimum concentration of 100  $\mu\text{g/ml}$  of anisomycin was needed to inhibit protein synthesis in a pure culture. For anaerobic digester sludge samples, the final concentration of anisomycin used was 250  $\mu\text{g/ml}$ .

Anaerobic digester sludge was collected from the Glendale Wastewater Reclamation Plant in Lakeland, FL, and 50 ml added to each of the 100 ml Balch-style serum bottles. The 80%  $\text{N}_2$  - 20%  $\text{CO}_2$  atmosphere in each reactor was injected by needle, and was refreshed whenever the plug was removed for reactor feeding or cycling. The reactors were operated at a 20 day hydraulic retention time, meaning that each day 5% of the volume in each reactor was replaced with fresh feed. The feed mixture used in this case was a mixture of primary sludge (PS) and waste activated sludge (WAS) blended in a dry solids ratio of 1.79:1 (PS/WAS) to simulate typical blended sludge for anaerobic digestion (Griffin *et al*, 1998). The reactors were operated for several days after the sludge acquisition from Glendale at 35° C and shaken at 150 rpm to ensure that the microbial populations were actively growing.

Four hours prior to sampling, the reactors were given an injection of 1M sodium acetate solution to provide a growth impetus for any acetoclastic methanogens present in the reactors. After four hours, a solution of anisomycin was added to each reactor to provide for a final concentration of 250  $\mu\text{g/ml}$  of anisomycin in each reactor. Samples were taken at time = 0, 4, 20, 24, and 48 hours after the addition of the sodium acetate solution. These samples were stored and the RNA extracted and purified as described in 3.2.3.

During the RNA extraction process, the cell disruptor used previously (Biospec Products Mini-Beadbeater-8) malfunctioned and needed to be replaced. The unit chosen (Scientific Industries Disruptor Genie<sup>®</sup>) required new protocol that took some time to optimize for samples of this nature. Once the RNA was extracted from the samples, further concentration was performed in order to maximize the chances of detecting the 16S and pre16S rRNA peaks with the CEQ-8000. In addition to concentration of samples, the longer fragment lengths expected from the Arch915 primer required that the MapMarker<sup>®</sup> 1000 (Bioventures, Inc.) size standard be used.

### **3.3.5 Analytical Methods**

For the experiments involving activated sludge from the HPO system at the Howard F. Curren Advanced Wastewater Treatment Plant in Tampa, two additional instruments were used. For the measurement of dissolved oxygen in the master reactor, the instrument used was the Traceable Portable Dissolved Oxygen Meter (Fisher Scientific, Hampton, NH). Filtered wastewater samples were taken from the master reactor during the experiment using a syringe filter and refrigerated for later COD analysis. COD samples were analyzed using a Hach DRB 200 system (Hach Company, Loveland, CO). pH was measured using an Oakton pH/°C/Ion/mV meter (Oakton Instruments, Vernon Hills, IL).

### 3.4 Results and Discussion

#### 3.4.1 RT-RiboSyn with Pure Bacteria Culture

Data from the capillary electrophoresis measurements is analyzed in a simple graphical manner. As described in 3.3.2, the pre16S to 16S ratio is determined from these data and plotted. Figure 10 shows an example of this calculation, in this case the sample taken at 30° C and using the Eub338 primer. In Figure 10, the y-axis is the pre16S:16S ratio, and the x-axis is time in minutes of exposure to chloramphenicol.

The solid line represents the linear trend line for the raw ratio values, with an equation of:

$$y = 0.0149x + 0.1221 \quad (27)$$

and an  $R^2$  of 0.9995. The dashed line represents the linear trend line for the “corrected data”, whereby the y-intercept is forced to zero by subtracting the initial pre16S:16S ratio at  $t=0$ , while maintaining almost the same slope as the raw ratios. Extending this “corrected data” trend line to the point where pre16S:16S = 1 will allow for the determination of the ribosome doubling time,  $t_D$ . This value is then used in Equation 26 to determine the specific growth rate of the microbial population.

Figures 11 and 12 show typical electropherograms from the fragment analysis of pure culture samples using the Eub338 and Acin0659 primers, respectively. In each of figures 11a and 12a, the sample is taken at zero minutes of exposure to chloramphenicol, whereas figures 11b and 12b are after 20 minutes of exposure. Both figures indicate an increase over time of the number of pre16S fragments relative to the 16S fragments. The

fragment analysis software used by the CEQ-8000 system calculates the area under each peak, which is the data used to calculate the pre16S:16S ratios.

Mean pre16S:16S values for each of the sub-samples collected from the four cultures are shown in Table 6. For all sub-samples, the low coefficient of variance indicates a strong reproducibility with the RT-RiboSyn method. For growing cultures, the mean pre16S:16S values increased with longer exposure to chloramphenicol, which is consistent with earlier work (Stroot, 2004).

A comparison of the specific rate of ribosome synthesis as measured by RT-RiboSyn and the specific growth rate of each culture as determined by spectrophotometry is shown in Table 7. When RT-RiboSyn was used with the Eub338 primer for the mid-log growth phase samples, the specific rates of ribosome synthesis were in good agreement (within 10.0%) with the specific growth rate measurements, while the Acin0659 primer resulted in slightly higher variation (within 21.0%).

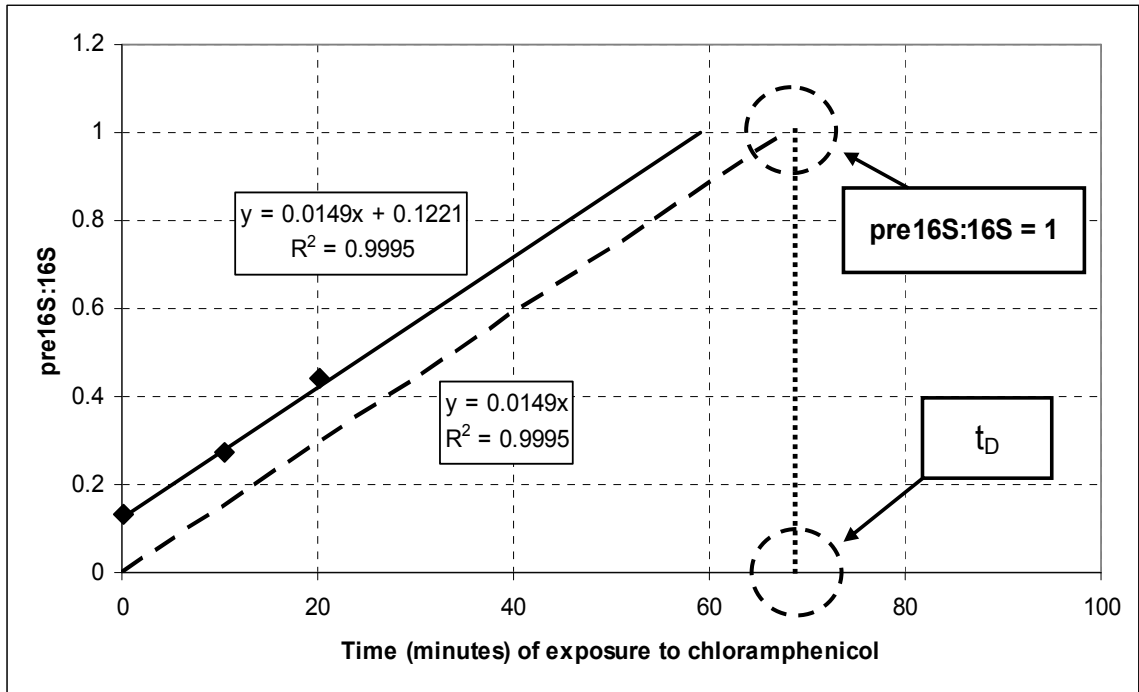


**Figure 10.** Example of pre16S:16S versus time, in this case a  $T = 30^\circ\text{C}$  sample using the Eub338 primer with *A. calcoaceticus*.

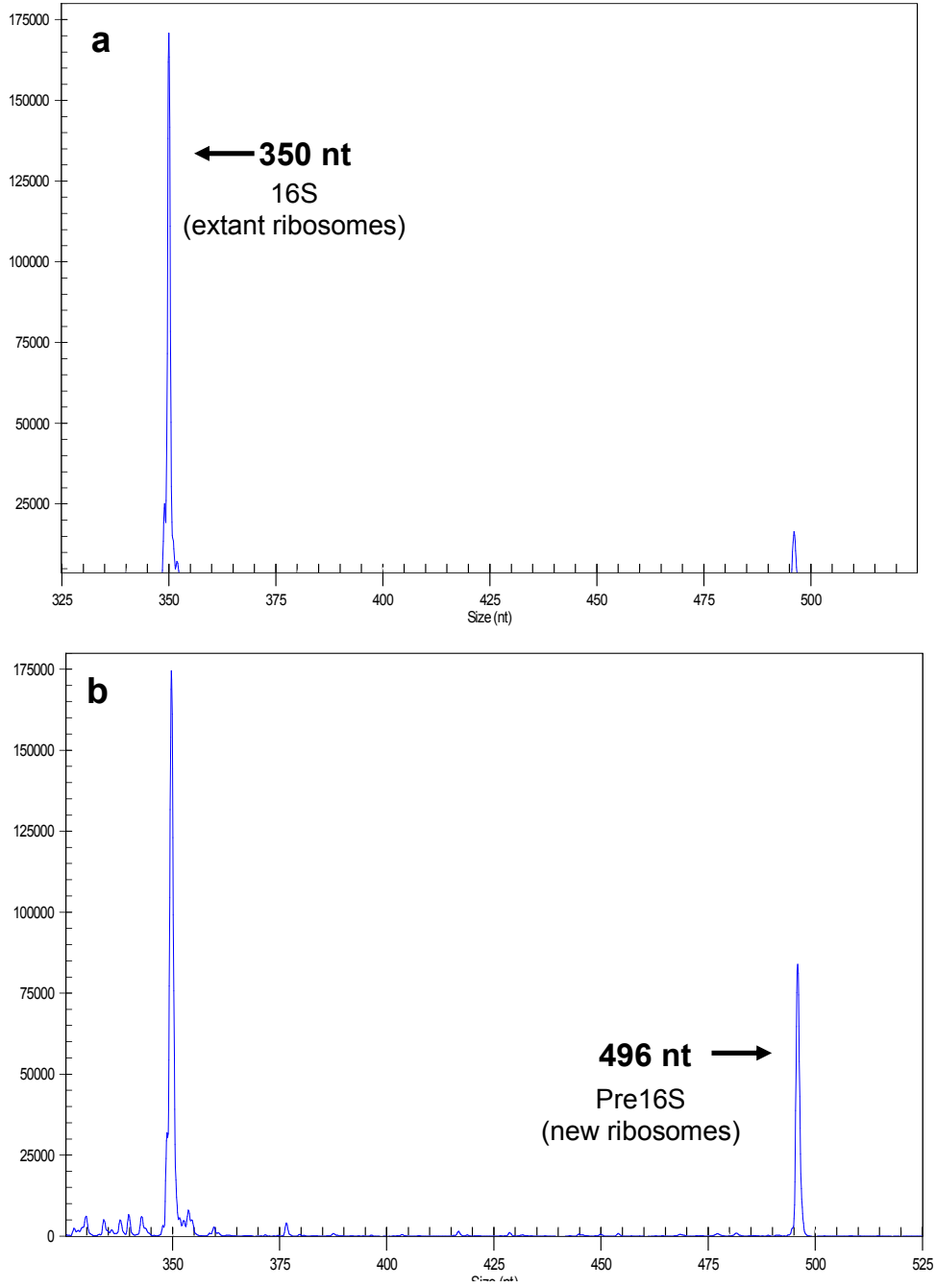


**Figure 11.** Typical electropherograms of RT-RiboSyn products derived from *A. calcoaceticus* incubated in nutrient broth at 25 °C after exposure to chloramphenicol for (a) zero minutes and (b) 20 minutes. The WellRed-labeled Eub338 primer was used.

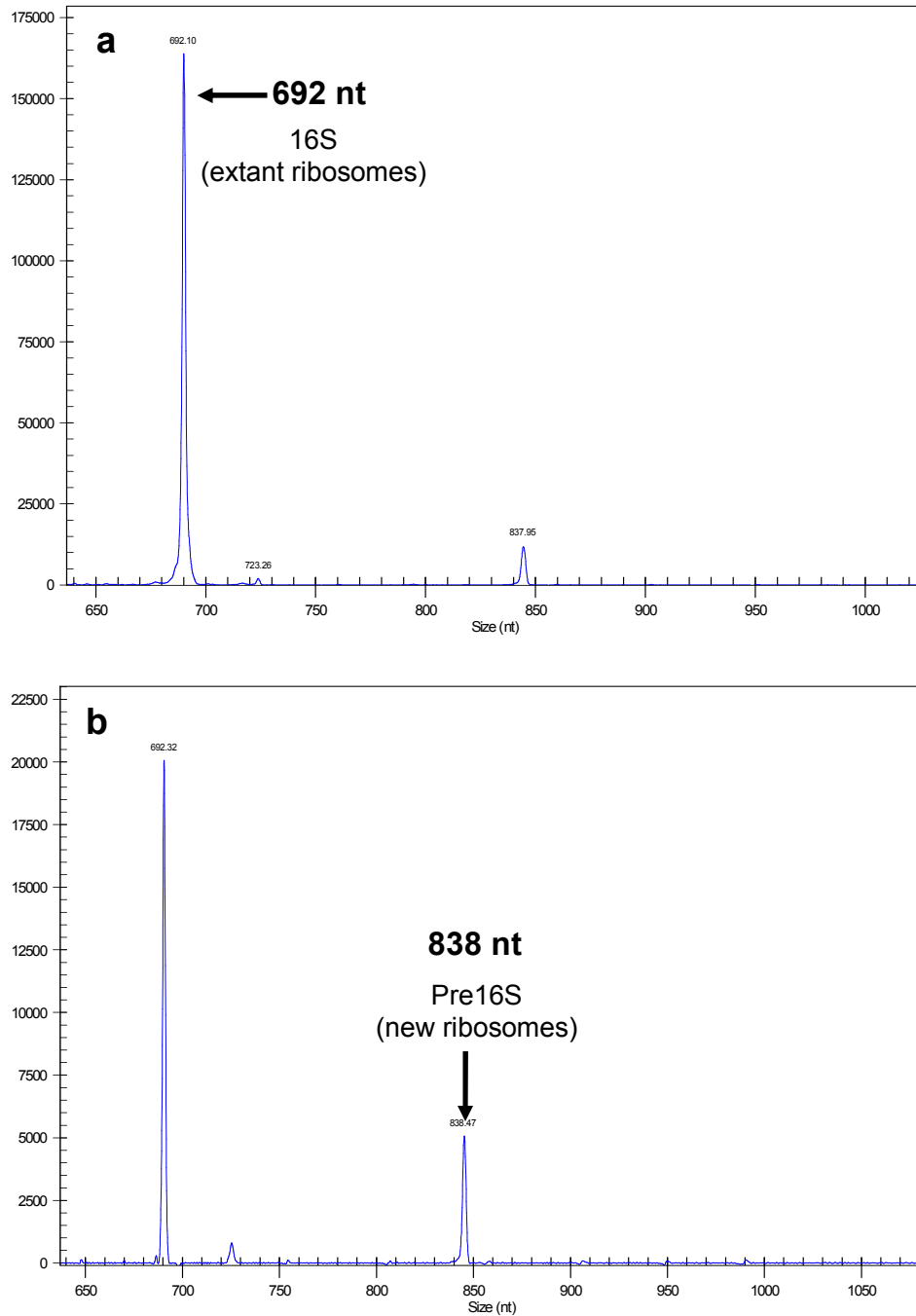


**Figure 12.** Typical electropherogram of RT-RiboSyn products derived from *A. calcoaceticus* incubated in nutrient broth at 25 °C after exposure to chloramphenicol for a.) zero minutes and b.) twenty minutes. The WellRed-labeled Acin659 primer was used.

**Table 6.** General and statistical data for calculated ratios of precursor 16S rRNA to mature 16S rRNA, including primer used, culture temperature (°C), time of exposure to chloramphenicol (minutes), mean pre16S:16S, standard deviation ( $\sigma$ ), number of samples (n), and the coefficient of variance (COV).

<b>Primer</b>	<b>Temperature (°C)</b>	<b>Time (min)</b>	<b>Mean pre16S:16S</b>	<b><math>\sigma</math></b>	<b>n</b>	<b>COV (%)</b>
<b>Eub338</b>	25	0	0.073	0.001	4	2.0
		10	0.145	0.002	3	1.0
		20	0.270	0.021	4	7.9
	30	0	0.126	0.014	3	11.0
		10	0.265	0.013	4	4.7
		30	0.571	0.011	3	1.9
	35	0	0.266	0.006	3	2.2
		20	0.513	0.010	5	2.0
		30	0.669	0.036	3	5.4
	30 stationary	0	0.104	0.014	3	13.4
		10	0.104	0.019	3	17.8
		20	0.093	0.012	3	12.6
<b>Acin0659</b>	25	0	0.136	0.005	4	3.6
		10	0.272	0.027	3	9.8
		20	0.390	0.01	3	2.6
	30	0	0.105	0.008	5	8.0
		10	0.195	0.006	4	10.6
		20	0.265	0.002	3	2.3
	35	0	0.473	0.025	5	5.3
		10	0.606	0.037	5	6.1
		30	0.957	0.008	3	0.9
	30 stationary	0	0.091	0.001	3	0.9
		10	0.094	0.003	3	2.8
		30	0.088	0.007	4	8.2

**Table 7.** Specific rate of ribosome synthesis,  $r$ , and specific growth rate,  $\mu$ , as calculated by RT-RiboSyn and spectrophotometry, as well as the % difference between the measurements. The  $R^2$  of the linear regression is included.

		25 °C	30 °C	35 °C	30 °C stationary
<b>Spectrophotometer</b>	$\mu$ (hr <sup>-1</sup> )	0.381	0.550	0.562	0.007
	$R^2$	0.811	0.988	0.925	0.476
<b>Eub335</b>	$r$ (hr <sup>-1</sup> )	0.387	0.611	0.545	-0.017
	$R^2$	0.971	0.999	0.996	0.706
	% diff	1.6	10.0	-3.1	N/A
<b>Acin0659</b>	$r$ (hr <sup>-1</sup> )	0.482	0.532	0.665	-0.004
	$R^2$	0.998	0.926	0.994	0.358
	% diff	21.0	-3.3	15.5	N/A

It is unclear why the specific rates of ribosome synthesis measured with the Acin0659 primer were different as compared to the Eub338 primer. It has been shown that chloramphenicol completely prevents pre16S rRNA degradation under all conditions in *E. coli* (Cangleosi and Brabant, 1997). Assuming this behavior holds true for *A. calcoaceticus*, the degradation of 16S rRNA during accumulation of pre16S rRNA may be the cause of higher specific rate of ribosome synthesis as compared to the specific growth rate. For the 30 °C stationary samples, the calculated specific rate of ribosome synthesis and specific growth rate were very low for both methods. However, it is important to note that the RT-RiboSyn method clearly distinguished between an actively growing culture and one with no growth.

While the RT-RiboSyn method shows promise as a useful new molecular biology tool, there are possible limitations that require further investigation. Chloramphenicol-resistant

bacteria may present one such limitation. It has been noted that the growth of many bacterial genera are inhibited by chloramphenicol concentrations of 1 to 10 mg/L (Brock, 1961). Our experiments were performed with chloramphenicol concentrations of 20 mg/L, which may render this resistance ineffective.

The analysis of the batch growth cultures in this study has yielded differences between the specific rate of ribosome synthesis and the specific growth rate. Ideally, RT-RiboSyn should be tested with cells collected from a chemostat operated over a broad range of specific growth rates to determine the limits of the method. However, these results from batch growth cultures are very promising. There is good agreement between the measurement of specific ribosome synthesis by RT-RiboSyn and the measurement of specific growth rate with the conventional spectrophotometric method for *A. calcoaceticus* under different growth conditions using standard culture media.

### **3.4.2 RT-RiboSyn Method with Activated Sludge from High-Purity Oxygen System**

Prior to attempting to use RT-RiboSyn with the sludge from the HPO system at the Howard Curren plant, a FISH analysis was performed on the sludge to determine whether or not *Acinetobacter* was present in the system. Figure 13 indicates the results of that analysis. The blue dye present is DAPI, which is a nucleic acid stain that will stain anything containing nucleic acids. The pink-red color is created by the Cy3 marker present in the Acin0659 probe used in the hybridization. Any organism showing as pink-red in color indicates that it is of the *Acinetobacter* genus. Figure 13 demonstrates that there was a significant population of *Acinetobacter* in the HPO system, and so it was

decided that RT-RiboSyn would be used to determine a specific growth rate for that population.

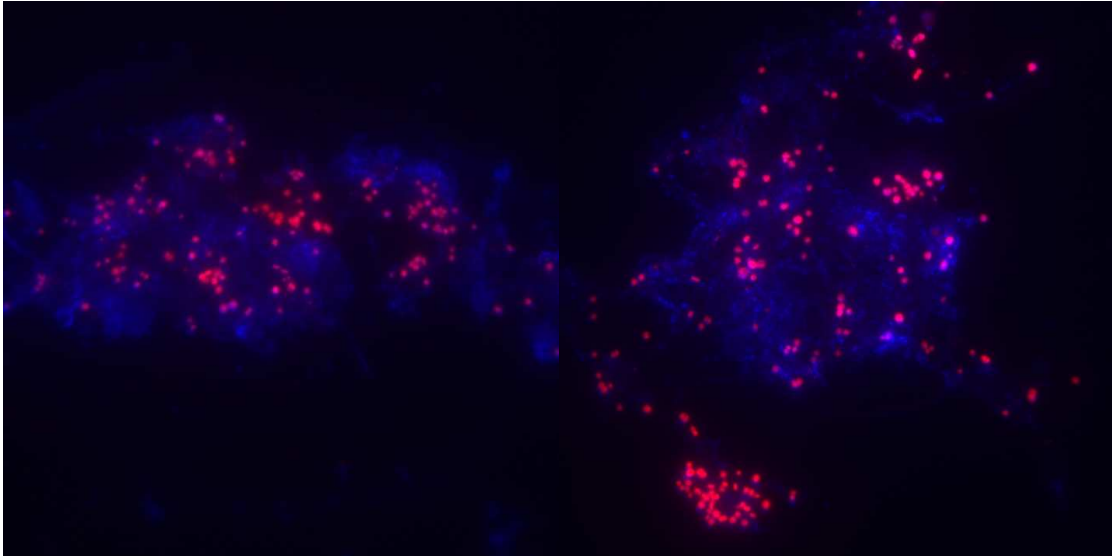


**Figure 13.** Images from FISH analysis of activated sludge from HPO system at Howard F. Curren Advanced Wastewater Treatment Plant. Magnification is 1000x. DAPI nucleic acid stain is indicated by blue, and the Acin0659 probe with Cy3 fluorescent marker is indicated by the pink-red color.

As described in 3.3.2, samples were taken from a reactor using activated sludge and primary effluent from the HPO system and exposed to chloramphenicol to produce RT-RiboSyn samples. Samples were also taken from the master reactor for COD analysis so that a determination could be made as to when the greatest microbial growth was occurring during the sampling period. Figure 14 shows the COD measurements over time from the master reactor.

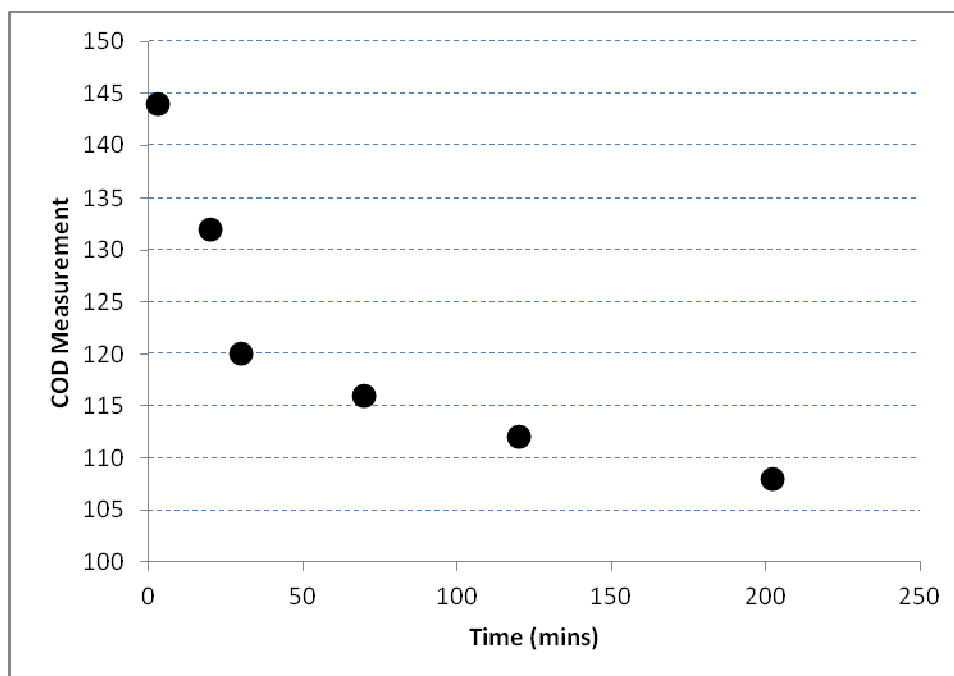


**Figure 14.** Filtered sample COD measurements versus time (minutes) from the master reactor.

COD measurements were taken as an indicator of bacterial activity in the sludge. These results were not available when sampling was being done, so sample sets were spread out over the course of the experiment in order to catch rapid growth or any abnormal growth behavior of interest. Based upon the results in Figure 14, the samples taken at 20 minutes after the mixing of the primary effluent and activated sludge in the master reactor were used for analysis. These samples represented as near to the maximum growth rates as possible.

As described in 3.2.2, RNA was extracted from the reactor samples and purified for the RT&PE process and analysis with the CEQ-8000 Beckman-Coulter Genetic Analysis system. Figure 14 shows two electropherograms of fragment analysis using the Eub338

primer that targets all bacteria. Parts (a) and (b) represent samples at zero and 28 minutes of exposure to chloramphenicol, respectively.

Figure 15 (a) and (b) both indicate a large cluster of peaks centered around fragment lengths of 350 nt, which is not unexpected as the Eub338 primer targets all bacteria present. If *Acinetobacter* genus organisms were present and growing at a rapid rate, what is expected is to have a peak or peaks at around 490 nt in length increasing in size between Figure 15 (a) and (b). There is a small peak in Figure 15b indicated at about 485 nt, however, it is below the threshold by which the CEQ-8000 can assign it a measured size. It is interesting to note, however, that there is a prominent peak at 447 nt. Since this peak represents fragments more than 40 nt shorter than the typical *Acinetobacter*, results as seen in Figure 11, the peak at 447 nt is not of the *Acinetobacter* genus. In order to determine the identity of the organism(s) creating that peak, a fragment analysis system that includes a sample collector would be needed so that the fragments could be sequenced.

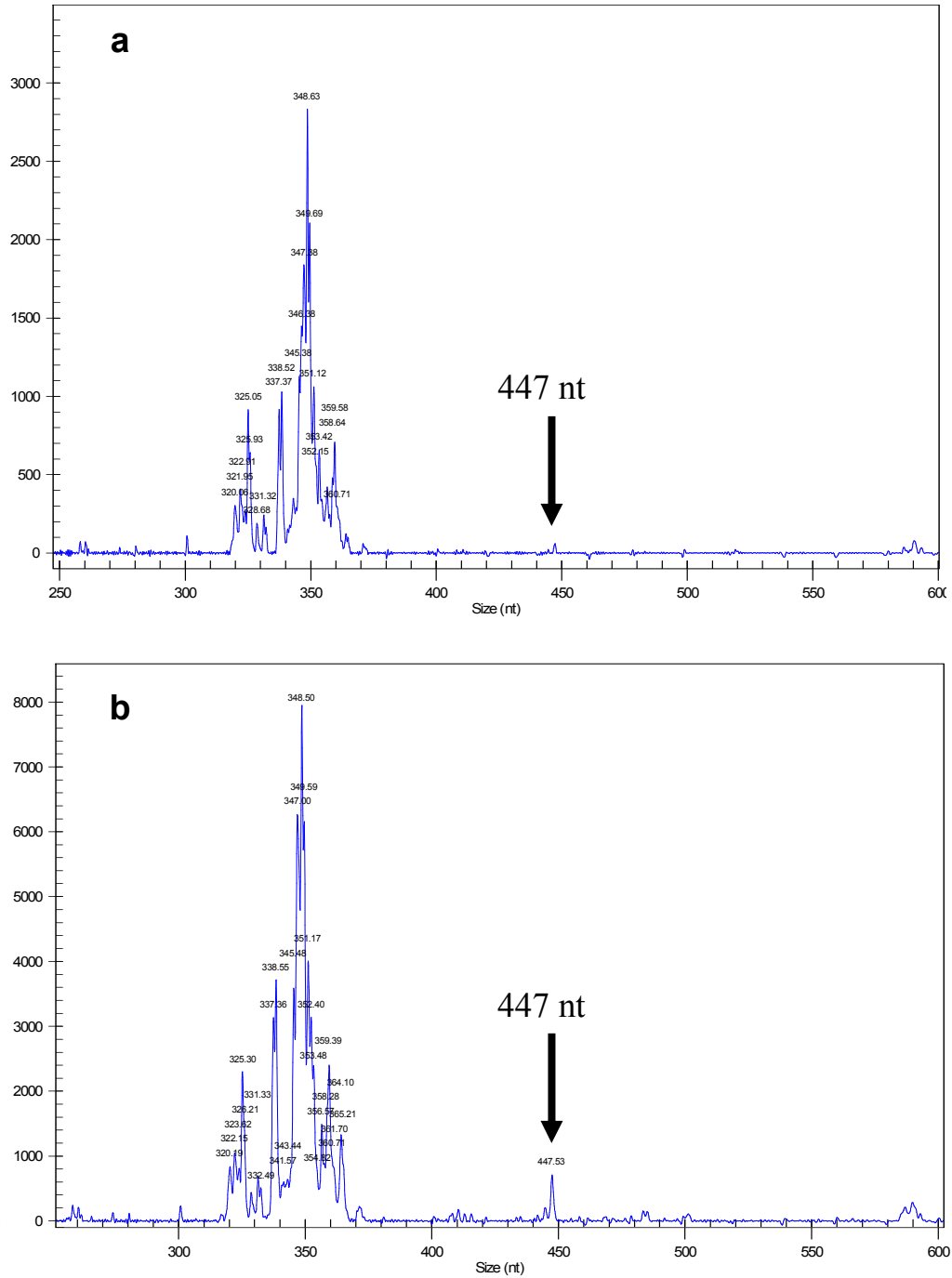


**Figure 15.** Electropherograms of RT-RiboSyn products taken from reactor with HPO system activated sludge at (a) zero minutes and (b) 28 minutes using the Eub338 primer.

Since this is the only significant peak indicated over the sampling period of this set of samples, it can only be assumed that this organism has the greatest specific growth rate under these conditions and may be responsible for the bulk of the decrease in COD over the sampling period. It is clear that the pre16S rRNA peak(s) expected at around 490 nt are not present, and so it must be concluded that *Acinetobacter* is not growing significantly during the sampling period.

An explanation for this low growth or stationary phase for *Acinetobacter* genus can be seen when looking at typical diurnal flow rate patterns for wastewater treatment plants. As mentioned earlier, the activated sludge and primary effluent samples were taken in the early morning. According to the typical diurnal pattern (Metcalf & Eddy, 2003), peak flows in wastewater treatment plants occur during the late morning to early afternoon (Curds, 1973), with a trough in flow rates at around 5 am. Based on this information, it is likely that most organisms in the HPO system at the time these samples were taken would be in stationary phase, and thus would not be growing. Further, Figure 14 indicates that it took over 200 minutes for the COD of the wastewater in the master reactor to drop by 36 mg/L, although most of that occurred within the first hour. As influent flow rates trough in the early morning hours, so do suspended solids and soluble biological oxygen demand (BOD). Organisms growing in those conditions may be adapted to grow on recalcitrant substrates, while other organisms such as *Acinetobacter* genus may require more readily-consumable substrates to grow at higher rates.

### **3.4.3 RT-RiboSyn Method with Pure Methanogen Culture and Anaerobic Digester Sludge**

It has been shown that the RT-RiboSyn method can be successfully applied to a pure eubacterial culture. RT-RiboSyn was also applied to a pure culture of methanogens, followed by targeting archaeal populations in anaerobic digester sludge.

#### **3.4.4 Results from *M. barkeri* RNA**

A culture of the methanogen *M. barkeri* was obtained from the Oregon Collection of Methanogens located at the Portland State University, and was grown using the starter media provided with the culture. An RT&PE was performed using the *M. barkeri* RNA and Arch915 primer as described in 3.3.2, with the exception of a 48° C primer extension step temperature. The product was analyzed via the CEQ-8000, and the results are shown in Figure 16, which represents eight RT&PE reactions. The average fragment size was 889.6 nt, with an average peak height and peak area of 33,789 and 71,284, respectively. The standard deviations for these three values are 0.41, 15,392, and 33,261, respectively.

These results indicate that the RT&PE method is applicable to archaeal populations. Using genome sequence data from 16S rRNA from the National Center for Biological Information (NCBI) (<http://www.ncbi.nlm.nih.gov/>), the predicted 16S fragment length for *M. barkeri* with the Arch915 primer is 879 nt, with a predicted length of 1037nt for the pre16S rRNA. The discrepancy between predicted and measured lengths of the 16S rRNA fragment in the electropherogram will be discussed later in this chapter. It should also be noted that the absence of the pre16S rRNA fragment in Figure 16 is expected, as it is simply beyond the scale of the CEQ analysis software.

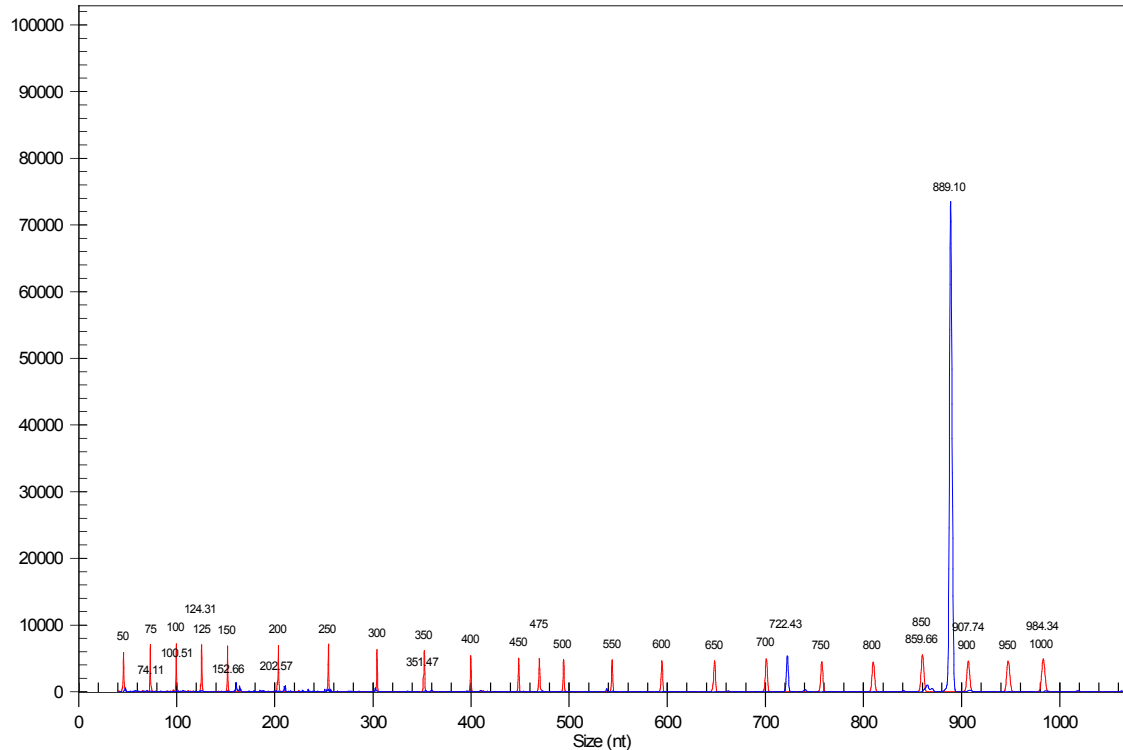


**Figure 16.** RT&PE fragment analysis for RNA from pure culture of *M. barkeri* generated with the Arch915 primer. The average fragment size for product from eight reactions is 889.6 nt with a standard deviation of 0.41 nt. The red peaks represent the size standard.

The method by which the 16S and pre16S fragment lengths are predicted for organisms of interest is shown in Figure 17. First, the Arch915 primer target site is found within the 16S rRNA sequence as shown, and then additional sequence information (200 nt on each end in this example and known as the intergenic spacer region) is added to the 5' and 3' ends of the 16S rRNA region.

To estimate the length of the pre16S "precursor" rRNA fragment, a sequence must be found in the 5' intergenic region that has a reverse complement in the 3' intergenic region. This is typically accomplished by using online tools such as the Basic Local Alignment

Search Tool (BLAST) (<http://blast.ncbi.nlm.nih.gov/Blast.cgi>) to aid in the search. Once the region is found, the length of the fragment between the 3' end of the Arch915 target site and the middle of the RNaseIII cut site in the 5' intergenic spacer region is the estimated length of the pre16S fragment. Using this method, the 16S and pre16S rRNA fragments for several methanogens of interest have been estimated, and the results are shown in Table 8.

Table 8 shows that there are predictions for fragment lengths that are similar amongst different organisms. This is to be expected due to the general nature of the primer (all archaea) and the similarity between the organisms. If a specific organism is to be targeted by this method, a genus or species-specific primer is needed to differentiate it from other organisms.

The length of the fragment between the 3' end of the Arch915 target site and the 5' end of the 16S rRNA sequence is the 16S "mature" rRNA fragment length.

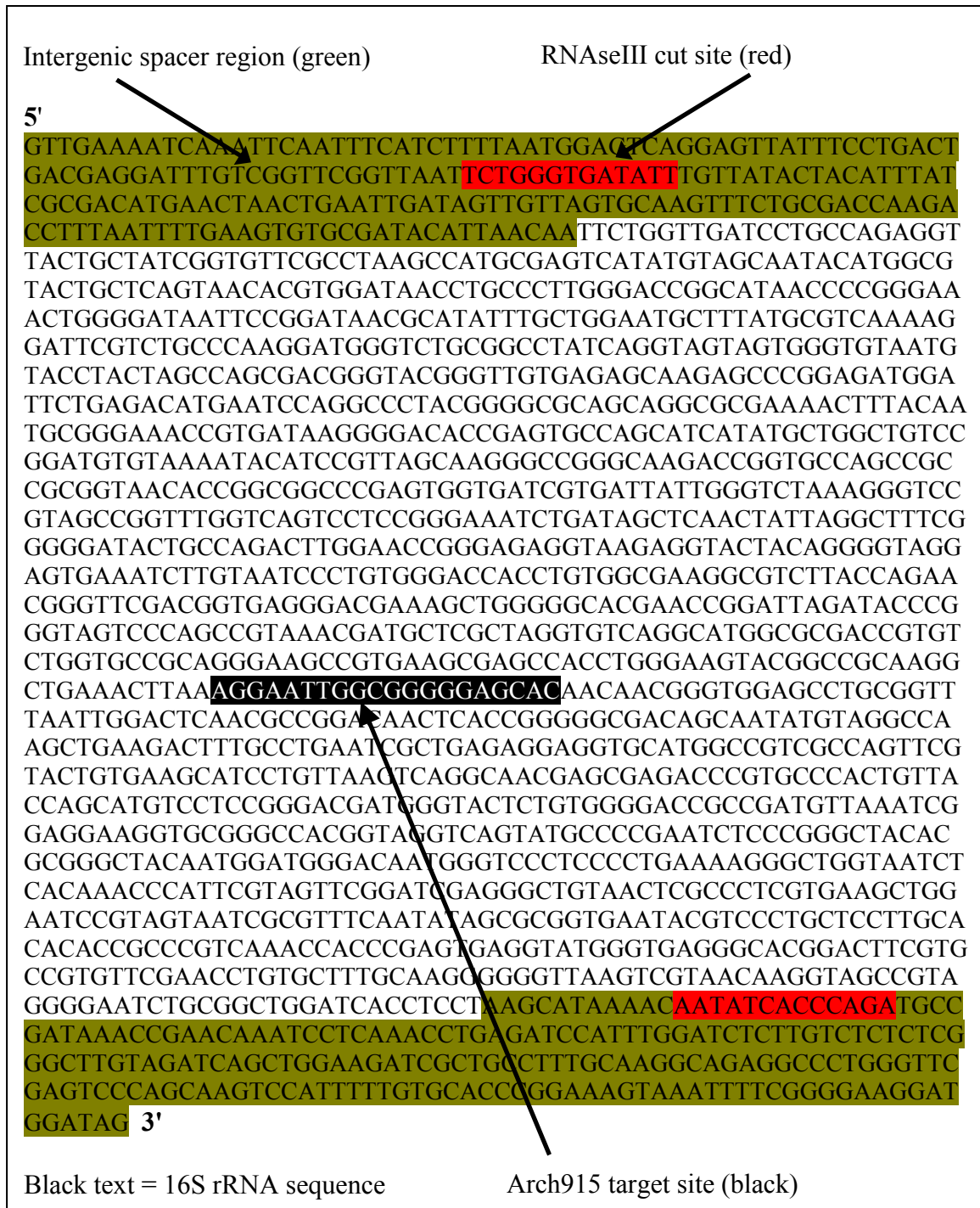


**Figure 17.** Example of how to estimate 16S and pre16S rRNA fragment lengths.

**Table 8.** Predicted lengths of 16S rRNA and pre16S rRNA fragments from RT&PE using the Arch915 primer for several methanogens.

Organism	NCBI Accession#	Fragment Length	
		16S	pre16S
<i>Methanosarcina barkeri</i>	NC_007355	879 nt	1037 nt
<i>Methanosarcina mazei</i>	NC_003901	875 nt	987 nt
<i>Methanococcus aeolicus</i>	NC_009635	870 nt	985 nt
<i>Methanobrevibacter smithii</i>	NC_009515	876 nt	963 nt
<i>Methanocorpusculum labreanum</i>	NC_008942	868 nt	990 nt
<i>Methanosphaera stadtmanae</i>	NC_007681	887 nt	967 nt
<i>Methanocaldococcus vulcanis</i>	NC_013407	875 nt	985 nt
<i>Methanococcoides burtonii</i>	NC_07955	877 nt	983 nt

### 3.4.5 RT-RiboSyn Results with Anaerobic Digester Sludge and Arch915 Primer

The final stage of this work was to apply this method to an environmental sample of interest, which in this case was anaerobic digester sludge.

Figures 18a and 18b present two electropherograms from the analysis of the  $t=4$  hours samples. The  $>800$  nt region of the electropherogram shown has been magnified for clarity. The two electropherograms are from two different wells in the well plate, however they are the same RT&PE product. The peaks present in the range of predicted

16S fragment lengths, as in Table 8, are 877 and 884 nt. The peak at 877 nt may represent either *M. burtonii* or *M. smithii*. Peaks further out at 950 and 987 nt may represent pre16S peaks, however Table 8 predicts only that the peak at 987 nt may be *M. mazei*.

Figures 19a and 19b are of two electropherograms from the analysis of the t=24 hours samples. Again, these are the same samples but from two different wells in the well plate. For Figure 19a, the peaks present in the range of predicted 16S lengths are 867, 876 and 884 nt, which may correspond to *M. labreanum* at 867 nt, and *M. vulcanis*, *M. mazei*, or *M. burtonii* at 876 nt. Figure 19b, indicates similar peaks and the same possible methanogens. Both figures also show peaks further out at 961 and 968 nt, which may pertain to the pre16S peaks of *M. smithii* and *M. stadtmannae*, respectively. However as in Figures 18a and 18b these do not correspond to any of the 16S peaks on the same electropherograms.

A few different explanations may account for these fragment size discrepancy issues. The first of these is that the genomic information from NCBI may not be correct, and the subsequent fragment length predictions are not correct as a result. Determining sequences for these organisms is beyond the scope of this work, so we are left to assume that these genomic data are correct. Another possibility is that the fragments being seen here are

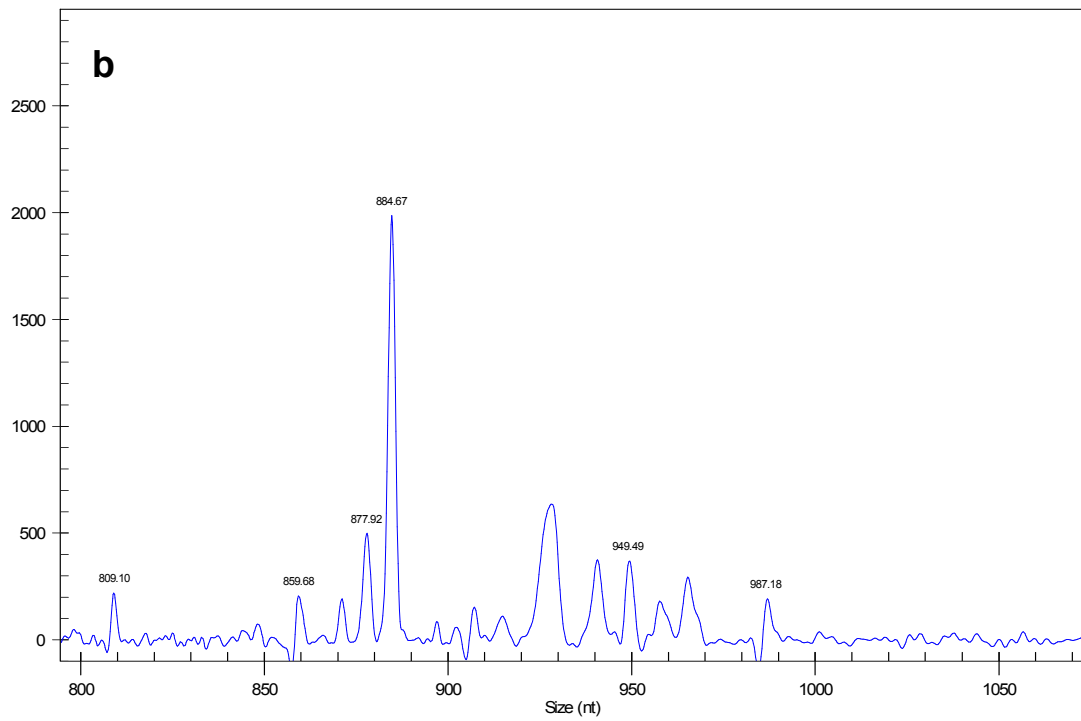
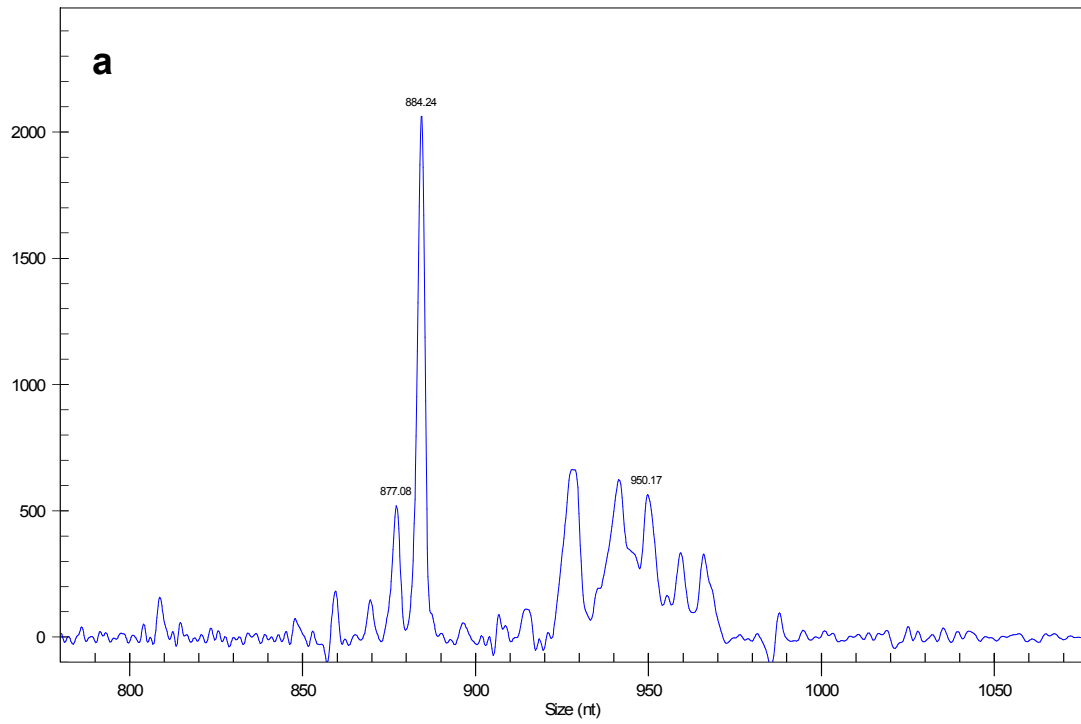


**Figure 18.** RT&PE fragment analysis for anaerobic digester sludge at t=4 hours using the Arch915 primer.

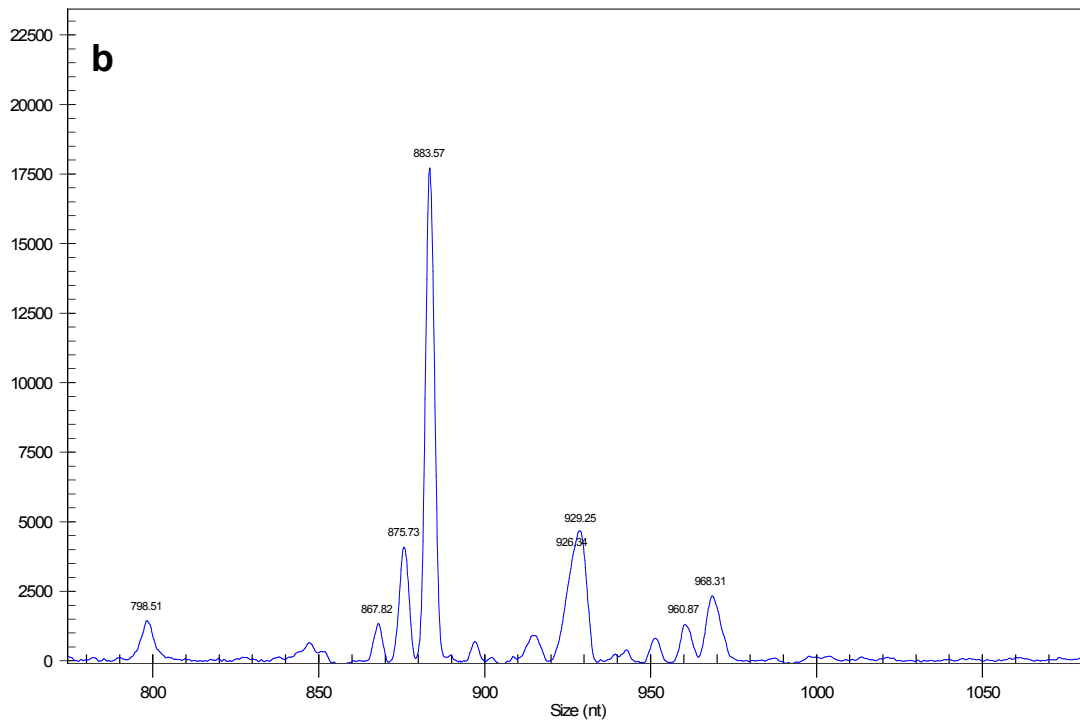
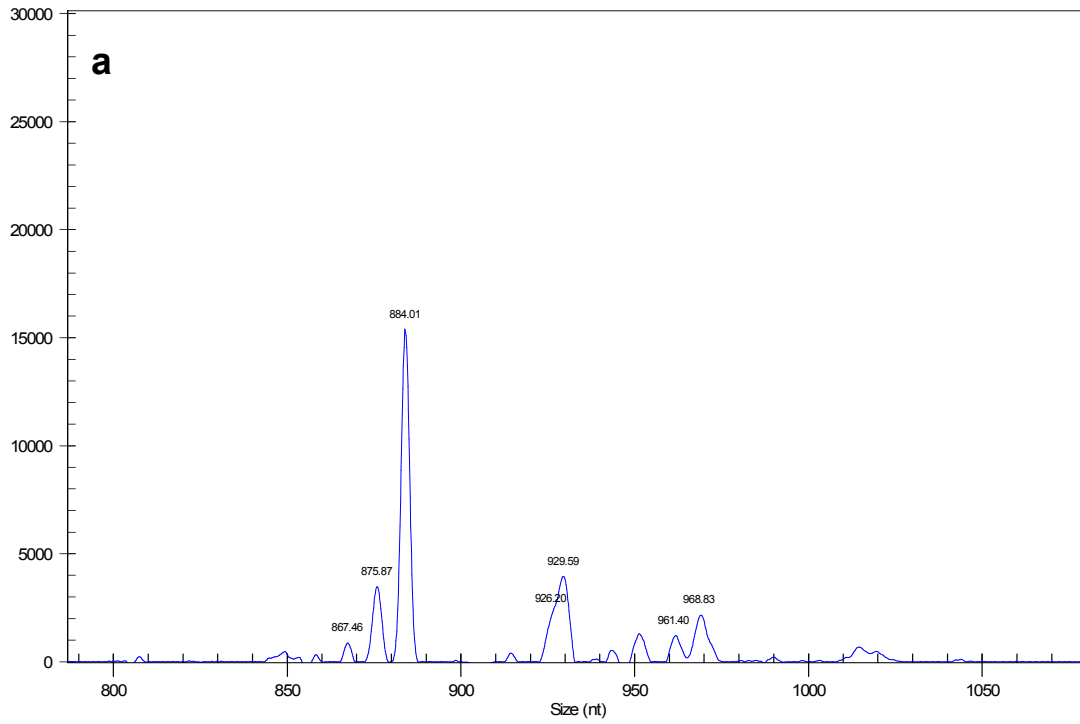


**Figure 19.** RT&PE fragment analysis for anaerobic digester sludge at t=24 hours using the Arch915 primer.

not the organisms predicted in Table 8, but are other (perhaps unsequenced) methanogens or other Archaea.

Another problem exists with the CEQ-8000 itself (S. Questa, personal communication, June 27, 2007). The company does not produce a size standard for the CEQ-8000 that is greater in length than 640 nt, therefore the machine itself does not support the use of size standards beyond this size. The reason for this is that the fragment analysis software uses a size calibration curve (fragment size vs. migration time) to determine the fragment sizes. As fragments get longer and further away from the 640 nt maximum, the fragment length prediction becomes more and more inaccurate. This can be seen in the size calibration curve results available from each electropherogram. The standard deviation from the calibration statistics from electropherograms for the Eub338 tests with the *A. calcoaceticus* fragments is typically about 0.5 nt. For the Arch915 tests using the 1000 nt size standard, the standard deviation averages 6.8 nt. This inaccuracy could account for the 10 nt difference between the predicted and actual size of the *M. barkeri* 16S fragments shown in Figure 15 and Table 8.

The CEQ-8000 is adequate for fragment peak detection in the >640 nt range. However accurate sizing is not guaranteed (S. Questa, personal communication, June 27, 2007). In addition, any peaks within the last 10% of the detection range (>900 nt) suffer from greater inaccuracy due to non-linearity in the size calibration curve in that range. Extending the capability of the CEQ-8000 has been discussed within Beckman-Coulter, focusing on creating a size standard out to 1000 nt or beyond and determining the accompanying operational parameters. However, they have no plans to do so at this time.

A further issue that may be present in these results is a lack of pre16S peak size due to slow growth conditions or low population concentration. Methanogens are known to be slow growing organisms, with typical doubling times on the order of days. They also typically represent a small percentage of the biomass present in anaerobic digester sludge. As the RT-RiboSyn method is dependent on the rate of ribosome synthesis, a slow-growing or low-population organism could be difficult to detect using the RT&PE method inherent in this procedure. Dismissing the problems with the CEQ-8000, and even if pre16S fragments were present in the sample, they may not be abundant enough due to slow growth conditions. This limitation renders the RT-RiboSyn method useful for organisms that are abundant or doubling at a rate that is detectable via production of pre16S fragments. Methanogens are both low in population and grow at a slow rate, indicating that they may not be easily detectable for specific growth rate analysis.

#### **3.4.6 RT-RiboSyn Results with Anaerobic Digester Sludge and Eub338 Primer**

In order to get a more complete picture of the application of the RT&PE method with anaerobic digester sludge, samples using the Eub338 primer were prepared in tandem with the Arch915 samples. It was expected that a large number of peaks at ~350 nt would be present in the fragment analyses from these samples, as the biomass of syntrophic bacteria is greater than that of the methanogens in anaerobic digester sludge. Figure 20 reveals this to be the case for a t=24 hour sample. At least two dozen peaks are labeled between 329 and 383 nt, indicating that there are many different bacterial organisms present. Due to the lack of chloramphenicol in the sample, there is no indication of pre16S fragment peaks beyond a few small peaks that are too small to be readable.

If one were to use this method to investigate the growth rate of a specific organism in an environmental sample such as anaerobic digester sludge, it is recommended that a more specific primer be used to target that organism than Eub338 or Arch915. Eub338 has the potential to produce many peaks as in Figure 20, and Arch915 to produce peaks that are within a size range that cannot be trusted to be accurate.

Using genomic information to synthesize a primer to target the methanogens of interest so that smaller fragments are generated is a possibility. Another option would be to use a different machine than the CEQ-8000, such as the Applied Biosystems 3130XL as an example.

Working with environmental samples such as anaerobic digester sludge in the future, one would also be advised to use other methods first to determine the populations present within the sample prior to investigation with RT-RiboSyn. Fingerprinting methods such as Terminal Restriction Fragment Length Polymorphism (T-RFLP) would be beneficial in determining which organisms to target with specific primers.

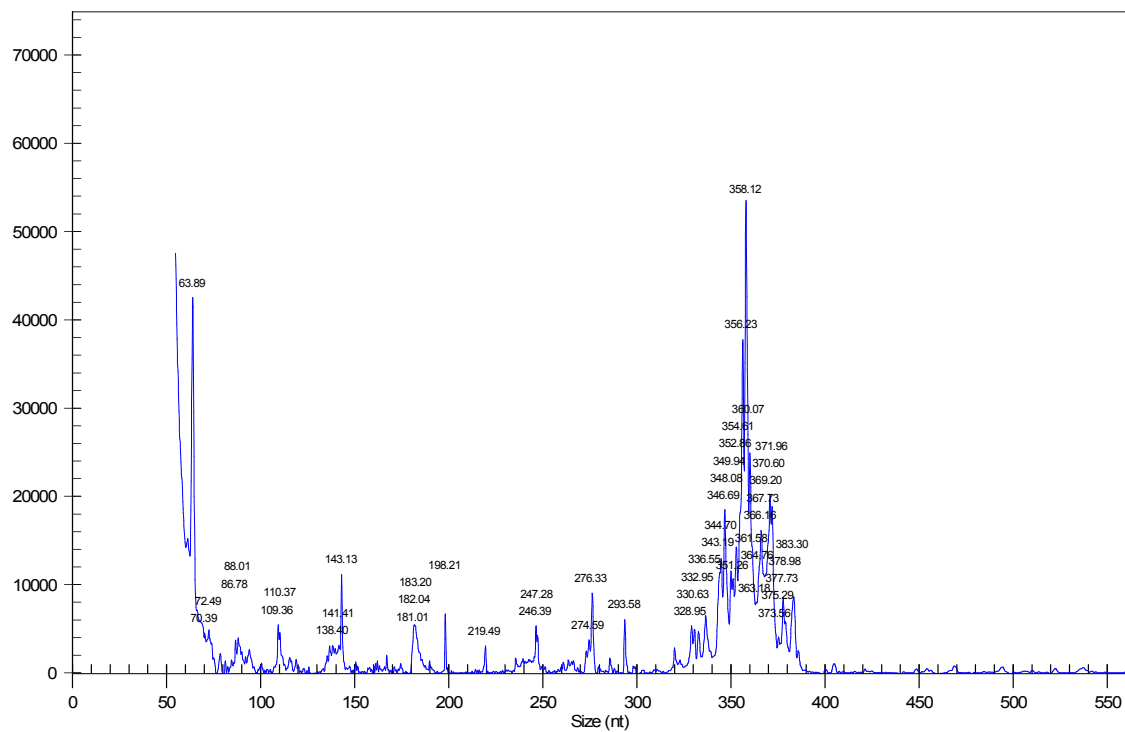


**Figure 20.** RT&PE fragment analysis for sludge at t=24 hours using the Eub338 primer.

## **CHAPTER 4: CONCLUSIONS**

A simple F/M-based anaerobic digestion model was designed that predicted biogas output more accurately than a commercially-available model. A molecular biology assay was created to take advantage of the reverse transcription and primer extension method to determine the specific growth rate of microorganisms. The following conclusions can be made from this work.

### **4.1 F/M-Based Anaerobic Digestion Model**

- The SBG test is simple and fast and allows for the calibration of the F/M model for the prediction of biogas production, which has been shown to be reasonably accurate in comparison to three laboratory-scale reactors. The model predicts and average steady-state biogas output within 5.0%, 14.3%, and 9.5% for 10-day, 15-day, and 20-day HRT reactors, respectively.
- A commercially-available model, BioWin 3, over-predicted the average biogas output of the anaerobic digesters by 52.4%, 108.5%, and 97.0% for 10-day, 15-day, and 20-day HRT reactors, respectively.
- The F/M model was less accurate for the reactor with a 20-day HRT, but this may be due to an initial overload condition or shifting microbial population dynamics.
- The parameter F/M is a function of OLR and HRT and monitoring it could improve the operation of existing anaerobic digesters.

- The F/M model is relatively simple to set-up and customize for an anaerobic digester without the need for dozens of parameters, which are inherent to more complex models such as BioWin 3. Rather than spending days or weeks to calibrate, the F/M model can be calibrated in a few hours.
- The F/M model is not restricted to a particular feed or sludge type, as it could be used to model a variety of anaerobic digestion processes after an SPC test. The model could also be useful for evaluating strategies for start-up of new reactors or the re-seeding of reactors that have been shut down for various reasons.

#### **4.2 RT-RiboSyn Method**

- The RT-RiboSyn method has been shown to closely predict the specific growth rate of *A. calcoaceticus* under different growth conditions using standard culture media. As compared to a traditional spectrophotometric method and using a Eub338 primer, the specific growth rate was measured within 1.6%, 10.0%, and 3.1% for cultures grown at 25°, 30°, and 35° C, respectively.
- The RT-RiboSyn method also indicated when a culture was in stationary phase.
- When applied to the sludge from a high-purity oxygen activated sludge system and using an Eub338 primer, the presence of many types of bacteria was determined but not the presence of pre16S rRNA for the *Acinetobacter* genus. The specific growth rate was not able to be determined. This may be due to a stationary phase condition.

- Attempts to grow a pure culture of a methanogen were not successful, but the RT-RiboSyn method was able to detect 16S rRNA from *M. barkeri*, indicating its applicability to Archaea.
- Application of the RT-RiboSyn method to determine the specific growth rates of methanogens in anaerobic digester sludge indicated the presence of Archaea, however growth rates were not able to be determined.
- Limitations of the capillary electrophoresis system used, as well as the small population concentration and slow growth rates of methanogens in anaerobic digester sludge appear to be the greatest hindrances to this method for these anaerobic digestion sludge samples.
- For microorganism populations that are slow growing or in low concentrations in a sample, a modified version of RT-RiboSyn may be needed. A new version incorporating real time quantitative reverse transcription polymerase chain reaction (Real Time qRT-PCR) could overcome the issues inherent to slow growth and low population concentration.

## REFERENCES

- Amann, R., H. Lemmer, and Wagner, M. (1998) Monitoring the community structure of wastewater treatment plants: a comparison of old and new techniques. *FEMS Microbiology Ecology*. 25:205-215.
- Amann, R., and Ludwig, W. (2000) Ribosomal RNA-targeted nucleic acid probes for studies in microbial ecology. *Fems Microbiology Reviews*. 24(5):555-565.
- American Public Health Association (1999) Standard Methods for Examination of Water & Wastewater 20th ed. Washington D.C., USA.
- Angelidaki, I., and Ahring, B.K. (1993) Thermophilic anaerobic digestion of livestock waste: effect of ammonia. *Environ. Biotech.* 38(4):560-564.
- Arnaiz, C., Gutierrez, J.C., and Lebrato, J. (2006) Biomass stabilization in the anaerobic digestion of wastewater sludges. *Biores. Tech.* 97(10):1179-1184.
- Balch, W.E., Fox, G.E., Magrum, L.J., Woese, C.W., and Wolfe, R.S. (1979) Methanogens: Reevaluation of a Unique Biological Group. *Microb. Rev.* 43:260-296.
- Batstone, D., Keller, J., Newell, B., and Newland, M. (1997) Model development and full scale validation for anaerobic treatment of protein and fat based wastewater. *Water Sci. and Tech.* 36:423-431.
- Batstone, D.J., Keller, J., Newell, R.B., and Newland, M. (2000a) Modeling anaerobic degradation of complex wastewater. I: model development. *Biores. Tech.* 75:67-74.

- Batstone, D.J., Keller, J., Newell, R.B., and Newland, M. (2000b) Modeling anaerobic degradation of complex wastewater. II: parameter estimation and validation using slaughterhouse effluent. *Biores. Tech* 75:75-85.
- Batstone, D.J., Keller, J., Angelidaki, I., Kalyuzhnyl, S.V., Pavlostathis, S.G., Rozzi, A., Sanders, W.T.M., Siegrist, H., and Vavilin, V.A. (2002) The IWA anaerobic digestion model No 1 (ADM1). *Water Sci. and Tech.* 45:65-73.
- Baumann, U., and Müller, M.T. (1997) Determination of anaerobic biodegradability with a simple continuous fixed-bed reactor. *Water Res.* 31:1513-1517.
- Bill Kruppa, Operations Manager of Lakeland Wastewater Reclamation Plant, Lakeland, FL (personal communication, November 3, 2011)
- Blumensaat, F., and Keller, J. (2005) Modeling of two-stage anaerobic digestion using the IWA anaerobic digestion model No. 1 (ADM1). *Water Res.* 39:171-183.
- Boone, D.R., Johnson, R.L. and Liu, Y. (1989) Diffusion of the interspecies electron carriers H<sub>2</sub> and formate in methanogenic ecosystems and its implications in the measurement of K<sub>m</sub> for H<sub>2</sub> or formate uptake. *Appl. Environ. Microbiol.* 55:1735-1741
- Boubaker, F., and Ridha, B.C. (2008) Modeling of the mesophilic anaerobic co-digestion of olive mill wastewater with olive mill solid waste using anaerobic digestion model No. 1 (ADM1). *Biores. Tech.* 99:6565-6577.
- Britschgi, T.B., Cangleosi, G.A. (1998) Rapid and Sensitive Detection of Antibiotic-Resistant Mycobacteria Using Oligonucleotide Probes Specific for Ribosomal RNA Precursors. US Patent #5,726,021.
- Brock, T. D. (1961) Chloramphenicol. *Bacteriol. Rev.* 25:32-48.
- Cakmakci, M. (2003) Adaptive neuro-fuzzy modeling of anaerobic digestion of primary sedimentation sludge. *Bioproc. and Biosys. Eng.* 30(5):349-357.

- Cangelosi, G.A., and Brabant, W.H. (1997) Depletion of Pre-16S rRNA in Starved *Escherichia coli* cells. *J. Bacteriol.* 179:4457-4463.
- Corominas, L., Rieger, L., Takács, I., Ekama, G., Hauduc, H., Vanrolleghem, P.A., Oehmen, A., Gernaey, K.V., van Loosdrecht, M.C.M., and Comeau, Y. (2010) New framework for standardized notation in wastewater treatment modeling. *Water Sci. and Tech.* 61(4):841-857.
- Costello, D.J., Greenfield, P.F., and Lee, P.L. (1991) Dynamic modeling of a single-stage high-rate anaerobic reactor. *Water Res.* 25:847-871.
- Curds, C.R. (1973) A theoretical study of factors influencing the microbial population dynamics of the activated-sludge process – II. A computer simulation study to compare two methods of plant operation. *Water Res.* 7(10):1439:1452.
- Cutter, M.R., and Stroot, P.G. (2008) Determination of Specific Growth Rate by Measurement of Specific Rate of Ribosome Synthesis in Growing and Nongrowing Cultures of *Acinetobacter calcoaceticus*. *Appl. Environ. Microbiol.* 74 (3):901-903.
- Dhillon, A., Level, M., Lloyd, K.G., Albert, D.B., Sogin, M.L., and Teske, A. (2005) Methanogen Diversity Evidenced by Molecular Characterization of Methyl Coenzyme M Reductase A (*mcrA*) Genes in Hydrothermal Sediments of the Guyamas Basin. *Appl. Environ. Microbiol.* 71:4592-4601.
- Eastman, J.A., Ferguson, J.F. (1981) Solubilization of particulate organic carbon during the acid phase of anaerobic digestion. *Journal Water Pollution Control Federation* 53:352-366.
- Forster, S., Snape, J.R., Lappin-Scott, H.M., and Porter, J. (2002) Simultaneous fluorescent gram staining and activity assessment of activated sludge bacteria. *Appl. Environ. Microbiol.* 68(10):4772-4779.

Galagan, J.E., Nusbaum, C., Roy, A., Endrizzi, M.G., Macdonald, P., FitzHugh, W., Calvo, S., Engels, R., Smirnov, S., Atnoor, D., Brown, A., Allen, N., Naylor, J., Stange-Thomann, N., DeArellano, K., Johnson, R., Linton, L., McEwan, P., McKernan, K., Talamas, J., Tirrell, A., Ye, W., Zimmer, A., Barber, R.D., Cann, I., Graham, D.E., Grahame, D.A., Guss, A.M., Hedderich, R., Ingram-Smith, C., Kuettner, H.C., Krzycki, J.A., Leigh, J.A., Li, W., Liu, J., Mukhopadhyay, B., Reeve, J.N., Smith, K., Springer, T. A., Umayam, L.A., White, O., White, R.H., de Macario, E.C., Ferry, J.G., Jarrell, K.F., Jing, H., Macario, A.J.L., Paulsen, I., Pritchett, M., Sowers, K.R., Swanson, R.V., Zinder, S.H., Lander, E., Metcalf, W.W., and Birren, B. (2002). The Genome of *M. acetivorans* Reveals Extensive Metabolic and Physiological Diversity. *Genome Res.* 12:532-542.

Garcia, J.L., Patel, B.K.C., and Olliver, B. (2000) Taxonomic, phylogenetic, and ecological diversity of methanogenic *Archaea*. *Anaerobe.* 6:205-226.

Gavala, H.N., Angelidaki, I., and Ahring, B.K. (2003) Kinetics and modeling of anaerobic digestion process. *Adv. in Biochem. Eng.* 81:57-93.

Griffin, M.E., McMahon, K.D., Mackie, R.I., and Raskin, L. (1998) Methanogenic population dynamics during start-up of anaerobic digesters treating municipal solids waste and biosolids. *Biotech. and Bioeng.* 57(3):342-355.

Hales, B.A., Edwards, C., Ritchie, D.A., Hall, G., Pickup, R.W., and Saunders, J.R. (1996) Isolation and Identification of methanogen-specific DNA from blanket bog peat by PCR amplification and sequence analysis. *Appl. Environ. Microbiol.* 62:668-675.

Hallam, S.J., Girguis, P.R., Preston, C.W., Richardson, P.M., and DeLong, E.F. (2003) Identification of Methyl Coenzyme M Reductase A (*mcrA*) Genes Associated with Methane-Oxidizing Archaea. *Appl. Environ. Microbiol.* 69:5483-5491.

Haug, R.T., Stuckey, D.C., Gosset, J.M., and McCarty, P.L. (1978) Effect of Thermal Pretreatment on Digestibility and Dewaterability of Organic Sludges. *Journal Water Pollution Control Federation* 50:73-85.

Hoh, C.Y., and Cord-Ruwisch, R. (1996) A practical kinetic model that considers endproduct inhibition in anaerobic digestion processes by including the equilibrium constant. *Biotech. and Bioeng.* 51:597-604.

- Ince, O. (1998) Performance of a two-phase anaerobic digestion system when treating dairy wastewater. *Water Res.* 32(9):2707-2713.
- Jemiolo, D.K. (1996) Processing of prokaryotic ribosomal RNA, p. 453-468. In R.A. Zimmermann and A.E. Dahlberg (ed.), *Ribosomal RNA. Structure, evolution, processing, and function in protein synthesis*. CRC Press, New York, NY.
- Kabouris, J., Pavlostathis, Sp., Tezel, U., Engelmann, M., Dulaney, J., Todd, A., and Gillette, B. (2008) Anaerobic Degradability of Pinellas County Sludge & FOG at Mesophilic & Thermophilic Temperatures. *Fla. Water Res. J.*, June:38-45.
- Kleerebezem, R., and Stams A.J.M. (2000) Kinetics of syntrophic cultures: a theoretical treatise on butyrate fermentation. *Biotech. and Bioeng.* 67:529-543.
- Kolář, L., Klimeš, F., Gergel, J., Kužel, S., Kobes, M., Ledvina, R., and Šindelářová, M. (2005) Methods to evaluate substrate degradability in anaerobic digestion and biogas production. *Plant Soil and Env.* 51:173-178.
- Lee, N., Nielsen, P.H., Andreasen, K.H., Juretschko, S., Nilesen, J.L, Schleifer, K-H., and Wagner, M.(1999) Combination of Fluorescent In Situ Hybridization and Microautordiography-- a New Tool for Structure-Function Analyses in Microbial Ecology. *Appl Environ. Microbiol.* 65(3):1289-1297.
- Leuders, T., Chin, K-J., Conrad, R., and Friedrich, M. (2001) Molecular analyses of methyl-coenzyme M reductase  $\alpha$ -subunit (*mcrA*) genes in rice field soil and enrichment cultures reveal the methanogenic phenotype of a novel archaeal lineage. *Env. Microbiol.* 3:194-204.
- Loy, A., Horn, M., Wagner, M. (2003) probeBase - an online resource for rRNA-targeted oligonucleotide probes. *Nucleic Acids Res.* 31:514-516.
- McMahon, K.D., Zheng, D., Stams, A.J.M., Mackie, R.I., and Raskin, L. (2004) Microbial population dynamics during start-up and overload conditions of anaerobic digesters treating municipal solid waste and sewage sludge. *Biotechnology and Bioengineering* 87(7):823-834.

- Michaud, S. Bernet, N., Buffière, P., Roustan, M., and Moletta, R. (2002) Methane yield as a monitoring parameter for the start-up of anaerobic fixed film reactors. *Water Res.* 36(5):1385-1391.
- Monod, J. (1942) Recherches sur la croissance des cultures bacteriennes. Herman et Cle., Paris.
- Monod, J. (1949) The Growth of Bacterial Cultures. *Ann. Rev. of Microbio.* 3:371-394.
- Morel, E., Tartakovsky, B., Guiot, S.R., and Perrier, M. (2006) ADM1 application for tuning and performance analysis of a multi-model observer-based estimator. *Water Sci. and Tech.* 54:93-100.
- Moss, A.R. (1993) Methane, Global Warming and Production by Animals. Chalcombe Publications, Kingston, UK.
- Newell, R.B., and Cameron I.T. (1991) Numerical integration of many balances for user simulation (NIMBUS): *Users manual*. CAPE Centre. The University of Queensland, Brisbane, Australia.
- Nielsen, J.L., Christensen, D., Kloppenborg, M., and Nielsen, P.H. (2003) Quantification of cell-specific substrate uptake by probe-defined bacteria under *in situ* by microautoradiography and fluorescence *in situ* hybridization. *Environ. Microbiol.* 5(3):202-211.
- Noike, T., Endo, G., Chang, J.E., and Matsumoto, J.I. (1985) Characteristics of carbohydrate degradation and the rate-limiting step in anaerobic digestion. *Biotech. and Bioeng.* 27:1482-1489.
- Oerther, D.B., Pernthaler, J., Schramm, A., Amann, R., and Raskin, L. (2000) Monitoring Precursor 16S rRNAs of *Acinetobacter* spp. in Activated Sludge Wastewater Treatment Systems. *Appl. Environ. Microbiol.* 66:2154-2165.
- Oerther, D.B., van Loosdrecht, M.C.M., and Raskin, L. (2002) Quantifying the impact of wastewater micronutrient composition on *in situ* growth activity of *Acinetobacter* spp. *Water Sci. and Tech.* 46:443-47.

- Pace, N.R. (1973) Structure and Synthesis of the Ribosomal Ribonucleic Acid of Prokaryotes. *Bacteriol. Rev.* 37:562-603.
- Parker, W.J. (2005) Application of the ADM1 model to advanced anaerobic digestion. *Biores. Tech.* 96:1832-1842.
- Pasztor, I., Thury, P., and Pulai, J. (2009) Chemical oxygen demand fractions of municipal wastewater for modeling of wastewater treatment. *Int. J. Environ. Sci. Tech.* 6(1):51-56.
- Pavlostathis, S.G., and Gossett, J.M. (1986) A kinetic model for anaerobic digestion of biological sludge. *Biotech. and Bioeng.* 28:1519-1530.
- Pollard, P.C. (1998) Estimating the Growth Rate of a Bacterial Species in a Complex Mixture by Hybridization of Genomic DNA. *Microb. Ecol.* 36(2):111-20.
- Possot, O., Gernhardt, P., Klein, A., and Sibold, L. (1988) Analysis of drug resistance in the archaeobacterium *Methanococcus voltae* with respect to potential use in genetic engineering. *Appl. Environ. Microbiol.* 54:734-740.
- Ramsay, I.R., Pullammanappallil, P., Newell, R.B., and Lee, P.I. (1994) Basis for dynamic modeling of anaerobic degradation of protein-based wastewater. *Proceedings of 22<sup>nd</sup> Australian Chemical Engineering Conference*, Perth, 25-28 September 1994. 232-242.
- Rittmann, B.E., and McCarty, P.L. (2001) *Environmental Biotechnology: Principles and Applications*. McGraw-Hill, New York, NY.
- Rodriguez-Fonseca, C., Amils, R., and Garrett, R.A. (1995) Fine structure of the peptidyl transferase centre on 23S-like rRNAs deduced from chemical probing of antibiotic-ribosome complexes. *J. Mol. Biol.* 247:224-235.
- Rosen, C., Vrecko, D., Gernaey, K.V., Pons, M.N., and Jeppsson, U. (2006) Implementing ADM1 for plant-wide benchmark simulations in Matlab/Simulink. *Water Sci. and Tech.* 54:11-19.

- Sanders, W.T.M., Geerink, M., Zeeman, G., and Letting, G. (2000) Anaerobic hydrolysis kinetics of particulate substrates. *Water Sci. and Tech.* 41:17-24.
- Schmid, M., Schmitz—Esser, S., Jetten, M., and Wagner, M. (2001) 16S-23S rDNA intergenic spacer and 23S rDNA of anaerobic ammonium-oxidizing bacteria: implications for phylogeny and *in situ* detection. *Environ. Microbiol.* 3:450-59.
- Siegrist, H., Vogt, D., Garcia-Heras, J.L., and Gujer, W. (2002) Mathematical Model for Meso- and Thermophilic Anaerobic Sewage Sludge Digestion. *Env. Sci. Tech.* 36(5):1113-1123.
- Sosnowski, P., Wieczorek, A., and Ledakowicz, S. (2003) Anaerobic co-digestion of sewage sludge and organic fraction of municipal solid wastes. *Adv. Env. Res.* 7(3):609-161.
- Srivastava, A.K., Schlessinger, D. (1990) Mechanism and Regulation of Bacterial Ribosomal RNA Processing. *Ann. Rev. Microbiol.* 44:105-129.
- Stahl, D.A., Flesher, B., Mansfield, H.R., and Montgomery, L. (1988) Use of phylogenetically based hybridization probes for studies of ruminal microbial ecology. *Appl. Environ. Microbiol.* 54:1079-84.
- Steve Questa, Beckman-Coulter, Inc., Brea, CA (personal communication, June 27, 2011)
- Stroot, P.G., and Oerther, D.B. (2003) Elevated precursor 16S rRNA levels suggest the presence of growth inhibitors in wastewater. *Water Sci. Technol.* 47:241-50.
- Stroot, P.G. (2004) Ph.D. Dissertation. University of Cincinnati, Cincinnati. Novel transcription method confirms growth inhibition of bacteria exposed to domestic wastewater.
- Tim Ware, Plant Manager of the Howard F. Curren Advanced Wastewater Treatment Plant, Tampa, FL (personal communication, October 28, 2011)

- Tchobanoglous, G., Burton, F.L., Stensel, H.D., and Metcalf & Eddy. (2003) Wastewater Engineering: Treatment and Reuse, McGraw-Hill (4<sup>th</sup> ed.), New York, NY.
- Tiehm, A., Nickel, K., Zellhorn, M., Neis, U. (2001) Ultrasonic waste activated sludge disintegration for improving anaerobic stabilization. *Water Res.* 35:2003-2009.
- Valentini, A., Garuti, G., Rozzi, A., and Tilche, A. (1997) Anaerobic degradation kinetics of particulate organic matter: a new approach. *Water Sci. and Tech.* 36:239-246.
- Vasiliev, V.B., Vavilin, V.A., Rytov, S.V., and Ponomarev, A.V. (1993) Simulation model of anaerobic digestion of organic matter by a microorganism consortium: Basic equations. *Water Res.* 20(6).
- Vavilin, V.A. (1996) Modeling of volatile fatty acids degradation kinetics and evaluation of microorganism activity. *Biores. Tech.* 57(1):69-80.
- Vavilin, V.A., Rytov, S., Lokshina, L., Pavlostathis S.G., and Barlaz M.A. (2003) Distributed model of solid waste anaerobic digestion: Effects of leachate recirculation and pH adjustment. *Biotech. and Bioeng.* 81:66-73.
- Vavilin, V.A., Lokshina, L., Jokela, J.P.Y., and Rintala, J.A. (2004) Modeling solid waste decomposition. *Biores. Tech.* 94:69-81.
- Woese, C. (1987) Bacterial Evolution. *Microb. Rev.* 51:221-271.

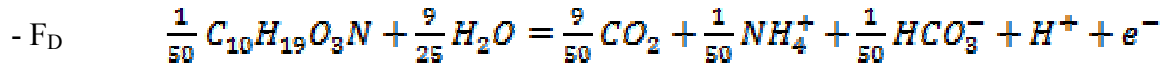
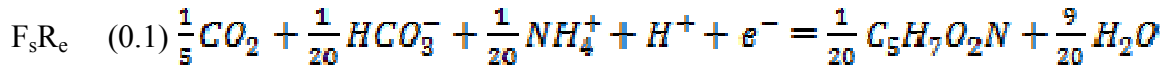
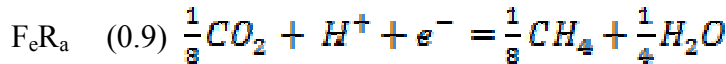
## **APPENDICES**

## Appendix A. F/M Anaerobic Digestion Model Supplemental Material

### A.1. Equations to Determine the Biogas Generation per Feed Destroyed

These calculations pertain to the blended feed used in the experimental reactors, and represent an upper limit on the production of biogas from PS and WAS. As wastewater is not 100% biodegradable, a degradable fraction for each feed stream ( $F_{PS}$ ,  $F_{WAS}$ ) is added in the model to allow the user to account for this limit.

Contribution to biogas production from digestion of primary sludge where  $F_s = 0.1$  and  $F_e = 0.9$ :



Resulting in the balanced equation:



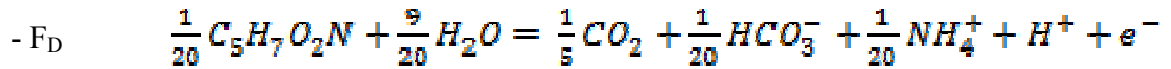
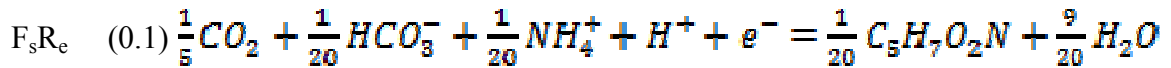
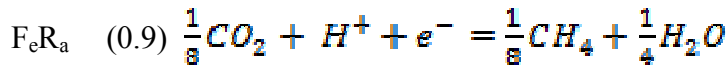
On a mass basis,  $C_{10}H_{19}O_3N = 201$  g/mol wastewater. For each 4.02 g wastewater ( $C_{10}H_{19}O_3N$ ), 1.8 g  $CH_4$  and 2.09 g  $CO_2$  is generated which is 0.16 mol of biogas:

Appendix A (continued)

$$\frac{0.16 \text{ mol biogas}}{0.002 \text{ mol } C_{10}H_{19}O_3N} \cdot \frac{22.4 \text{ L biogas}}{\text{mol}} \cdot \frac{1000 \text{ mL}}{\text{L}} \cdot \frac{1 \text{ mol } C_{10}H_{19}O_3N}{201 \text{ g}}$$

$$= 891.5 \frac{\text{mL biogas}}{\text{g PS wastewater}} = 0.892 \frac{\text{m}^3 \text{ biogas}}{\text{kg VS destroyed}}$$

Contribution to biogas production from digestion of waste activated sludge where  
 $F_s = 0.1$  and  $F_e = 0.9$ :



Resulting in the balanced equation:



On a mass basis,  $C_5H_7O_2N = 113 \text{ g/mol biomass (WAS)}$ . For each 5.65 g WAS  
 ( $C_5H_7O_2N$ ), 1.8 g  $CH_4$  and 2.97 g  $CO_2$  is generated which is 0.18 mol of biogas:

$$\frac{0.18 \text{ mol biogas}}{0.05 \text{ mol } C_5H_7O_2N} \cdot \frac{22.4 \text{ L biogas}}{\text{mol}} \cdot \frac{1000 \text{ mL}}{\text{L}} \cdot \frac{1 \text{ mol } C_5H_7O_2N}{113 \text{ g}}$$

$$= 713.6 \frac{\text{mL biogas}}{\text{g PS wastewater}} = 0.714 \frac{\text{m}^3 \text{ biogas}}{\text{kg VS destroyed}}$$

## Appendix A (continued)

As the wastewater feed blend is mixed in known quantities, the biogas contributions are averaged:

$$G_{FD} = 0.803 \frac{m^3 \text{ biogas}}{kg \text{ VS destroyed}}$$

This is in agreement with the 0.75-1.12 m<sup>3</sup> biogas/kg VSS destroyed as published previously (Metcalf and Eddy, 2003).

## Appendix A (continued)

### A.2. F/M Anaerobic Digestion Model Code

```
□ degradable_primary(t) = degradable_primary(t - dt) + (incoming_degradable_primary - wasted_degradable_primary -
digested_primary) * dt
INIT degradable_primary = 0.61
INFLOWS:
  ↳ incoming_degradable_primary = PULSE(((Daily_primary_feed*degradable_fraction_of_PS))/cycles,0,1/cycles)
OUTFLOWS:
  ↳ wasted_degradable_primary = PULSE(((degradable_primary/retention_time)/cycles),0,1/cycles)
  ↳ digested_primary = (Primary_gas_production/gpfd)
□ degradable_WAS(t) = degradable_WAS(t - dt) + (incoming_degradable_WAS - wasted_degradable_WAS - digested_WAS) * dt
INIT degradable_WAS = 0.46
INFLOWS:
  ↳ incoming_degradable_WAS = PULSE((((Daily_WAS_feed)*degradable_fraction_of_WAS))/cycles,0,1/cycles)
OUTFLOWS:
  ↳ wasted_degradable_WAS = PULSE(((degradable_WAS/retention_time)/cycles),0,1/cycles)
  ↳ digested_WAS = (WAS_gas_production/gpfd)
□ Microbes(t) = Microbes(t - dt) + (microbe_growth - wasted_microbes - decay) * dt
INIT Microbes = 9.06
INFLOWS:
  ↳ microbe_growth = (yield_primary*digested_primary)+(yield_WAS*digested_WAS)
OUTFLOWS:
  ↳ wasted_microbes = PULSE((((Microbes/retention_time)/cycles)),0,1/cycles)
  ↳ decay = Microbes*decay_rate
□ nondegradable_primary(t) = nondegradable_primary(t - dt) + (incoming_ND_primary - wasted_ND_primary) * dt
INIT nondegradable_primary = 0
INFLOWS:
  ↳ incoming_ND_primary = PULSE(((Daily_primary_feed)*(1-degradable_fraction_of_PS))/cycles,0,1/cycles)
OUTFLOWS:
  ↳ wasted_ND_primary = Pulse((((nondegradable_primary/retention_time)/cycles)),0,1/cycles)
□ nondegradable_WAS(t) = nondegradable_WAS(t - dt) + (incoming_ND_WAS - wasted_ND_WAS) * dt
INIT nondegradable_WAS = 0
INFLOWS:
  ↳ incoming_ND_WAS = PULSE((((Daily_WAS_feed)*(1-degradable_fraction_of_WAS)))/cycles,0,1/cycles)
OUTFLOWS:
  ↳ wasted_ND_WAS = PULSE(((nondegradable_WAS/retention_time)),0,1/cycles)
UNATTACHED:
  ↳ Primary_gas_production = (prim_constant+(prim_x_coeff*FM_PS)+(prim_x2_coeff*FM_PS^2))*Microbes
UNATTACHED:
  ↳ WAS_gas_production = (WAS_constant+WAS_x_coeff*FM_WAS+WAS_x2_coeff*FM_WAS^2)*Microbes
```

---

## Appendix A (continued)

- Cycles = 1
- Daily\_primary\_feed = 0.61
- Daily\_WAS\_feed = 0.457
- Decay\_gas = gpfd\*decay
- decay\_rate = 0.1
- degradable\_fraction\_of\_PS = 1
- degradable\_fraction\_of\_WAS = 1
- FM\_PS = degradable\_primary/Microbes
- FM\_WAS = degradable\_WAS/Microbes
- gpfd = 803
- prim\_constant = 640.55
- prim\_x2\_coeff = -1.3465
- prim\_x\_coeff = 71.061
- retention\_time = 20
- Total\_Biogas\_Production = Primary\_gas\_production+WAS\_gas\_production+(gpfd\*decay)
- Total\_FM = (degradable\_primary+decay)/Microbes
- WAS\_constant = 39.885
- WAS\_x2\_coeff = 0
- WAS\_x\_coeff = 5.5132
- yield\_primary = 0.24
- yield\_WAS = 0.17

## **Appendix B. Expanded Methods and Materials**

### **B.1. Sampling Protocol for RT-RiboSyn**

The RT-RiboSyn method requires a careful sampling procedure prior to RNA extraction and purification. Whether dealing with a pure culture or an environmental sample, the procedure is largely the same, however the concentration of chloramphenicol added to the sample will differ. Prior to sampling, a concentrated solution of chloramphenicol will need to be prepared and stored on ice. Solutions that will be used at a later date can be frozen for long term storage.

Chloramphenicol powder is added to DI water or DEPC-treated (RNase-free) water to a concentration of 1000 mg/L. This can be made more concentrated to 5000 mg/L if dilution of the target sample is a concern. A mixing table makes this step easier, as a stir bar can be added to the bottle and left to mix over a longer period of time. A low level of heat (no more than 35-45° C) can also be added to the solution to speed up the dissolution of the powder. Once the liquid is clear, it should be aliquoted to smaller tubes for freezer storage and ease of use.

Based on experiences with different kinds of samples, it has been found that pure culture samples (grown in broth) respond favorably to a final concentration of 20 µg/L of chloramphenicol. For environmental samples, such as wastewater, a final concentration of 100-200 µg/L of chloramphenicol is best to overcome absorption by extraneous material in the sample.

## **Appendix B (continued)**

The time frame for sampling should be estimated based on the assumed specific growth rate of the target organism(s) in the sample. Faster growing organisms should be sampled at shorter time intervals than slower growing organisms. For instance, *Escherichia coli* should be sampled every few minutes, whereas slower growing organisms might be sampled every 4-6 hours. Samples should be taken from a chloramphenicol-treated sample at least five to six times over the course of the sampling time frame.

### **B.1.1. Protocol**

- 1.) Chloramphenicol solution is added to a subsample of the master biological sample to reach the desired final concentration of chloramphenicol in the sample.
- 2.) A timer is started and the first sample is taken. Typically, samples are taken in 2 ml screw-top microcentrifuge tubes for later RNA extraction. Two to four samples are taken at each time step.
- 3.) Centrifuge samples immediately for 3-5 minutes at a minimum 10,000 g force.
- 4.) Decant samples and immediately place in -80° C freezer for storage until ready for RNA extraction.
- 5.) Repeat steps 2-4, taking samples at regular desired intervals.

## **Appendix B (continued)**

### **B.2. Phenol-Chloroform RNA Extraction Method (Stahl *et al*, 1988)**

Materials needed: pH 5.1 Phenol and buffer, 10% Sodium dodecyl sulfate (SDS) solution, Chloroform, RNase-free water, Pure Ethanol, 0.1 mm diameter RNase-free Zirconium beads, 2mL snap-cap and screw-cap micro centrifuge tubes

Equipment needed: Water bath (set to 60° C), Micro centrifuge, Vortex Genie, Freezers (-20° C and -80° C), Cell disruptor (such as Disruptor Genie® or Beadbeater)

#### **B.2.1. Sample Preparation**

Samples are prepared in 2 mL screw-cap tubes to allow for cell disruption without spillage. The most crucial part of the sample preparation is to not overload the Phenol with organic material that does not contain RNA. Depending on the sample type, samples may need to be split into several tubes to prevent overloading. A typical sample should be 100-300 mg of wet cell mass.

In each sample tube, add the following to the sample in order listed: pH 5.1 buffer to bring volume to 0.5 mL, 0.5 g Zirconium beads, 100 µL 10% SDS solution, and then pH 5.1 Phenol to within about 5 mL of the top of the sample tube. It is important to leave some headspace in order to allow the cell disruptor to work properly. In subsequent steps, each sample must be maintained in separate tubes. Meaning, samples should not be combined.

## **Appendix B (continued)**

### **B.2.2. Cell Disruption and RNA Isolation**

- 1.) Place sample tubes in cell disruptor and turn it to maximum power. If using the Beadbeater, set the time for 2 minutes. If using the Disruptor Genie®, set it for 5 minutes.
- 2.) Place samples in 60° C water bath for 10 minutes.
- 3.) Repeat step 1.
- 4.) Centrifuge samples at 5000 rpm for 5 minutes to pelletize the Zirconium beads.
- 5.) Transfer aqueous (clear) and organic phase (remaining liquid) to a new snap-cap tube. Leave zirconium beads in screw-cap tube.
- 6.) Rinse beads with 200 mL of the pH 5.1 buffer. Vortex tube to ensure good washing.
- 7.) Place samples in cell disruptor for 1 min (Beadbeater) or 3 minutes (Disruptor Genie®).
- 8.) Centrifuge samples at 5000 rpm for 5 minutes to pelletize the Zirconium beads.
- 9.) Transfer remaining aqueous and organic phases to the previously collected samples.
- 10.) Centrifuge samples at 10,000 rpm for 10 minutes to separate aqueous and organic phases.
- 11.) Transfer the aqueous phase to a new snap-cap tube. Avoid transferring the protein (white layer) to the new tube.
- 12.) If needed, the samples can be refrigerated at this point for a short time

## **Appendix B (continued)**

### **B.2.3. RNA Purification**

- 1.) Add 1 mL of pH 5.1 Phenol to each sample and vortex tube to mix thoroughly.
- 2.) Centrifuge samples at 10,000 rpm for 10 minutes to separate aqueous and organic phases.
- 3.) Transfer aqueous phase to a new tube.
- 4.) Prepare a mixture of four parts Phenol to 1 part Chloroform. Avoid adding the buffer phase from the Phenol tube.
- 5.) To each sample, add an equal volume of 4:1 Phenol:Chloroform and vortex the tubes to mix thoroughly.
- 6.) Centrifuge the samples at 10,000 rpm for 10 minutes to separate aqueous and organic phases.
- 7.) Transfer the aqueous phase to a new tube.
- 8.) Repeat steps 17 through 19.
- 9.) Add an equal volume of Chloroform to each sample and vortex the tubes to mix thoroughly.
- 10.) Centrifuge the samples at 10,000 rpm for 10 minutes to separate aqueous and Chloroform phases. Tilting the tube back about 30° and pipetting from the front of the tube will aid in extracting the aqueous phase from the Chloroform.
- 11.) Transfer the aqueous phase to a new tube. Add two volumes of pure Ethanol to each sample and vortex to mix thoroughly. Place the samples in a -20° C freezer overnight or a -80° C freezer for 30 minutes.

**Appendix B (continued)**

- 12.) Centrifuge the samples at 13,200 rpm (maximum speed) for 30 minutes.
- 13.) Decant each sample carefully and leave caps open. Place sample tubes on their sides on a clean surface to dry. Depending on conditions, this could take a few hours.
- 14.) Once dry, resuspend the bead of nucleic acids in the sample tubes in RNase-free water to a desired volume. 10-30  $\mu\text{L}$  is typical.
- 15.) Store samples at  $-80^{\circ}\text{C}$  for long term storage.

## **Appendix B (continued)**

### **B.3. RNAqueous® Kit for RNA Purification**

The RNAqueous® kit is a molecular biology product made by Ambion, Inc. (Austin, TX) that can be used to purify total RNA from small samples of tissue or cultured cells. It utilizes a guanidinium thiocyanate solution to lyse cells inactivate ribonucleases. For this work, it is used to further purify the RNA extracted with the Phenol-Chloroform RNA extraction method. Prior to using this method, a dry bath should be preheated to 70° C. Equipment needed: Dry bath (set to 70° C), Micro centrifuge, Vortex Genie, Freezer (-80° C)

#### **B.3.1. Protocol**

- 1.) Samples are mixed with twelve (12) times the volume of the Lysis/Binding solution. Vortex the sample tubes and let the samples sit for a few minutes at room temperature. This solution makes the RNA stick to the cartridge filter used in the following steps.
- 2.) Add 60 µL of the Elution Solution for each sample being treated to two 500 µL tubes. It is advised to use more than is needed, since some evaporation may occur. Depending on the number of samples being treated, more than two tubes may be needed.
- 3.) Add an equal volume of 64% ethanol solution to each sample tube.

## **Appendix B (continued)**

- 4.) Place a filter cartridge into fresh tubes (both provided with kit) so that you have a filter/tube combination for each sample tube. Add up to 700  $\mu\text{L}$  of each sample to the corresponding filter cartridge tube. Centrifuge the filter cartridge tubes at 10,000 g for 1 minute. Discard filtered liquid.
- 5.) If there is more than 700  $\mu\text{L}$  to filter, repeat step 3 until all the liquid has been filtered.
- 6.) Apply 700  $\mu\text{L}$  of Wash Solution #1 to each tube and centrifuge at 10,000 g for 1 minute. Discard filtered liquid.
- 7.) Apply 500  $\mu\text{L}$  of Wash Solution #2/#3 to each tube and centrifuge at 10,000 g for 1 minute and discard filtered liquid.
- 8.) Repeat step 7. Once filtered liquid has been discarded, replace the filter cartridge and centrifuge for an additional 30 seconds.
- 9.) Move the filter cartridges to fresh sample tubes, and discard the original tubes.
- 10.) Place the sample tubes into the centrifuge with the snap caps opened. Aliquot 60  $\mu\text{L}$  of the hot Elution Solution to the middle of each filter. This step must be completed swiftly.
- 11.) Once the Elution Solution has been added to each tube, quickly close the snap cap on each tube and centrifuge the tubes at 10,000 g for 30 seconds.
- 12.) Repeat step 10 and collect the 120  $\mu\text{L}$  of filtrate in the same tube.
- 13.) Discard the filter cartridge and add half the volume (60  $\mu\text{L}$ ) of Lithium Chloride to each sample and vortex for 1 second to mix thoroughly.
- 14.) Incubate the samples at  $-20^{\circ}\text{C}$  for 30 minutes.

**Appendix B (continued)**

- 15.) Centrifuge at maximum speed (13,200 rpm) for 15 minutes to concentrate the RNA at the bottom of the tubes. Use a pipette to carefully remove the supernatant from each tube.
- 16.) Add 25  $\mu$ L of cold 70% ethanol solution to each tube. Centrifuge at maximum speed for 5 minutes. Carefully remove supernatant.
- 17.) Leave caps open and place sample tubes on their sides on a clean surface to dry. Depending on conditions, this could take a few hours.
- 18.) Once dry, resuspend the bead of nucleic acids in the sample tubes in RNase-free water to a desired volume. 10-30  $\mu$ L is typical. Store samples at  $-80^{\circ}$  C for long term storage.

## **Appendix B (continued)**

### **B.4. DNA-free™ DNase Treatment Kit for DNA Removal**

The DNA-free™ DNase Treatment kit is a molecular biology reagent kit manufactured by Ambion, Inc. (Austin, TX) that can be used to remove trace amounts of contaminant DNA from RNA samples. It utilizes DNase I to remove DNA from RNA samples, followed by a DNase Removal Reagent to deactivate the DNase I. For this work, this kit is used after the RNAqueous® kit as a final purification step prior to the reverse transcription (RT) step.

Equipment needed: Water bath (set to 37° C), Micro centrifuge, Vortex Genie, Freezer (-80° C)

#### **B.4.1. Protocol**

- 1.) Add 0.1 volume of 10x DNase I buffer to each sample.
- 2.) Add 2 µL of DNase I to each sample. Mix each sample gently using a Vortex Genie.
- 3.) Place samples in 37° C water bath for 1 hour.
- 4.) Add 0.1 volume of DNase Removal Agent to each sample. Flick tubes gently to mix samples with agent.
- 5.) Incubate samples at room temperature for 2 minutes, gently mixing several times during the incubation period.
- 6.) Centrifuge samples at 10,000 g for 1.5 minutes.

## **Appendix B (continued)**

- 7.) Transfer supernatant of each sample to new tubes. Leave the DNase I Removal Agent (white) behind. Store the purified RNA samples at  $-80^{\circ}\text{C}$  for long term storage.

## **Appendix B (continued)**

### **B.5. ImProm-II™ Reverse Transcription System**

The ImProm-II™ Reverse Transcription System is a molecular biology kit manufactured by Promega Corporation (Madison, WI) for the synthesis of first-strand cDNA typically for preparation of samples prior to PCR amplification. For this work, we are not using PCR, so in fact we utilize just the cDNA copies synthesized by this process.

If these samples are to be analyzed using the Beckman-Coulter CEQ-8000 system, the primer used will need to have a WellRed fluorescent label. If the user is interested in extending the life of the kit, the reactions can be cut volumetrically in half.

Equipment needed: Water bath or heating block set to 25° C, Heating block set to 85° C, Water bath set to 37° C, and Water bath set to temperature required for primer (e.g. 42° C for Eub338, or 47° C for Acin0659 primer), Vortex Genie, shaved ice with container, Freezer (-80° C)

#### **B.5.1. Protocol**

- 1.) Prepare a master mix in one tube from the materials in the kit in the following order and amounts for each sample: 6.5 µL RNase-free water, 4.0 µL 5x Reaction buffer, 2.0 µL MgCl<sub>2</sub> solution, 1.0 µL dNTP mix, 0.5 µL RNAsin inhibitor, and 1.0 µL RTase. While preparing this mix, place the tube in an ice bath.

## **Appendix B (continued)**

- 2.) Prepare samples on ice by mixing them with the primer to be used. This mixture can be up to 5  $\mu\text{L}$  for each sample. For instance, a sample/primer mix might be 3  $\mu\text{L}$  RNA solution with 2  $\mu\text{L}$  primer solution. However, the amount of RNA should be limited to 1  $\mu\text{g}$  of material.
- 3.) Add 15  $\mu\text{L}$  of master mix to each sample. Anneal the samples at 25° C for 5 minutes.
- 4.) Anneal the samples for 1 hour in a water bath at the temperature required for the primer being used.
- 5.) Move the samples to the 85° C heating block for 15 minutes to deactivate the RNAsin inhibitor.
- 6.) While waiting during Step 5, prepare an ice/water bath so as to create a firm slurry. Once the 15 minutes are elapsed, quickly move the samples to the ice bath and leave them there for 5 minutes.
- 7.) Add two volumes (usually 40  $\mu\text{L}$ ) of RNase A cocktail to each sample.
- 8.) Place the samples in a 37° C water bath for 30 minutes.
- 9.) The samples are now ready for fragment analysis.

**Appendix B (continued)**

**Table B1.** Annealing temperatures for selected WellRed-labelled primers.

<b>Primer</b>	<b>Annealing Temperature (°C)</b>
Eub338	42° C
Acin0659	47° C
Arch915	48° C

## Appendix B (continued)

### B.6. Fluorescence *in situ* Hybridization (FISH) Protocol (Amman *et al*, 1990)

#### B.6.1. Buffer Preparation

##### 1.) Hybridization buffer

Combine the following (in order) in a 2 ml microcentrifuge tube:

360  $\mu$ L 5M NaCl solution

40  $\mu$ L 1M Tris-HCl solution

X  $\mu$ L deionized formamide (depending on needed % for chosen probe)

e.g. a probe requiring 20% formamide would need 400  $\mu$ L formamide

Deionized water to 2 mL total volume

2  $\mu$ L 10% SDS solution

Preheat a hybridization oven to 46° C

##### 2.) Washing buffer

Combine the following (in order) in a 50 mL conical tube:

1 mL 1M Tris-HCl solution

Y  $\mu$ L 5M NaCl solution (see Table B2 to determine required volume)

e.g. Y=2150  $\mu$ L for 20% formamide concentration in the hybridization buffer

Z  $\mu$ L 0.5M EDTA solution (see Table B2 to determine required volume)

e.g. Z=500  $\mu$ L for 20% formamide concentration in the hybridization buffer

Fill to 50 mL using deionized water

## **Appendix B (continued)**

50  $\mu$ L 10% SDS solution

Place cap on tube and put tube in 48° C water bath (upright)

### **B.6.2. Placing Sample(s) on Slide**

- 1.) Mark slides with pencil, as pen or marker will wash off in the Washing Buffer
- 2.) Dot ~2  $\mu$ L of stored FISH sample per slide well (see Figure B1)
- 3.) Place the slide in the hybridization oven for 5 minutes
- 4.) Dehydrate slides in 50%, 80%, and 100% ethanol for 1 minute each – this is best accomplished by having three 50 mL conical tubes of these solutions ready for use.  
  
Lower the slide into the 50% ethanol/water solution for 1 minute, remove with tweezers and shake to remove excess liquid, and place into the 80% ethanol tube.  
  
Repeat with the 100% ethanol tube.
- 5.) Dry slide in hybridization oven for 1 minute.

### **B.6.3. *In situ* Hybridization Buffer**

- 1.) For each slide well containing sample, 10  $\mu$ L of *in situ* hybridization buffer will be required.

## Appendix B (continued)

- 2.) Prepare the *in situ* hybridization buffer by mixing 1  $\mu\text{L}$  of fluorescently labeled probe (50 ng/ $\mu\text{L}$ ) with 9  $\mu\text{L}$  of hybridization buffer for each sample being tested. For instance, 8 samples will require 8  $\mu\text{L}$  of fluorescently labeled probe mixed with 72  $\mu\text{L}$  of hybridization buffer. It is also prudent to mix an extra quantity to ensure full coverage of the samples with *in situ* hybridization buffer. A good practice is to mix 20% more than is needed.

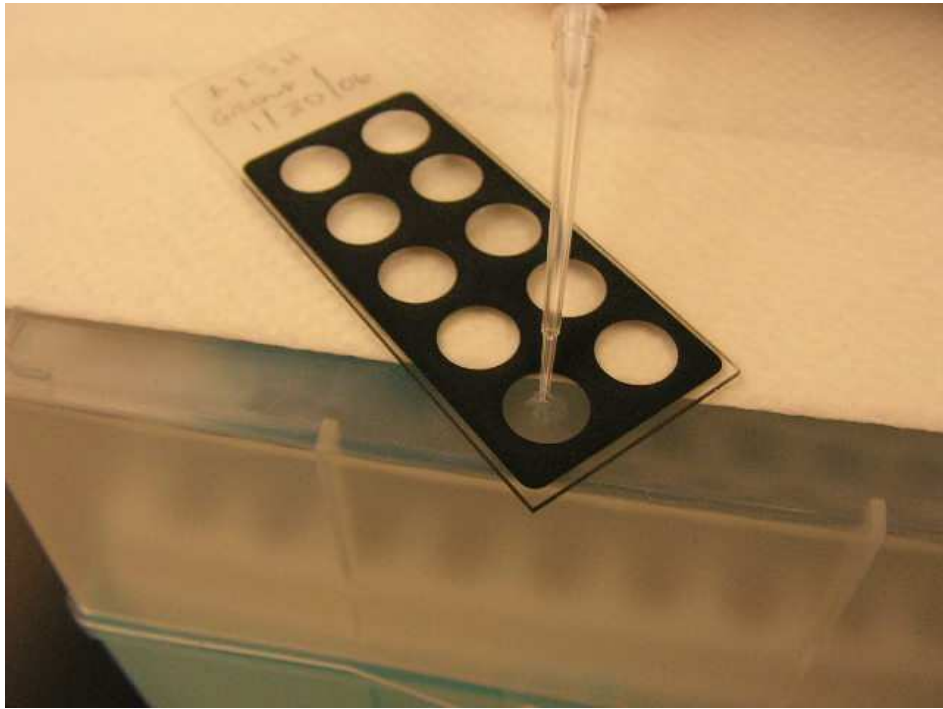


**Figure B1.** Dotting sample(s) on slide well(s).

- 3.) Apply 10  $\mu\text{L}$  of *in situ* hybridization buffer (from step 3b) to each well containing sample. Make sure the material in the sample is covered completely by the buffer.

## Appendix B (continued)

- 4.) Add the sample slide well-side up to the hybridization chamber and place a folded Kimwipe into the hybridization chamber as shown in Figure B2. Add remainder of hybridization buffer to the Kimwipe so that it is soaked.
- 5.) Keep the chamber horizontal as to prevent contamination of the slide wells and the samples they contain. Replace lid on hybridization chamber.
- 6.) Place hybridization chamber(s) in hybridization oven at 46° C for 60-120 minutes.

### B.6.4. Move Slides to Washing Buffer

- 1.) Remove sample slide from hybridization chamber(s) and rinse them with a small amount of Washing Buffer. This is to remove excess probe.
- 2.) Place the slide into the tube of Washing Buffer for 30 minutes at 48° C. Replace cap on the tube of Washing Buffer.

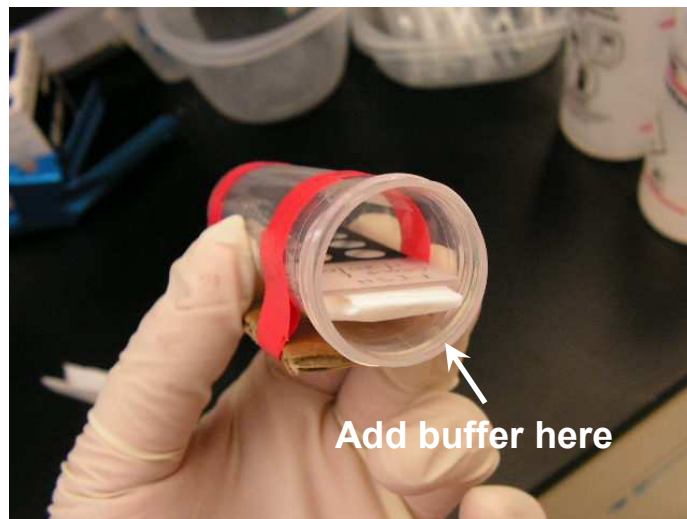


**Figure B2.** Placing sample slide and folded Kimwipe in hybridization chamber.

## **Appendix B (continued)**

### **B.6.5. Rinse Slide and Store**

- 1.) Remove slide from Washing Buffer and rinse in a beaker of deionized water.
- 2.) Shake slide to remove excess water and store at an angle to allow for drying. Keep the slide out of direct light to prevent bleaching of fluorescent label of the probe.
- 3.) Slides can be stored in a container (50 mL conical tube is ideal) in the dark at -20° C at this point if desired. Otherwise, carry on to DAPI staining. Drying should take no more than 15 minutes.

### **B.6.6. Counter Stain Cells with DAPI Nucleic Acid Stain**

- 1.) Prepare a DAPI solution of 1 µg/mL. The volume required is 100 µL per sample well. As was the case with the *in situ* hybridization buffer, it is prudent to make more than needed to ensure total coverage of the sample wells.
- 2.) Using a pipette, add approximately 100 µL of DAPI stain solution to each sample well on the slide and let sit undisturbed for 1 minute.
- 3.) Shake slide in sink to remove DAPI stain from slide, and then gently swirl the slide in a beaker of deionized water. This entire step should be performed in just a few seconds.
- 4.) Shake slide to remove excess water and store at an angle to allow for drying. Keep the slide out of direct light to prevent bleaching of DAPI or fluorescent label of the probe. Drying should take no more than 15 minutes.
- 5.) Once dry, the samples are ready for epifluorescent microscope examination.

**Appendix B (continued)**

**Table B2.** Washing buffer formulation depending on formamide concentration in the hybridization buffer.

<b>% formamide in hybridization buffer</b>	<b>NaCl mM</b>	<b>5M NaCl (=Y) μl</b>	<b>0.5M EDTA μl</b>
0	900	9000	-
5	636	6300	-
10	450	4500	-
15	318	3180	-
20	225	2150	500
25	159	1490	500
30	112	1020	500
35	80	700	500
40	56	460	500
45	40	300	500
50	28	180	500
55	20	100	500
60	14	40	500
65	10	-	500
70	7	-	350
75	5	-	250
80	3.5	-	175
85	2.5	-	125
90	1.75	-	88
95	1.24	-	62

For formamide concentrations of 65% and greater, enough NaCl is present in the EDTA for adequate washing.

## Appendix C. Reprint of Published RT-RiboSyn Article

### C.1. Full AEM Article

APPLIED AND ENVIRONMENTAL MICROBIOLOGY, Feb. 2008, p. 901–903  
0099-2241/08/\$08.00+0 doi:10.1128/AEM.01899-07  
Copyright © 2008, American Society for Microbiology. All Rights Reserved.

Vol. 74, No. 3

## Determination of Specific Growth Rate by Measurement of Specific Rate of Ribosome Synthesis in Growing and Nongrowing Cultures of *Acinetobacter calcoaceticus*<sup>†</sup>

Matthew R. Cutter and Peter G. Stroot\*

Department of Civil and Environmental Engineering, University of South Florida, 4202 East Fowler Ave., ENB118, Tampa, Florida 33620-5350

Received 17 August 2007/Accepted 29 November 2007

**RT-RiboSyn measures the specific rate of ribosome synthesis in distinct microbial populations by measuring the generation rate of precursor 16S rRNA relative to that of mature 16S rRNA when precursor 16S rRNA processing is inhibited. Good agreement was demonstrated between specific rate of ribosome synthesis and specific growth rate of *Acinetobacter calcoaceticus*.**

A new molecular-biology-based method was developed to determine the specific growth rate of a distinct microbial population in an environmental sample by measurement of the specific rate of ribosome synthesis. This new method has been named RT-RiboSyn, based upon the use of reverse transcription and primer extension (RT&PE) to measure the specific rate of ribosome synthesis as shown in equation 1:

$$r = \frac{\ln 2}{t_D} \quad (1)$$

where  $t_D$  is the ribosome doubling time.

RT-RiboSyn utilizes the antibiotic chloramphenicol, which disrupts the processing of precursor 16S (pre-16S) rRNA to mature 16S rRNA over time (6). When exposed to chloramphenicol, the bacterial cells continue to generate pre-16S rRNA while the mature 16S rRNA remains constant (9), excluding low rates of degradation. Monitoring pre-16S rRNA synthesis has been used in previous work (2, 5, 8, 9) as an indicator of growth response, and pre-16S rRNA synthesis has been shown (5) to dramatically increase compared to the sum of pre-16S and mature 16S rRNA levels. RT-RiboSyn expands on this concept to determine a specific rate of ribosome synthesis by using a primer that specifically targets a population of interest.

*Acinetobacter calcoaceticus* (ATCC 23055) was cultured in nutrient broth and shaken at 250 rpm to generate four distinct growth conditions, including mid-log growth phase cultures incubated at 25, 30, and 35°C and a stationary-phase culture incubated at 30°C. Chloramphenicol (final concentration, 20 mg/liter) was added to a 50-ml sample from each culture to inhibit the secondary processing of pre-16S rRNA (6). Subsamples (4 ml) were collected from each 50-ml sample at 0, 10, 20, and 30 min of exposure to chloramphenicol, centrifuged

(10,000 × g for 5 min), decanted, and stored promptly at –80°C.

The optical densities of the four cultures were measured periodically at 684 nm by using a spectrophotometer, and the specific growth rates were determined for the time of sample collection.

RNA was extracted from the subsamples by using the phenol-chloroform method (7), followed by purification with an RNAqueous kit (Ambion, Inc.). Residual DNA was removed using DNase I treatment (DNAfree kit by Ambion, Inc.). Finally, RT&PE using the ImProm-II reverse transcription system (Promega Corporation) was performed according to the manufacturer's instructions, with an MgCl<sub>2</sub> concentration of 2.5 mM. The WellRed-labeled primers (Sigma-Genosys) used in the RT&PE reaction were Eub338 (5' GCTGCCCTCCCGT AGGAGT 3') and Acin0659 (5' CTGGAATTCTACCATCC TCTCCCA 3'), which target conserved sites of the pre-16S and 16S rRNA for all *Eubacteria* and *Acinetobacter* species, respectively (3, 4). The primer extension step was 1 h at 42°C and 47°C for the Eub338 and Acin0659 primers, respectively. Samples were then incubated at 85°C for 15 min to inactivate any RNase inhibitor present, followed by quenching in an ice slurry for 5 min. Samples were then mixed with RNase A (Sigma) cocktail (40 μl) and incubated at 37°C for 30 min. The RT&PE samples were analyzed by capillary electrophoresis with the CEQ 8000 genetic analysis system (Beckman-Coulter), with resulting electropherograms used for analysis (see the supplemental material). The size standards for the WellRed-labeled primers were the GenomeLab DNA size standard kit (600 nucleotides) for the Eub338 RT&PE samples and the MapMarker 1000 (Bioventures, Inc.) sizing standard for the Acin0659 RT&PE samples.

Capillary electrophoresis separates the two RT&PE products by length, and using the same primer for both products allows for the comparison of the two peaks by area (Fig. 1; also see the supplemental material). The fragment lengths correspond to the predicted lengths of the pre-16S and 16S RT&PE products (10). The ratio of the pre-16S and 16S RT&PE products (pre-16S:16S) was determined for each subsample and plotted versus time of chloramphenicol exposure. A trend line was fitted to these data, and the equation was determined.

\* Corresponding author. Mailing address: 4202 East Fowler Ave., ENB118, Tampa, FL 33620-5350. Phone: (813) 396-9323. Fax: (813) 974-9341. E-mail: pstroot@cug.usf.edu.

<sup>†</sup> Supplemental material for this article may be found at <http://aem.asm.org/>.

<sup>‡</sup> Published ahead of print on 14 December 2007.

## Appendix C (continued)

902 CUTTER AND STROOT

APPL. ENVIRON. MICROBIOL.

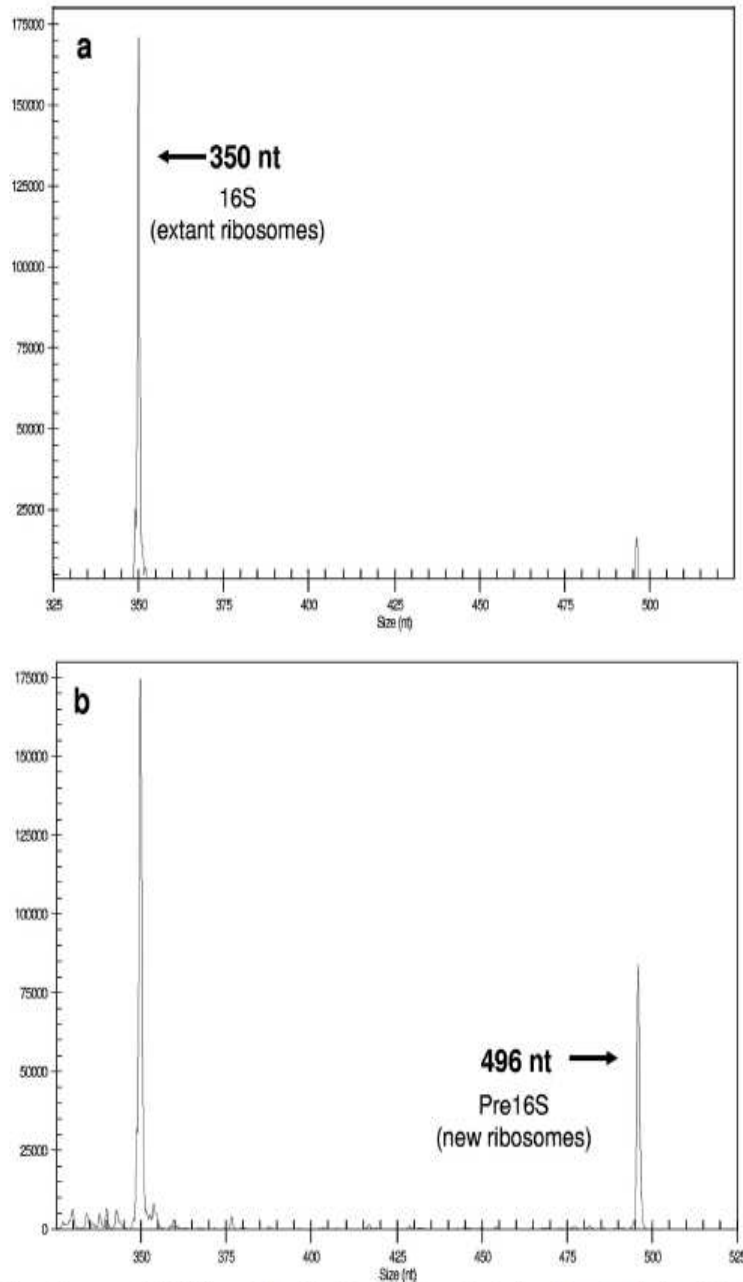


FIG. 1. Electropherograms of RT-RiboSyn products derived from *A. calcoaceticus* incubated in nutrient broth at 25°C after exposure to chloramphenicol for 0 min (a) and 20 min (b). The WellRed-labeled Eub338 primer was used. nt, nucleotides.

Using the slope of the equation, the ribosome doubling time was determined. Specific rates of ribosome synthesis were then determined using equation 1.

Table 1 shows the mean pre-16S:16S values for each of the subsamples collected from the four cultures. For all sub-

samples, the low coefficient of variance indicates a strong reproducibility with the RT-RiboSyn method. For growing cultures, the mean pre-16S:16S values increased with longer exposure to chloramphenicol, which is consistent with earlier work (10).

Appendix C (continued)

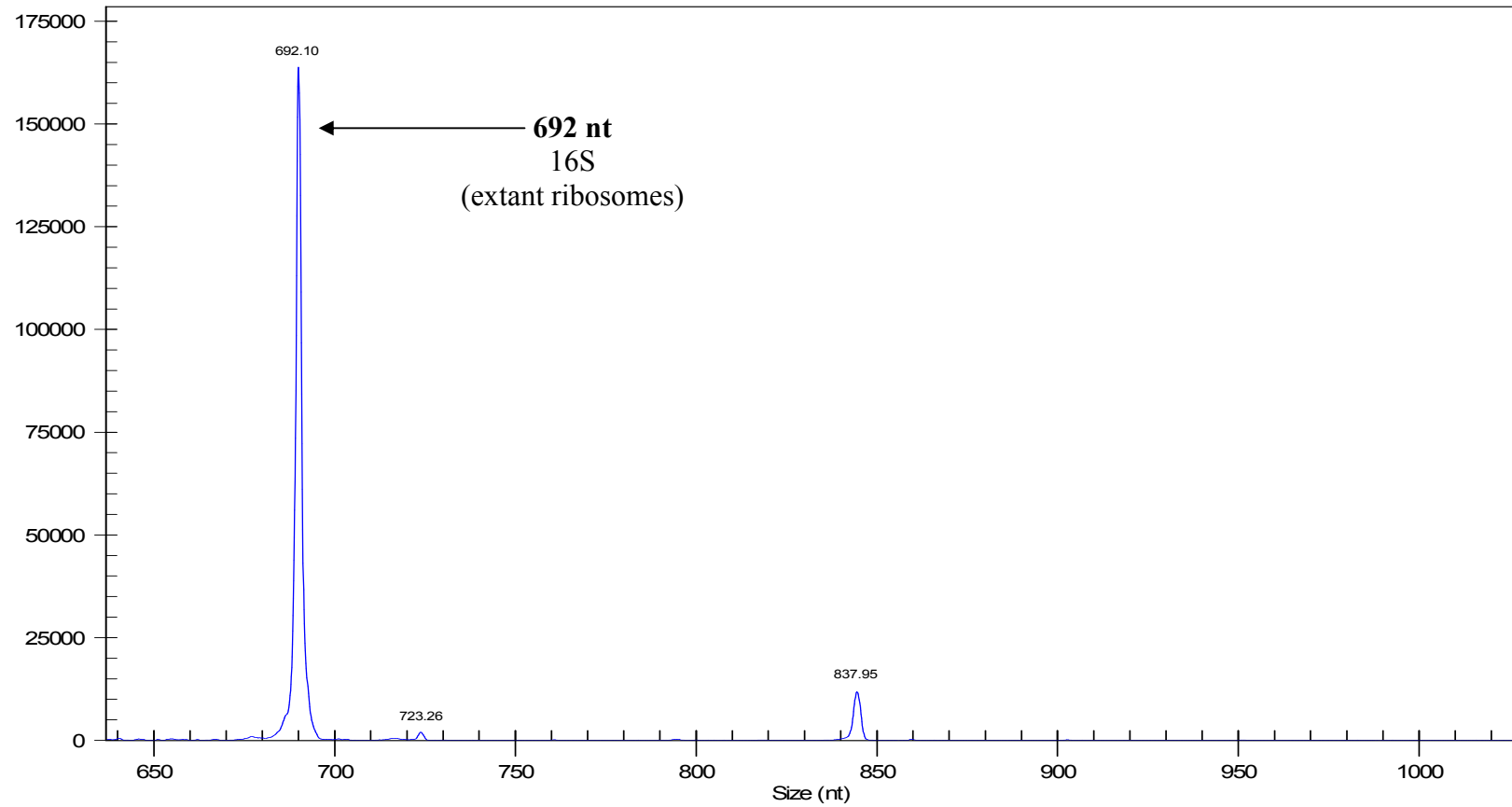


**Figure C1.** Electropherogram of RT-RiboSyn products derived from *A. calcoaceticus* incubated in nutrient broth at 25 °C after exposure to chloramphenicol for zero minutes.

Appendix C (continued)

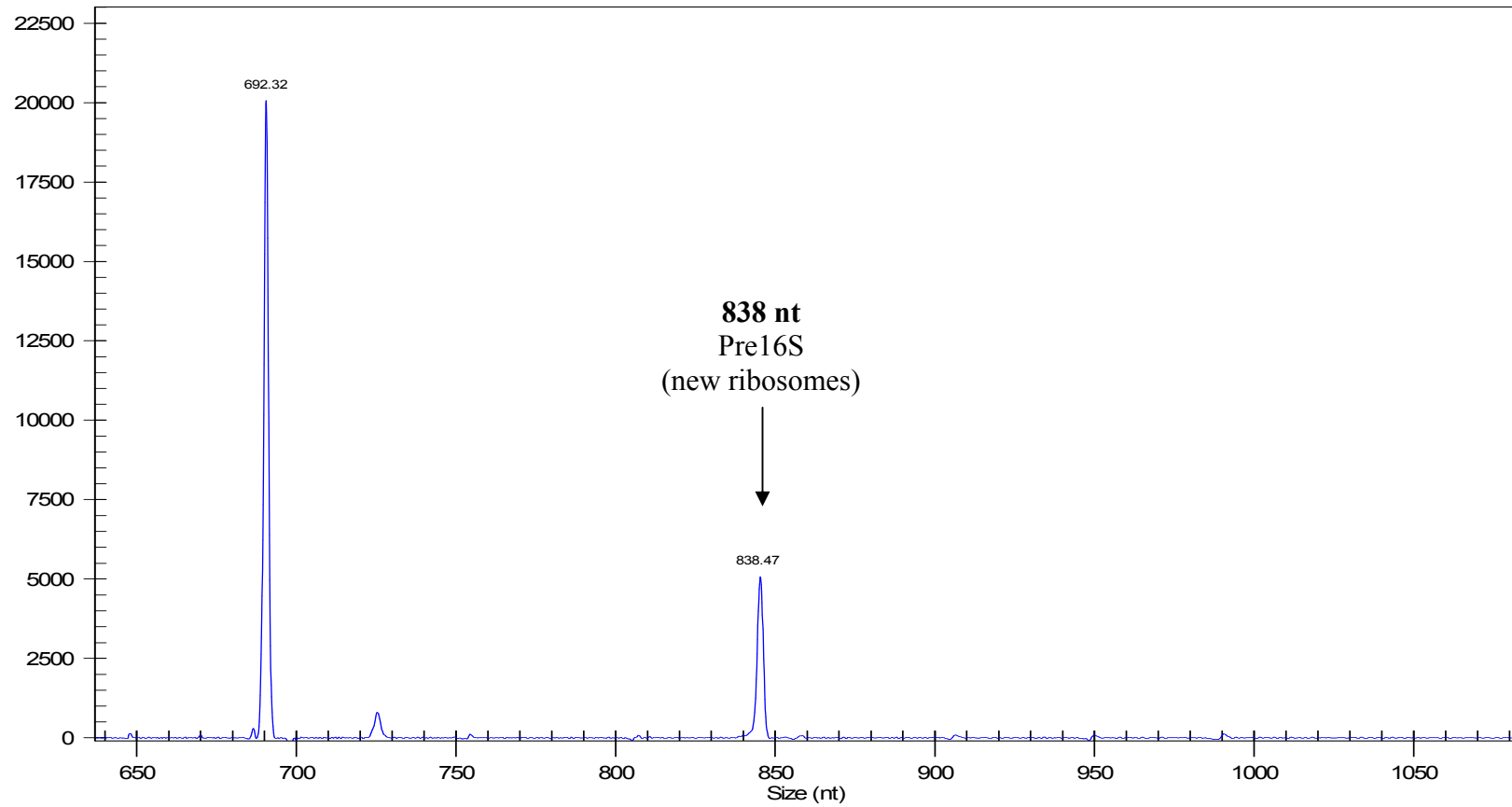


**Figure C2.** Electropherogram of RT-RiboSyn products derived from *A. calcoaceticus* incubated in nutrient broth at 25 °C after exposure to chloramphenicol for twenty minutes



## **Appendix D. Beckman-Coulter CEQ-8000 Detection Limits**

### **D.1. CEQ-8000 Genetic Analysis System**

The Beckman-Coulter CEQ-8000 Genetic Analysis System is the principal instrument used in this work to detect the ssDNA fragments generated from the RT-RiboSyn method. The CEQ-8000 system (CEQ) is an automated capillary gel electrophoresis system capable of analyzing fragment lengths and abundance from eight samples at a time. Beckman-Coulter manufactures size standards up to 640 nt in length, with greater length size standards offered by another vendor. After analysis, a signal strength vs. fragment length electropherogram is created for each sample along with the numerical data used to create the graph. It is this list of fragment lengths and abundance that are used to determine the pre16S:16S data as shown in Figure 10.

In order to use the CEQ and be confident that sample fragments are being accurately detected, the minimum mass detection limit for the instrument must be determined. While this may not be as big a concern for pure culture samples in which specific RNA is plentiful, in environmental samples such as anaerobic digester sludge, a targeted population may only exist in small concentrations within that sample. For instance, it has been demonstrated that methanogen populations make up only 3-9% of the microbial community in anaerobic digester sludge (Griffin *et al*, 1997) (McMahon *et al*, 2004). The question then becomes whether or not the CEQ will even detect these populations in a fashion that will provide useful information to allow for the determination of pre16S:16S data.

## Appendix D (continued)

### D.2. Determination of CEQ-8000 Detection Limits

The manner in which this lower detection limit was determined was simple. RNA was extracted from frozen concentrated cell pellets of *Acinetobacter calcoaceticus* as described in Chapter 3. Three cell pellets were used in the extraction, representing a time series of 0, 10, and 20 minutes of exposure to chloramphenicol before centrifugation and freezing. Final concentration of the extracted RNA was determined by using the Invitrogen Qubit™ Quantitation Platform, which is a highly sensitive fluorometer that can distinguish between RNA and DNA through the use of an Quant-iT™ RNA Assay Kit. After an initial full-concentration ssDNA mass of 49.2, 62.4, and 75.0 ng for the time= 0, 10, and 20 minute samples, respectively, a dilution series (10x to 1000000x) was created for each of the three samples. The CEQ fragment analysis of these samples is presented in Figures C1 through C4. Figures C1 and C2 present the average 16S and pre16S peak height, respectively, for each sample in the dilution series for each of the three time series samples. Figures C3 and C4 present the 16S and pre16S, respectively, peak height versus the total fragment mass per sample.

These data indicate that dilution factors greater than three will eliminate detection of either 16S or pre16S peaks, with final lower detection limits of about 0.1 ng. In order to achieve levels great enough to be detected and measured, the peak height must be greater than about signal noise inherent in . The best use of these data are for determination of microorganism presence rather than fragment mass, as variations such as temperature and capillary array/gel age within the CEQ are likely to render these attempts outside of the

## Appendix D (continued)

purpose of the instrument. For detecting the presence of minor populations, concentrating samples is a good practice to maximize the chance to generate detectable fragments.

Earlier work (McMahon *et al*, 2004) has estimated the mass levels of typical anaerobic digester sludge populations that can be expected. Table C1 indicates that we can expect adequate mass of RNA to be extracted from samples of anaerobic digester sludge to be detectable by the CEQ.

**Table D1.** Expected mass of rRNA available in a standard sample of anaerobic digester sludge (2 mL) and per RT reaction (10 µg total) for several examples of syntrophic bacteria and methanogens found in anaerobic digester sludge.

Organism type	Genus and species	Total mass (µg)	Mass in RT reaction (µg)
Syntrophs	<i>Syntrophobacter fumaroxidans</i>	78.4	0.03
	<i>Syntrophobacter pfennigii</i>	100.45	0.04
	<i>Syntrophobacter wolinii</i>	105.35	0.04
	<i>Syntrophomonadacea spp.</i>	267.05	0.11
Methanogens	<i>Methanosarcina spp.</i>	29.4	0.01
	<i>Methanosaeta concilii</i>	595.35	0.24
	<i>Methanobacteriaceae spp.</i>	29.4	0.01

Appendix D (continued)

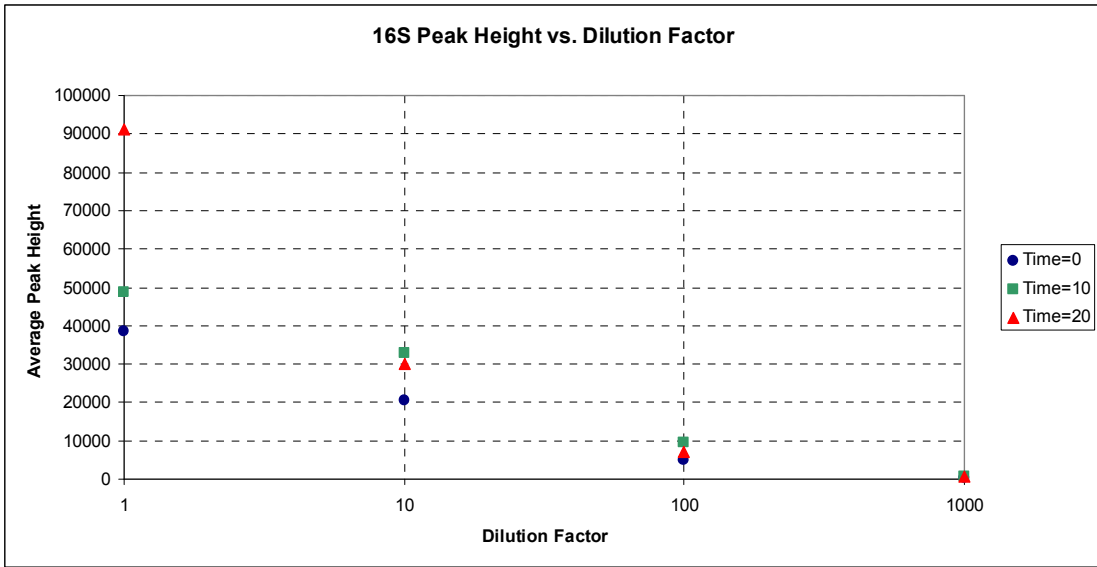


Figure D1. 16S peak height vs. dilution factor from CEQ fragment analysis

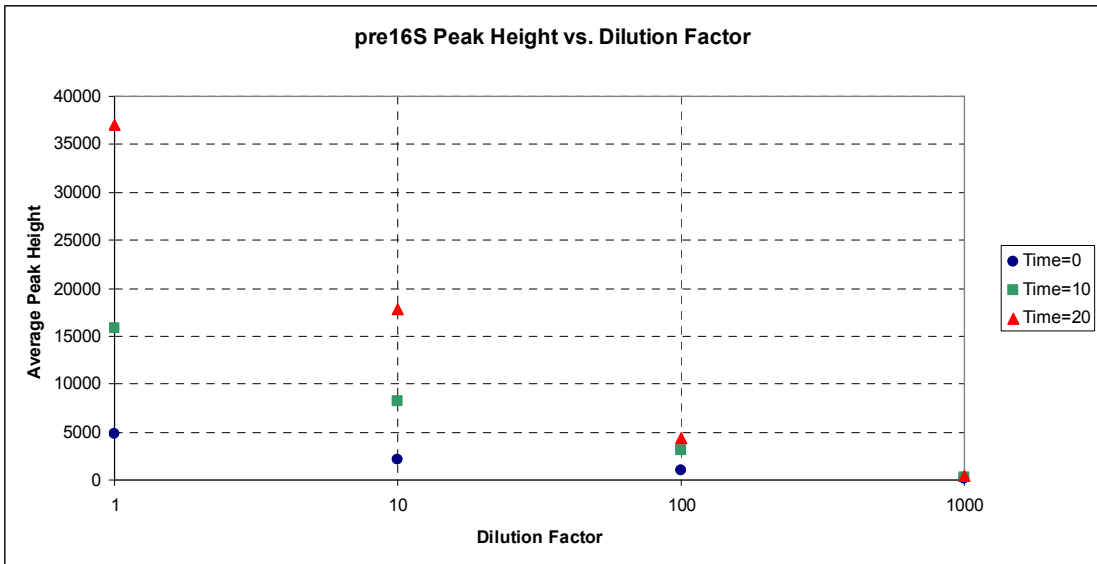


Figure D2. Pre16S peak height vs. dilution factor from CEQ fragment analysis

Appendix D (continued)

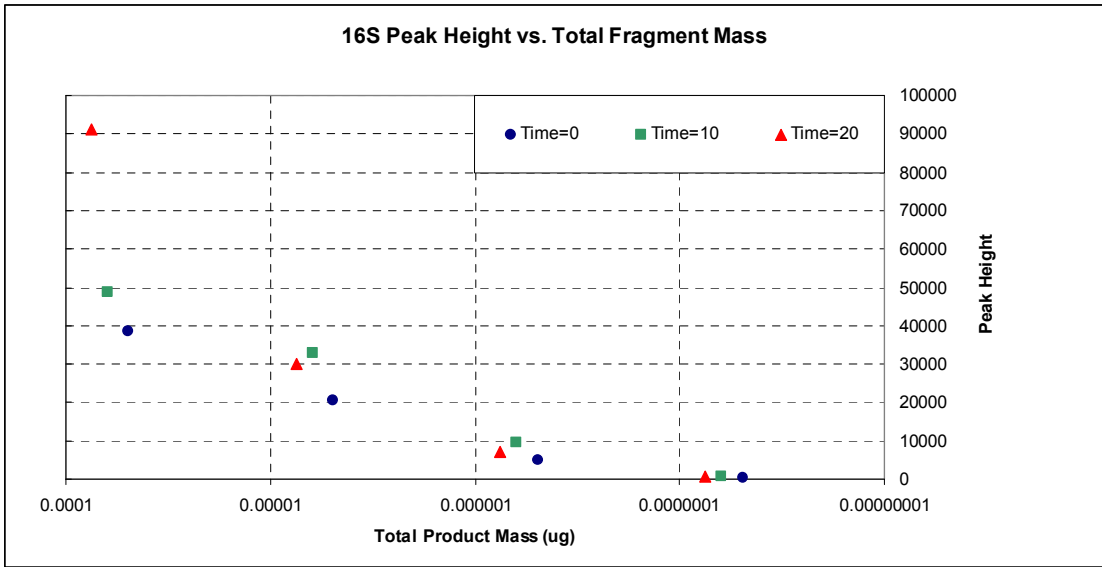


Figure D3. 16S peak height vs. total fragment mass

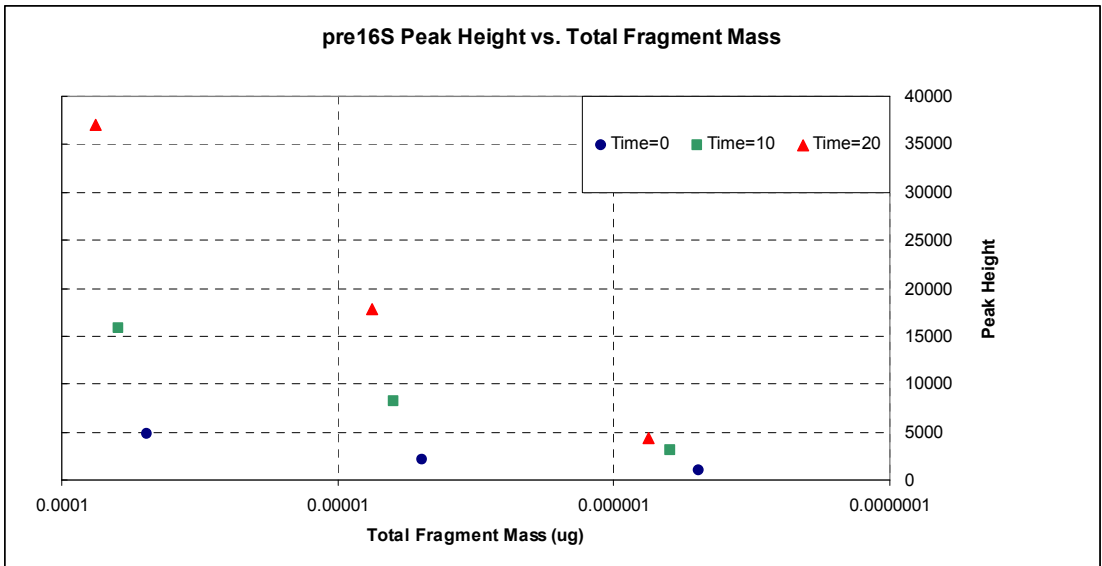


Figure D4. Pre16S peak height vs. total fragment mass

## **ABOUT THE AUTHOR**

Matthew R. Cutter grew up just north of Cincinnati, Ohio and attended The Ohio State University, graduating with a Bachelor of Science degree in Metallurgical Engineering in 1993. After working in the aluminum foundry and stainless steel industries for 8 years, and after earning an Master of Business Administration degree in 2000, Matt decided to pursue higher education in the field of Environmental Engineering. After earning a Master of Science degree (Hydraulics) in 2004 at the University of Cincinnati, he began his Ph.D. studies at the University of South Florida. While there, he developed an interest in waste water treatment and molecular biology methods. He has earned or applied for three patents in these fields. Matt has a variety of interests and enjoys finding new ones from time to time.